



Carla Isabel Lopes Daniel

Mestre em Engenharia Química e Bioquímica

Development and Modulation of Magnetic Responsive Supported Ionic Liquid Membranes

Dissertação para obtenção do Grau de Doutor em

**Engenharia Química e Bioquímica
Especialidade Engenharia Química**

Orientador: João Paulo Goulão Crespo, Professor Catedrático,
Faculdade de Ciências e Tecnologia - Universidade
Nova de Lisboa

Co-orientadora: Carla Alexandra Moreira Portugal, Investigadora,
Faculdade de Ciências e Tecnologia - Universidade
Nova de Lisboa

Júri

Presidente: Prof. Doutor Manuel Nunes da Ponte

Arguentes: Prof. Doutora Patrícia Luís Alconero
Prof. Doutor Carlos Manuel Silva

Vogais: Prof. Doutor Pedro José Oliveira Sebastião
Prof. Doutor Carlos Afonso



FACULDADE DE
CIÊNCIAS E TECNOLOGIA
UNIVERSIDADE NOVA DE LISBOA

Dezembro, 2015

Development and Modulation of Magnetic Responsive Supported Ionic Liquid Membranes

Copyright © Carla Isabel Lopes Daniel, Faculdade de Ciências e Tecnologia, Universidade NOVA de Lisboa.

A Faculdade de Ciências e Tecnologia e a Universidade NOVA de Lisboa têm o direito, perpétuo e sem limites geográficos, de arquivar e publicar esta dissertação através de exemplares impressos reproduzidos em papel ou de forma digital, ou por qualquer outro meio conhecido ou que venha a ser inventado, e de a divulgar através de repositórios científicos e de admitir a sua cópia e distribuição com objetivos educacionais ou de investigação, não comerciais, desde que seja dado crédito ao autor e editor.

ACKNOWLEDGEMENTS

Com imenso gosto, quero agradecer em primeiro lugar aos meus orientadores João Paulo Crespo e Carla Portugal, pela oportunidade de fazer parte deste projecto de investigação que durante estes 5 anos desenvolvemos em conjunto. Foi pela orientação científica, disponibilidade, sentido crítico, exigência e rigor da vossa parte que me fizeram aprender cada dia mais e mais e crescer muito a nível profissional. Agradeço sempre a amizade e apoio demonstrados a nível pessoal em todos os momentos passados ao longo destes anos, os quais não esquecerei nunca. Agradeço também as oportunidades de colocações científicas nacionais e internacionais que me aconselharam a experienciar, pois sem dúvida, foram as que mais me fizeram crescer a todos os níveis, profissional e pessoal, onde conheci pessoas inesquecíveis. Um gigante Obrigado por tudo João Paulo e Carla!!!

Quero agradecer ao Professor Pedro Sebastião, do Instituto Superior Técnico, pela oportunidade de colaborar e integrar o seu grupo de investigação durante quatro anos. Ao longo desta colaboração aprendi um novo mundo sobre a “encantada” Física, que me fez interligar com todo o meu PhD e foi crucial para todos os avanços que fui alcançando com a imensa ajuda, apoio, paciência que o Pedro teve para comigo. Foram as longas e inúmeras discussões sobre o trabalho que mais fizeram ter uma visão de qual o passo seguinte! Aprendi imenso e cresci muito com esta colaboração! Um grande obrigado a si Pedro!

Ao Professor Angel Irabien, da Universidade de Cantabria, Santander - Espanha, quero agradecer pela oportunidade do meu primeiro estágio em 2012, no seu grupo de investigação, no qual desenvolvi uma parte do meu PhD, e também agradecer a colaboração no Projecto ERA-CHEMISTRY no qual tive oportunidade de trabalhar. Agradeço a todo o grupo com quem trabalhei em Santander, pois jamais esquecerei o quanto me ajudaram desde o primeiro dia até ao ultimo!

Aos Professores Paul Scovazzo e Jonh O´Haver da Universidade do Mississippi, Oxford - EUA, agradeço pela colaboração na recta final da minha tese, no desenvolvimento de micelas magnéticas, e pelo facto de me ter recebido no seu grupo em 2013 no meu segundo estágio, nos EUA! Foi uma experiência inesquecível, a trabalhar com pessoas fantásticas, tendo aprendido imenso.

Ao Professor Carlos Afonso, da Univerdade de Lisboa, Faculdade de Farmácia, quero agradecer imenso ter-me recebido dois meses no seu laboratório para trabalhar em colaboração neste projecto. Todo o apoio, reuniões e sugestões o meu muito Obrigado!

Aos Professores Gaspar Martinho e José Paulo Farinha, do Instituto Superior Técnico, pela ajuda nas análises por DLS, na última parte deste trabalho.

À Professora Isabel Marrucho, do ITQB, pela oportunidade que me facultou de fazer medidas de condutividade no seu laboratório.

À Professora Margarida Cardoso, da FCT/UNL, pela ajuda na última parte deste trabalho, pelas sugestões e reuniões que tivemos. Obrigada pela disponibilidade!

Ao Doutor Fabian Chávez, da Universidade Nacional de Córdoba, com quem trabalhei no IST em colaboração com o Professor Pedro Sebastião, quero agradecer a imensa ajuda desde o primeiro dia até ao final da minha tese, toda a disponibilidade e atenção e interesse por este trabalho e toda a simpatia demonstrados sempre!

Gostaria de agradecer a todos colegas do grupo BPEG e aos que já não estão no grupo e que a amizade e contacto ficaram, por ao longo destes anos demonstrarem sempre interajuda e disponibilidade para quando no dia a dia precisei de ajuda nas questões e dúvidas de trabalho. A todas as pessoas que conheci ao longo deste PhD que foram mais que muitas, em cursos e conferências, e que de alguma forma também ajudaram!

Em especial quero agradecer à minha grande amiga Luísa, pela amizade gigante, apoio incondicional, disponibilidade total e por me conhecer como ninguém, sempre esteve e está lá comigo!!! OBRIGADA!!! OBRIGADA!!!

Igualmente especial à Mónica e Cristiana, pela grande amizade, todo o apoio no dia a dia, momentos muito bem passados e o companheirismo ao longo deste anos. O meu muito Obrigado!!!

Um agradecimento também muito muito especial, aos meus queridos amigos espanhóis, Jonathan e Esther, pela amizade, apoio, diversão, ânimo, durante os estágios que fiz em Espanha e vocês em Portugal! Foram dos momentos mais bem passados e aproveitados!!! A todos os grandes amigos que ficam para toda a vida que conheci em Espanha, os quais me fizeram sentir muito feliz!!! Fortísimos sempre!!

Agradeço aos amigos que conheci nos EUA e que ficam também para sempre, Frances e família, Martinha, Rui, Fábio e todas as outras pessoas, o muito Obrigada ao apoio que tive a Kms de Portugal durante dois meses!!! Outstanding!!!

À Liliana e Sandra, as minhas meninas do ITQB, pela amizade, apoio e indiscutíveis melhores momentos de pura diversão!!! Principalmente além fronteiras!

Ao pessoal do grupo de investigação da FFarmácia, principalmente, Carlos, Jaime, Andreia, Roberta, Filipa e todos os que conheci, pelo companheirismo, imensa ajuda e muita diversão que passámos no Lab! Muito Obrigada!

Agradeço a imensa e fundamental ajuda do Bruno Candeias do DI/FCT na parte de edição da tese em Latex!

À minha grande amiga e mana Isabel, que apesar de separadas, estamos sempre juntas com toda a amizade, carinho e apoio, que já dura à 24 anos!

A todos os outros grandes grandes amigos como, Ana Rodrigues, Alice, Natacha, Lina, Humberto, Joana, Pedro, agradeço a imensa amizade, ajuda, conversas, cafés, e tudo o que já passámos juntos!!! O meu muito Obrigado!

A todos os outros amigos e colegas que são mais que muitos, que mesmo longe, sei que me apoiam e agradeço pelas lembranças sempre! Aos mais recentes amigos, Liliana, Telmo, Cláudia pela amizade, boa disposição e todos os momentos de grandes risadas!

Aos meus manos, cunhadas e sobrinhos, pelos momentos em família bem passados, e pelo apoio e preocupação demonstrados e pelas conversas sempre!

Por último, mas o maior dos agradecimentos aos MEUS PAIS, Teresa e Daniel! As duas pessoas mais presentes na minha vida, apesar da distância física, e que muitas vezes fizeram falta estarem mais perto, agradeço por me conhecerem como mais ninguém sabe, pelo apoio, as longas conversas por telefone, os conselhos que foram, são e serão tudo para seguir em frente! Obrigada mãe e pai por acreditarem em mim e nos momentos que mais foram difíceis, vocês estão sempre comigo, e por todos os mimos!

Agradeço a todos por terem acreditado em mim!

ABSTRACT

The work presented in this thesis aims at developing a new separation process based on the application of supported magnetic ionic liquid membranes, SMILMs, using magnetic ionic liquids, MILs. MILs have attracted growing interest due to their ability to change their physicochemical characteristics when exposed to variable magnetic field conditions. The magnetic responsive behavior of MILs is thus expected to contribute for the development of more efficient separation processes, such as supported liquid membranes, where MILs may be used as a selective carrier. Driven by the MILs behavior, these membranes are expected to switch reversibly their permeability and selectivity by *in situ* and non-invasive adjustment of the conditions (e.g. intensity, direction vector and uniformity) of an external applied magnetic field.

The development of these magnetic responsive membrane processes were anticipated by studies, performed along the first stage of this PhD work, aiming at getting a deep knowledge on the influence of magnetic field on MILs properties. The influence of the magnetic field on the molecular dynamics and structural rearrangement of MILs ionic network was assessed through a $^1\text{H-NMR}$ technique. Through the $^1\text{H-NMR}$ relaxometry analysis it was possible to estimate the self-diffusion profiles of two different model MILs, [Aliquat][FeCl_4] and [P_{66614}][FeCl_4]. A comparative analysis was established between the behavior of magnetic and non-magnetic ionic liquids, MILs and ILs, to facilitate the perception of the magnetic field impact on MILs properties. In contrast to ILs, MILs show a specific relaxation mechanism, characterized by the magnetic dependence of their self-diffusion coefficients. MILs self-diffusion coefficients increased in the presence of magnetic field whereas ILs self-diffusion was not affected.

In order to understand the reasons underlying the magnetic dependence of MILs self-diffusion, studies were performed to investigate the influence of the magnetic field on MILs' viscosity. It was observed that the MIL's viscosity decreases with the increase of the magnetic field, explaining the increase of MILs self-diffusion according to the modified Stokes- Einstein equation.

Different gas and liquid transport studies were therefore performed aiming to determine the influence of the magnetic behavior of MILs on solute transport through SMILMs. Gas permeation studies were performed using pure CO_2 and N_2 gas streams and air, using

a series of phosphonium cation based MILs, containing different paramagnetic anions. Transport studies were conducted in the presence and absence of magnetic field at a maximum intensity of 1.5T. The results revealed that gas permeability increased in the presence of the magnetic field, however, without affecting the membrane selectivity. The increase of gas permeability through SMILMs was related to the decrease of the MILs viscosity under magnetic field conditions.

Two distinct case studies were performed to evaluate the influence of magnetic field in the transport of two model solutes, ibuprofen and α -pinene, in organic liquid phases, dodecane and hexane. Transport studies in liquid phase were carried out using SMILMs prepared by immobilization of imidazolium based MILs, which depicted good structural stability when in contact with the selected organic phases. Identical to that observed in gas transport studies, the magnetic field induced an increase of the permeability of ibuprofen and α -pinene through the SMILMs tested. In this case, the increase of solute permeability was not only ascribed to the magnetically induced decrease of MILs viscosity but also to the increase of solutes solubility in MILs, promoted by the magnetic field.

This work demonstrates the possibility to modulate the physicochemical characteristics of MILs, e.g. self-diffusion and viscosity, by non-invasive and *in situ* adjustment of the magnetic field conditions. It was also shown that the magnetic modulation of such variables impacts on the permeability of the SMILMs and on solute diffusion in gas and liquid separations.

Keywords: Magnetic Ionic Liquids (MILs), Proton Nuclear Magnetic Resonance (^1H -NMR), Supported Magnetic Ionic Liquid Membranes (SMILMs), magnetic field, gas and liquid transport.

RESUMO

O trabalho apresentado nesta tese tem como objetivo o desenvolvimento de uma nova geração de processos de separação baseados na aplicação de membranas líquidas suportadas, usando líquidos iônicos magnéticos. Estes líquidos iônicos magnéticos têm merecido um interesse crescente devido à sua capacidade em modificar reversivelmente as suas propriedades físico – químicas quando sujeitos à presença de um campo magnético. Enquanto transportadores líquidos, integrantes de membranas líquidas suportadas, será de esperar que o seu comportamento magnético se possa traduzir na capacidade de modular de modo não-invasivo, a permeabilidade e o transporte seletivo de solutos através destas membranas, por ajuste das condições (intensidade, direção do vetor magnético e uniformidade de campo) de um campo magnético externo. Como tal, poderão contribuir para o desenvolvimento de processos de separação mais eficientes de forma não invasiva.

O desenvolvimento destes processos de separação, baseados em membranas com propriedades magnéticas, foi antecipado por estudos realizados numa primeira fase deste trabalho de douramento, que tiveram como objetivo obter um conhecimento profundo acerca da influência do campo magnético nas propriedades dos líquidos iônicos magnéticos. O impacto do campo magnético na dinâmica molecular e nos rearranjos estruturais da rede iónica destes líquidos foi avaliado através da técnica $^1\text{H-NMR}$ (Relaxação Magnética Nuclear de Protão). Esta técnica de análise de relaxometria permitiu estimar os perfis de autodifusão de dois líquidos iônicos magnéticos modelo, [Aliquat][FeCl₄] e [P₆₆₆₁₄][FeCl₄] em função do campo magnético. Foi efetuada uma análise comparativa entre o comportamento dos líquidos magnéticos e não magnéticos, de modo a facilitar a compreensão do impacto do campo magnético nas propriedades dos líquidos iônicos magnéticos. Contrariamente aos líquidos não magnéticos, os líquidos iônicos magnéticos evidenciaram a presença de um mecanismo específico de relaxação, caracterizado pela dependência magnética dos seus coeficientes de autodifusão. Foi verificado que os coeficientes de autodifusão destes líquidos aumentam na presença de um campo magnético. Contudo a autodifusão dos seus análogos não magnéticos não foi afetada.

De modo a compreender a dependência magnética dos coeficientes de autodifusão destes líquidos iônicos, foram efetuados estudos para investigar a influência do campo magnético na viscosidade dos mesmos. Verificou-se que a viscosidade destes líquidos

magnéticos diminuí com o aumento da intensidade do campo magnético, o que, em concordância com a equação modificada de Stokes-Einstein, permitiu explicar o aumento da autodifusão dos líquidos iônicos.

Foram realizados estudos de transporte em meio gasoso e líquido com o objetivo de determinar a influência do comportamento magnético dos líquidos iônicos no transporte de diferentes gases, CO₂, N₂ e Ar, através de membranas líquidas suportadas. Estes estudos de permeação gasosa foram realizados usando diferentes membranas líquidas suportadas, preparadas por imobilização de líquidos iônicos magnéticos distintos, compostos pelo cátion fosfônio e diferentes aniões paramagnéticos. Estes estudos de transporte foram feitos na presença e ausência de campo magnético a uma intensidade máxima de 1.5 Tesla. Os resultados revelaram que a permeabilidade dos gases aumentou na presença do campo magnético, no entanto, sem efeito na seletividade da membrana líquida suportada. O aumento de permeabilidade de solutos na presença de campo magnético foi relacionada com a diminuição da viscosidade destes líquidos quando expostos ao efeito do campo magnético.

Foram testados dois casos de estudo distintos para verificar a influência do campo magnético no transporte de solutos presentes entre fases líquidas: transporte de ibuprofeno e α -pineno, em meio orgânico de dodecano e hexano. Os estudos de transporte foram realizados usando membranas líquidas suportadas com a incorporação dos líquidos iônicos magnéticos com o cátion imidazolium, as quais demonstraram possuir boa estabilidade mediante o contacto com as fases orgânicas selecionadas. Identicamente ao que foi observado no transporte de gases, o campo magnético induziu um aumento da permeabilidade dos dois solutos, ibuprofeno e α -pineno através das membranas líquidas suportadas testadas. Neste caso, o aumento da permeabilidade dos solutos não foi apenas atribuído à diminuição da viscosidade dos líquidos iônicos induzida pelo campo magnético, mas também devido ao aumento da solubilidade dos solutos nos líquidos iônicos magnéticos, promovido pelo campo magnético aplicado.

Este trabalho demonstra a possibilidade de modular as propriedades físico-químicas dos líquidos iônicos magnéticos, tais como, autodifusão e viscosidade, de forma não invasiva por ajuste das condições do campo magnético. Foi também possível mostrar que a modulação magnética destas variáveis tem impacto na permeabilidade das membranas magnéticas líquidas suportadas e na difusão dos solutos em fase gasosa e líquida.

Palavras-chave: Líquidos Iônicos Magnéticos, Ressonância Magnética Nuclear, Membranas Líquidas Suportadas com líquidos iônicos magnéticos, campo magnético, transporte em meio líquido e gasoso.

Abbreviations

[Aliquat ⁺]	Methyltrioctylammonium cation
[Aliquat][Cl]	Methyltrioctylammonium chloride
[Aliquat][FeCl ₄]	Methyltrioctylammonium tetrachloroferrate
B	Magnetic field, <i>Tesla</i>
BPP	Bloemberger, Purcel and Pound relaxation model
[C ₁₁ H ₂₁ N ₂ O][GdCl ₃ Br ₃]	1-butyl-3-(3-hydroxy-2-methylpropyl)imidazolium hexabromidechlorogadolinium
[C ₄ mim][FeCl ₄]	1-butyl-3-methylimidazolium tetrachloroferrate
[C ₈ mim][FeCl ₄]	1-octyl-3-methylimidazolium tetrachloroferrate
[C _n mim] ⁺	Imidazolium cation
[CoCl ₄] ⁻²	Cobalt tetrachloride
CMC	Critical Micellar concentration, <i>mM</i>
CR	Cross relaxation contribution
DMSO	Dimethyl sulfoxide
[FeCl ₄] ⁻	Iron tetrachloride
[GdCl ₆] ⁻³	Gadolinium hexachloride
GC	Gas Chromatography
¹ H-NMR	Proton Nuclear Magnetic Resonance Relaxometry
¹ H-NMRD	Proton Nuclear Magnetic Resonance Relaxometry Dispersion
ICP	Inductively coupled plasma
ILs	Ionic Liquids
[MnCl ₄] ⁻²	Manganese tetrachloride
MILs	Magnetic Ionic Liquids
MPD	Mean percentage deviation
mVFT	modified Vogel-Fulcher-Tamman equation
[n-bmim][FeCl ₄]	1-butyronitrile-3-methylimidazolium tetrachloroferrate
[P ₆₆₆₁₄] ⁺	Trihexyl(tetradecyl)phosphonium cation
[P ₆₆₆₁₄][Cl]	Trihexyl(tetradecyl)phosphonium chloride
[P ₆₆₆₁₄][FeCl ₄]	Trihexyl(tetradecyl)phosphonium tetrachloroferrate
[P ₆₆₆₁₄] ₂ [CoCl ₄]	Trihexyl(tetradecyl)phosphonium tetrachlorocobaltate
[P ₆₆₆₁₄] ₂ [MnCl ₄]	Trihexyl(tetradecyl)phosphonium tetrachloromanganate
[P ₆₆₆₁₄] ₃ [GdCl ₆]	Trihexyl(tetradecyl)phosphonium hexachlorogadolinium
PM	Paramagnetic relaxation contribution
PRE	Proton relaxation enhancement
PFG	Pulse field-gradient
PVDF	Polyvinylidene fluoride
Rot	Molecular rotations/reorientations contribution
RTILs	Room Temperature Ionic Liquids
SD	Translational self-diffusion contribution
SLMs	Supported liquid membranes

SMILMs	Supported Magnetic Ionic Liquid Membranes
VFT	Vogel-Fulcher-Tamman equation
ZFS	Zero-field-splitting

Variables

a, b and c	Coefficients of density equation
A and B	Orrick-Erbar model parameters for the viscosity estimation
A^* and B^*	Normalized parameters of Orrick-Erbar model
A^- and B^-	Parameters of anion contribution for the viscosity estimation
A^+ and B^+	Parameters of cation contribution for the viscosity estimation
A_m	Membrane area, cm^2
A_{CRi}	Parameter related to the strength of interaction in cross relaxation, s^{-2}
A_{Rot_i}	Parameter related to the strength of interactions in rotations/reorientations, s^{-2}
A_{Rot_1}, A_{Rot_2}	Parameters related with the strength of the interaction in rotations/reorientations contribution, s^{-2}
c	Quantity proportional to the molar concentration of magnetized particles, $[M]$, $molL^{-1}$
$[C]$	Concentration of the paramagnetic particles, $molL^{-1}$
C	Constant that depends on the MIL molar mass M_w and the molar volume V to calculate the viscosity
C_F	Concentration in the feed phase, $mol\ cm^{-3}$
C_S	Concentration in the stripping phase, $mol\ cm^{-3}$
d	Molecular width, m
D	Diffusion Coefficient, m^2s^{-1}
D_0	Diffusion Coefficient at zero magnetic field, m^2s^{-1}
D_{i0}	Diffusion coefficient of the solute i in the impregnated liquid phase, $m^2\ s^{-1}$
d_1 and e	Parameters of the accumulation equation
H	Gas partition coefficient
J_F	Flux of the solute in the feed phase, $mol\ cm^{-2}\ s^{-1}$
J_S	Flux of the solute in the stripping phase, $mol\ cm^{-2}\ s^{-1}$
K	Overall mass transfer coefficient, $cm\ s^{-1}$
$k_i m_0$	Mass transfer coefficient through the liquid phase impregnated in the support, $cm\ s^{-1}$
M_w	Molar mass, $gmol^{-1}$
n	Density of 1H spins, $spins\ m^{-3}$
n_i	number of chains of the phosphonium cation
N	Avogadro constant, mol^{-1}
p_{perm}	Pressure in the permeate compartment, Pa
p_{feed}	Pressure in the feed compartment, Pa
P	Permeability, Barrer or $cm^2\ s^{-1}$

P_1	Pressure, <i>MPa</i>
r_{FeH}	Distance between the magnetic ions and the solvent DMSO molecules for <i>is</i> relaxation contribution, \AA
r_1	Relaxivity of the contrast agent, $mM^{-1}s^{-1}$
$r_{i_{\text{eff}}}$	Effective inter-spin distance, <i>m</i>
R_1	Relaxation rate, s^{-1}
R_{FeH}	Distance between the magnetic ions and the solvent DMSO molecules for <i>os</i> relaxation contribution, \AA
Rot_1, Rot_2	Molecular rotations/reorientations contribution
<i>S</i>	Solubility
S_1	Electronic spin
S_c	Sub component of electronic spin - time average spin
<i>t</i>	Time, <i>s</i>
<i>T</i>	Absolute temperature, <i>K</i> or $^{\circ}\text{C}$
T_1	Spin-lattice relaxation time, <i>s</i>
T_2	Spin-spin relaxation time, <i>s</i>
$(T_1^{-1})_{is}$	Relaxation rate of inner-sphere relaxation contribution, s^{-1}
$(T_1^{-1})_{os}$	Relaxation rate of outer-sphere relaxation contribution, s^{-1}
<i>V</i>	Molar volume, m^3mol^{-1} or \AA^3
V_F	Volume of the feed phase, cm^3
V_S	Volume of the stripping phase, cm^3
Y^* and X^*	Normalized variables
$(VC)_{acc}$	Term for solute accumulation in the membrane, <i>mol</i>
$\sqrt{\langle r^2 \rangle}$	Mean-square jump distance, <i>m</i>

Greek Letters

α_1	Association degree
α and β	Fitted parameters of the density correlation, $\text{\AA}^3 Kg^{-1}MPa$ and $\text{\AA}^3 K^{-1}Kg^{-1}$
β_1	Geometric factor, m^{-1}
γ	^1H gyromagnetic ratio, <i>MHz</i>
γ_S	Electron's gyromagnetic ratio, <i>MHz</i>
δ	Gradient length, <i>ms</i>
δ_1	Membrane thickness, <i>m</i>
Δ	Delay between the gradients experiment, <i>ms</i>
Δ^2	Mean square fluctuations of the electronic zero-field-splitting (ZFS) relaxation contribution, s^{-2}
ϵ	Porosity of the membrane
η	Viscosity, <i>Pa.s</i> or <i>cP</i>
η_0	Viscosity at zero field, <i>Pa.s</i>

λ	Wavelength, <i>nm</i>
ν_L	Proton Larmor frequency, <i>Hz</i>
Ω	spectral density function
\mathcal{T}	dimensionless analytical function depends on the average time between diffusion jumps
ρ	Density, <i>g cm⁻³</i>
ω	Proton angular Larmor frequency, <i>Hz</i>
τ_1, τ_2	Correlation times in rotations/reorientations contribution, <i>s</i>
τ_{CRi}	Correlation time of the cross relaxation contribution, <i>s</i>
τ_d	Diffusion correlation time of paramagnetic contribution, <i>s</i>
τ_{d1}	Diffusion translational correlation time of paramagnetic contribution, <i>s</i>
τ_{d0}	Diffusion correlation time of paramagnetic contribution at zero magnetic field, <i>s</i>
τ_D	Diffusion correlation time of self-diffusion contribution, <i>s</i>
τ_{D0}	Diffusion correlation time of self-diffusion contribution at zero magnetic field, <i>s</i>
τ_m	Membrane tortuosity
τ_{mH}	Correlation time for the <i>is</i> inner relaxation, <i>s</i>
τ_{Rot_i}	Correlation time related with the rotations/reorientations, <i>s</i>
τ_s	Longitudinal electronic relaxation time, <i>s</i>
τ_{v_1} and p_1	Parameters that explained the decay of viscosity with <i>B</i>
χ_{mT}	Magnetic susceptibility, <i>emu.K. mol⁻¹</i>

Subscripts

0	absence of magnetic field
B	presence of magnetic field
cal	calculated property (density and viscosity)
exp	experimental(density and viscosity)
max	maximum value of the variables
min	minimum value of the variables
i	initial conditions
f	feed phase
s	stripping phase
eq	equilibrium

CONTENTS

List of Figures	xxi
List of Tables	xxiii
1 Introduction	1
1.1 Background and Motivation	1
1.2 Research strategy	4
1.3 Thesis Outline	6
2 ¹H-NMR and viscometry studies of MILs and ILs	9
2.1 Summary	9
2.2 Introduction	10
2.3 Experimental	11
2.3.1 Materials	11
2.3.2 Methods	12
2.3.2.1 Viscosity measurements	12
2.3.2.2 Nuclear Magnetic Resonance	12
2.4 Results	13
2.5 Analysis and discussion	15
2.5.1 Theoretical models	16
2.5.1.1 Translational self-diffusion	16
2.5.1.2 Rotations/reorientations	16
2.5.1.3 Cross-relaxation	16
2.5.1.4 Paramagnetic relaxation	17
2.5.2 Model fits to the experimental results	17
2.6 Conclusions	23
3 ¹H-NMR study of a MIL as a potential contrast agent	25
3.1 Summary	25
3.2 Introduction	26
3.3 Experimental	28
3.3.1 Materials	28
3.3.2 Methods	28

3.3.2.1	¹ H-NMR assays	28
3.3.2.2	Viscosity measurements	29
3.4	Results	29
3.5	Analysis and Discussion	31
3.6	Conclusions	37
4	A group contribution method for MILs viscosity	39
4.1	Summary	39
4.2	Introduction	40
4.3	Experimental	41
4.3.1	Materials and Methods	41
4.4	Results and Discussion	41
4.5	Conclusions	51
5	Permeability modulation of SMILMs	53
5.1	Summary	53
5.2	Introduction	54
5.3	Experimental	55
5.3.1	Materials	55
5.3.1.1	Gas Permeation experiments in Supported Magnetic Ionic Liquid Membranes (SMILMs)	55
5.3.1.2	Experimental viscosity determination	57
5.4	Results and Discussion	57
5.4.0.1	Permeability-viscosity data in the absence of a magnetic field	57
5.4.0.2	Separation performance of SMILMs in the presence of an external magnetic field	58
5.4.0.3	Permeability dependence on magnetic susceptibility	60
5.4.0.4	Influence of the magnetic field on MILs viscosity and CO ₂ permeability of SMILMs	61
5.4.0.5	Permeability-viscosity correlation in the presence of a mag- netic field	61
5.5	Conclusions	63
6	Magnetic modulation of the transport in SMILMs	65
6.1	Summary	65
6.2	Introduction	66
6.3	Experimental	67
6.3.1	Materials and Methods	67
6.3.1.1	Magnetic Ionic Liquids (MILs)	67
6.3.1.2	Model organic Solutes	68

6.3.1.3	Preparation of Supported Magnetic Ionic Liquid Membranes (SMILMs)	69
6.3.1.4	Transport studies	69
6.3.1.5	Analytical methods	70
6.3.1.6	Viscosity Measurements	71
6.4	Results and Discussion	71
6.4.0.1	Transport results	71
6.4.0.2	Viscosity results	76
6.5	Conclusions	79
7	General Conclusions	81
8	Future Work	85
	Bibliography	89
A	Appendix - Supporting Information	99
A.0.1	Theoretical models	99
A.0.1.1	Translational self-diffusion	99
A.0.1.2	Rotations/reorientations	99
A.0.1.3	Cross-relaxation	100
A.0.1.4	Paramagnetic relaxation induced by superparamagnetic particles	100
A.0.1.5	Relaxivity Dispersion	101
A.0.1.6	DMSO/FeCl ₃ and DMSO/[P ₆₆₆₁₄][FeCl ₄]	101

LIST OF FIGURES

1.1	Scheme description of the facilitated transport using a magnetic responsive membrane in the presence and absence of a magnetic field.	4
2.1	Molecular structure of the [Aliquat] cation.	12
2.2	Larmor dependence of the proton spin lattice relaxation rate R_1 for the studied systems: non-magnetic ionic liquid [Aliquat][Cl], a) and MIL [Aliquat][Cl]/[Aliquat][FeCl ₄] 1% (v/v) mixture, b).	14
2.3	Viscosity measured for the [Aliquat][Cl] and [Aliquat][Cl]/[Aliquat][FeCl ₄] systems. The solid line corresponds to the fit using eq. 2.9. Dashed curves correspond to the extrapolated values of viscosity as a function of the magnetic field estimated using also eq. 2.9.	18
2.4	Experimental results and model fitting curves for the two spin-lattice relaxation rates as a function of frequency for the IL systems, as explained in the text.	20
2.5	Viscosity [full and empty black circles] and translational self-diffusion [full and empty black squares] measured for the [Aliquat][Cl] and [Aliquat][Cl]/[Aliquat][FeCl ₄] systems. The patterned squares (red and blue online only) refer to the estimated diffusion values from the model fit of eq. 2.8, as explained in the text. Flat dashed curves correspond to the extrapolated values of viscosity and diffusion as a function of the magnetic field. The dashed-dot curve and the red (online only) patterned circle were obtained using eq. 2.9. The self-diffusion coefficient measured at 7T and 14.1 T were fitted together with the value at zero field obtained from NMRD. The phenomenological magnetic field dependence of α_1 for both [Aliquat][Cl] and [Aliquat][Cl]/[Aliquat][FeCl ₄] are also plotted.	22
3.1	Molecular structure of the [P ₆₆₆₁₄] ⁺ cation. The charge is localized at the phosphorous atom.	29
3.2	Larmor frequency dependence of proton spin lattice relaxation rates for the systems [P ₆₆₆₁₄][Cl] and MIL [P ₆₆₆₁₄][Cl]/[P ₆₆₆₁₄][FeCl ₄] 1% (v/v) mixture: R_{12} , a) and R_{11} , b).	30

3.3	Experimental results and model fitting curves for the two spin-lattice relaxation rates as a function of frequency for the IL systems, as explained in the text.	33
3.4	Experimental results and model fitting curves for the relativity as a function of frequency for the 10mM DMSO/[P ₆₆₆₁₄][FeCl ₄] system, as explained in the text.	35
3.5	Experimental results of the DMSO spin-lattice relaxation as a function of [P ₆₆₆₁₄][FeCl ₄] concentration. Relaxivities were estimated for three selected Larmor frequencies, as explained in the text. The arrow in the inset figure represent the concentration corresponding to the mixture [P ₆₆₆₁₄][Cl]/[P ₆₆₆₁₄][FeCl ₄] studied here.	36
4.1	Normalized viscosity fitted for all the MILs by Orrick-Erbar correlation using <i>Fitteia</i> software.	46
4.2	Experimental and calculated dimensionless MILs viscosity results using Orrick-Erbar correlation.	48
5.1	Experimental setup for CO ₂ separation in the presence of an external magnetic field.	57
5.2	Correlation for CO ₂ permeability versus viscosity.	58
5.3	Upper bound correlation for CO ₂ /N ₂ separation (1 Barrer = 10 ⁻¹⁰ cm ³ (STP)cm ⁻² s ⁻¹ cmHg ⁻¹)	60
5.4	Gas permeability behavior depending on MILs magnetic susceptibility. . . .	61
5.5	CO ₂ permeability ratio (P _(B) /P ₍₀₎) at different magnetic field intensities. . . .	62
5.6	CO ₂ permeability vs.MILs viscosity ratio	63
6.1	Experimental set-up showing the diffusion cell placed between the electromagnet poles during a transport study.	70
6.2	Normalized solute concentration profiles fitted along time in the stripping phase for the α - pinene transport through SMIMLs with immobilized [C ₈ mim][FeCl ₄] and [C ₄ mim][FeCl ₄]	74
6.3	Normalized solute concentration profiles fitted along time in the feed and stripping phases for the ibuprofen transport through SMIMLs with immobilized [C ₁₁ H ₂₁ N ₂ O] ₃ [GdCl ₃ Br ₃]	74
6.4	Ibuprofen normalized accumulation fittings curves along the time for the MIL	75
6.5	Normalized viscosity of pure MILs in the presence and absence of a magnetic field with intensities up to 2.0 Tesla	76
8.1	[Aliquat][FeCl ₄] micelles solution (dark region) in equilibrium with D ₂ O (clear region): a) with magnetic field OFF and b) with magnetic field ON.	87

LIST OF TABLES

2.1	IL physical parameters. The molar concentration of [Aliquat][FeCl ₄] in the [Aliquat][Cl]/[Aliquat][FeCl ₄] mixture is 0.012 mol/L.	12
2.2	Viscosity and diffusion experimental results for the [Aliquat][Cl]/ [Aliquat][FeCl ₄] 1% (v/v) MIL (in parenthesis the values for the [Aliquat][Cl] IL).	15
2.3	Relaxation model parameters obtained for the best fit of eq. 2.8 to the R_1 experimental results for the [Aliquat][Cl] and [Aliquat][Cl]/ [Aliquat][FeCl ₄] 1% (v/v) IL systems, as explained in the text. The follow fitting parameters are common for both IL systems: $\tau_{D_0} = (2.8 \pm 0.2) \times 10^{-9} s$, $d \simeq 7.3 \times 10^{-10} m$, $M \simeq 0.012 mol/L$, $S_1 \simeq 370 \pm 10$, $n = 8 \times 10^{28} spins/m^3$, $p_1 \simeq 2.4$, and $\tau_{v_1} \simeq 7 \times 10^{-10} s$, $p_2 \simeq 1.2$, and $\tau_{v_2} \simeq 9.3 \times 10^{-10} s$, $\omega_1/(2\pi) \simeq 33 MHz$, and $\omega_2/(2\pi) \simeq 18 MHz$. .	19
3.1	Physical parameters of the ionic liquid systems used. The molar concentration of [P ₆₆₆₁₄][FeCl ₄] in the [P ₆₆₆₁₄][Cl]/[P ₆₆₆₁₄][FeCl ₄] mixture is 0.014 mol/L.	29
3.2	Viscosity determined experimentally as a function of applied magnetic field for the [P ₆₆₆₁₄][Cl]/[P ₆₆₆₁₄][FeCl ₄] 1% (v/v) solution (in parenthesis the values for the [P ₆₆₆₁₄][Cl] IL). The viscosity of DMSO/[P ₆₆₆₁₄][FeCl ₄] 1% (v/v) was $\eta_{DMSO} = 2.15 Pa.s$, independent of the applied magnetic field.	31
3.3	Relaxation model parameters obtained for the best fit of eq 3.1 to the R_1 experimental results for the [P ₆₆₆₁₄][Cl] and [P ₆₆₆₁₄][Cl]/[P ₆₆₆₁₄][FeCl ₄] systems. The follow fitting parameters are common for both systems: $\tau_{D_0} = (1.46 \pm 0.06) \times 10^{-8} s$, $d \simeq 7.3 \times 10^{-10} m$, $M \simeq 0.014 mol/L$, $S_1 \simeq 400$, $n = 7 \times 10^{28} spins/m^3$, $p \simeq 1.13$, and $\tau_v \simeq 3.85 \times 10^{-10} s$, $\omega_1/(2\pi) \simeq 33 MHz$, and $\omega_2/(2\pi) \simeq 20 MHz$	34
4.1	Properties of the magnetic ionic liquids	42
4.2	Experimental Viscosities and densities of the MILs at different temperatures	43
4.3	Fitted parameters for the prediction of the density of the studied MILs . . .	44
4.4	Absolute and normalized variables for MILs viscosity and temperature . . .	45
4.5	Group contribution to the dimensionless viscosity	46
4.6	MILs viscosity, dimensionless viscosity Y^* and group contribution descriptors	47
4.7	Group contribution parameters fitted by Orrick-Erbar correlation eq 4.2 for the normalized viscosity and temperature of the MILs	48
4.8	Statistic parameters of the datasheet	49

4.9	Absolute values of the parameters of Orrick-Erbar correlation for viscosity of the MILs	49
4.10	Comparison of the A and B parameters of Orrick-Erbar correlation for different cations of MILs and ILs	50
4.11	Comparison of the A and B parameters of Orrick-Erbar correlation for different anions of MILs and ILs	50
5.1	Main properties of the Magnetic Ionic Liquids (MILs) studied.	56
5.2	Literature data used for the permeability-viscosity correlation shown in Figure 5.2	59
5.3	Gas permeability (P) increase at 1.5 Tesla intensity magnetic field and gas permeability ratio.	60
5.4	MILs viscosity at different magnetic field intensities from 0 to 2 Tesla.	62
5.5	Gas permeability - viscosity product for the different SMILMs studied.	63
6.1	MILs properties	68
6.2	K and P values resulting from the mathematical fittings for the two sets of experiments for α - pinene	75
6.3	K and P values resulting from the mathematical fittings for the ibuprofen	76
6.4	Absolute viscosity results and percentage of reduction under a magnetic field.	77
6.5	Estimation of the D values using the Wilke Chang and Scheibel correlations and solubility values calculated for each MIL and system	78

INTRODUCTION

1.1 Background and Motivation

Membrane separations are attracting a significant attention due to their versatility and potential application in different fields, such as: environment protection, energy, chemical industry, biomedicine, food and pharmaceutical industry. Efficient separation processes require membranes with high permselectivity and high chemical, mechanical and thermal stability [1]. A key property, is the ability of the membrane to control the permeation rate of chemical species. Over the years different strategies have been developed to design new membranes and improve their properties, mainly, their permeability, selectivity and stability, for a high performance in a broad range of fields [2].

Supported Liquid Membranes (SLMs), based processes have turned out to be an alternative technique to conventional membrane processes for the separation and isolation of many different compounds in dilute streams [3, 4, 5, 6, 7]. SLMs offer the possibility of achieving high separation factors, while allowing for a one step mass transfer using small amounts of carrier (internal liquid phase). However, the main limitation of this kind of membrane system is its low stability [8], which is due to volatilization and solubilization of the carrier and loss into the adjacent phases during the process. This behavior impacts in the membrane fluxes, permeability and selectivity, reducing the efficiency of these membrane systems, limiting their implementation in large scale processes [7].

Different procedures have been followed and suggested as an attempt to circumvent short-term membrane performances and enhance the mass transport: incorporation of high stable liquid phases in supported liquid membranes [9], use of more suitable control of processing conditions and new membrane surface modification strategies [10, 11]. Among them, membrane functionalization using stimuli-responsive materials [12, 13] is one promising approach for the improvement of selectivity and permeability.

The functionalization of materials with reversibly switchable physicochemical properties allows for the development of stimuli-responsive membranes capable to adjust their properties to an external stimuli: temperature, pH, solution ionic strength, light, electric and magnetic fields. An interesting fact that could be translated in an advantage is that reversible changes may occur locally at a fast rate and with high selectivity. Some strategies have been adopted to develop responsive membranes, according to their nature, and with the type of the stimulus applied. Porous membranes are usually made stimuli responsive, by grafting responsive polymer layers from the membrane external surface and the pore walls. Non-porous membranes are generally made responsive by incorporating stimuli-responsive groups in the bulk of the membrane material. Stimuli-responsive membranes characteristics are based on changes of conformation, polarity, solubility and reactivity of the responsive materials, leading to reversible changes in the permeability and selectivity of the membranes, influencing their ability to bind and release a target compound. Modified responsive polymers have been used in many systems and devices that require reversibly switchable material properties [14].

Magnetic responsive materials/particles have been studied due to their promising unique features under an applied external magnetic field [15, 16, 17, 18]. Among the responsive materials, Magnetic Ionic Liquids, MILs [19, 20, 21], are a specific class of Ionic Liquids, ILs, which due to the presence of a paramagnetic component are able to respond to the magnetic field, by changing their physicochemical properties. ILs, have been recognized as an alternative to classic organic solvents, due to their unique properties. These liquids are salt-like materials, usually composed by a large asymmetric organic cation and an inorganic or organic anion. They present advantageous characteristics such as, extremely low volatility, good thermal stability and capacity over a wide range of temperatures 300-400 °C, good electric and ionic conductivity, have a reduced solubility in various solvents, being non-flammable and reusable [22]. Moreover, ILs are versatile solvents, which can be designed in order to meet the desirable characteristics by simple combination of suitable cations and anions along their synthesis. All these properties have motivated the selection of ILs as main components in different applications, namely as selective separation media. In this way, they are regarded as alternative liquid carriers, which may integrate the structure of SLM, conferring them improved stability, thus eliminating the problems of the solvent displacement by the evaporation that typically occur in these membranes [22, 23, 24].

MILs have been recently applied in different areas, including, fluid-fluid separation, extraction processes, catalytic reactions, polymer chemistry, electrochemical and medical devices [25]. A variety of MILs under study, showed the influence of the magnetic field on their properties (e.g. solubility in gas and liquid medium) [19, 20, 21]. A mixture of MIL and water under magnetic field conditions, demonstrated an increase of the MIL solubility in water, in comparison with no magnetic field applied [19]. Moreover, the benzene solubility increases in a MIL when applying a rotational magnetic field [21]. These evidences motivated the present work for studying the modulation of MILs physicochemical

properties under a magnetic stimuli, with a potential impact of their magnetic behavior on the transport of solutes through SLMs.

The recovery or removal of a specific compound or contaminant, from a liquid or gas stream, are important challenges in membrane technology, since it requires high separation selectivity. SLMs have been designed with this purpose, namely for separation/capture of CO₂ and the recovery of added value compounds [26].

The different environmental problems posed by the high and prejudicial CO₂ emissions and consequent amplification of greenhouse effect, have been discussed over the years, in order to define solutions that may allow for an improved CO₂ capture from gases mixtures with minimal impact to the economic feasibility of the processes. The environmental problems involving CO₂, due to the high and prejudicial emission, since CO₂ acts as a trap for UVs rays, have been discussed over the years, in order to improve the efficiency to capture and separate the CO₂ from gas mixtures and reduce the costs associated with this process [27, 28, 29, 30]. The processes used for the capture of CO₂ include: absorption, adsorption, cryogenic separation and membrane processes. Membranes for gas separation, have been widely investigated in order to define an alternative solution to absorption, adsorption cryogenic separation, with improved CO₂ removal capacity. Ideal membrane systems should exhibit high permeability and selectivity to CO₂. Also they should present enhanced chemical, mechanical and thermal stability at high temperatures and pressures. In this respect, SLMs, have been intensive explored due to the high diffusivity and solubility of gases through them, leading to higher permeability values, when compared with dense membranes.

As for gas streams, the membranes systems using SLMs are intensively applied for separation, purification and recovery of added value compounds contained in liquid streams obtained from: metal ions from wastewater, amines in rainwater, sugars, amino acids from aqueous solution, and some drugs from body fluid samples [3, 4, 5, 6, 7]. The development of these membranes requires an enhancement of their permeability and selectivity, through the selection of the suitable carrier used for a task specific application.

This PhD project aims at developing Supported Magnetic Ionic Liquid Membranes (SMILMs) with tunable permeability and selectivity, profiting from the unique properties of MILs. The design of SMILMs with good performance requires to understand the impact of magnetic field on the MILs physicochemical properties, since they are expected to rule the magnetic responsive ability of the SMILMs. Thus, the first objective of the work is focused on the characterization of the physicochemical properties (solubility, rheological behavior, solvation capacity) and structural characteristics of the MILs, and how they are influenced by an uniform magnetic field. The magnetic influence on the ability of the MILs to change reversibly their properties may be accessed through the establishment of relationships between the structural characteristics of MILs and their physicochemical properties (e.g. viscosity, solubility and self-diffusion). The second major objective is the evaluation of the potential impact of MILs magnetic response on the transport solutes through magnetic responsive membranes. These membranes are expected to allow for

an *in situ* dynamic control of solute transport as described in Figure 1.1, contributing to the enhancement of the separation processes efficiency under a magnetic field. The evaluation of membrane performance is based on SMILMs descriptors, such as: membrane permeability and selectivity.

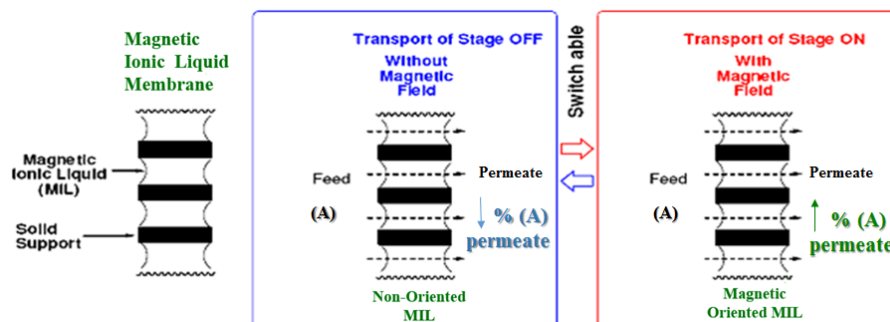


Figure 1.1: Scheme description of the facilitated transport using a magnetic responsive membrane in the presence and absence of a magnetic field.

1.2 Research strategy

The work was carried out to evaluate the impact of an external magnetic field on the intrinsic physicochemical and structural properties of MILs used as carriers, for the development of SLMs with modulated transport properties.

The MILs [Aliquat][FeCl₄], [P₆₆₆₁₄][FeCl₄], [P₆₆₆₁₄]₂[CoCl₄], [P₆₆₆₁₄]₂[MnCl₄], [P₆₆₆₁₄]₃[GdCl₆], [C₄mim][FeCl₄], [C₈mim][FeCl₄] and [C₁₁H₂₁N₂O]₃[GdCl₃Br₃] composed by paramagnetic anions with different magnetic susceptibility, like, [FeCl₄]⁻, [GdCl₆]³⁻, [CoCl₄]²⁻ and [MnCl₄]²⁻ and comprising cations with different alkyl chains, such as quaternary ammonium – [Aliquat]⁺, phosphonium – [P₆₆₆₁₄]⁺ and imidazoliums – [C_{*n*}mim]⁺ were studied.

Characterization studies of the physicochemical properties of the MILs were conducted in order to evaluate the ability to modulate intrinsic properties - viscosity and molecular dynamics of the MILs when a magnetic stimulus is applied. Uniform magnetic field was applied at intensities up to 2.5 T, using an electromagnet (GMW electromagnet 3473-70, GMW Associates, USA). The influence of the magnetic field on the molecular dynamics of MILs was investigated through ¹H-NMR – proton nuclear magnetic resonance relaxometry analysis. Based on the detection of proton mobility, this technique provided information about the diffusion mechanisms which are related with the structure, motion and orientation of the MILs molecules under magnetic field. The ¹H-NMR relaxation technique is described by the energy that is exchanged between the proton spins of the hydrogen nuclei and the energy exchanged between the spin system and the surrounding lattice [31]. The energy exchanged can be described by two different relaxation times:

spin-lattice relaxation time: T_1 (exchange energy between spins of protons and the environment) and spin-spin relaxation time: T_2 (exchange energy between the spins of the protons in the system). These relaxation times are obtained after the application of the magnetic field by a radiofrequency irradiation in the sample, being the spins of the protons polarized. Returning the spins system to the equilibrium, $^1\text{H-NMR}$ electrical signals are detected and the relaxation times are measured. The relaxation values of T_1 were the main focus of this study, depending on the temperature, diffusion constant, intermolecular distance and concentration of the magnetic anion.

The strategy adopted to follow this study involved the selection of two different magnetic ionic liquids systems, each one composed by the MIL and its non-magnetic analogue. The model MILs were composed by the same anion, $[\text{FeCl}_4]^-$, but different cations having different alkyl chains with distinct lengths: $[\text{Aliquat}]^+$ and $[\text{P}_{66614}]^+$. Their relaxation behavior and the impact on the self-diffusion of the two MIL systems over a wide range of frequencies was determined and compared to the proton relaxation profiles obtained for a pure solution of the non-magnetic ionic liquid. Furthermore, this technique allows at inferring about the ability of MILs to undergo fast and reversible switch of their intrinsic physical properties and consequently their capacity to promote modulated separation processes. Magnetic induced molecular dynamics of the MILs were correlated to the magnetic dependence exhibited by some intrinsic physicochemical properties of MILs, such as viscosity and self-diffusion. It was used a modified Stokes-Einstein equation to relate the viscosity and diffusion [32, 33].

After concluding about the impact of the magnetic field on the MILs behavior, the second objective of this thesis was the development and characterization of new magnetic membranes: supported magnetic ionic liquid membranes – SMILMs. The main objective was to develop magnetic responsive membranes with high stability, able to switch their permeability to specific solutes and membrane selectivity through a fine tuning of the magnetic field conditions. Supported liquid membranes were prepared by immobilization of MILs in the porous structure of a polymeric membrane, following an adequate methodology which lead to an efficient pore filling and good membrane stability. Different transport case-studies were performed in gas and liquid media, using a diffusion cell under different magnetic conditions. Transport studies in gas and liquid phases were performed in the absence and presence of an external magnetic field. The performance of SMILMs was evaluated taking into account the membrane permeability to target solutes, separation selectivity and membrane stability as performance descriptors.

The impact of magnetic field on gas permeation was tested using three different gas streams: CO_2 , N_2 and air. Transport studies in liquid phase were also conducted. In this case, α -pinene, an apolar compound, and ibuprofen, with amphiphilic character were selected as model compounds. The influence of the magnetic field on the permeability of these compounds contained in organic feed solutions through SMILMs was evaluated.

1.3 Thesis Outline

The present work is divided into eight chapters. Chapters 2, 3 and 4 describe the studies dedicated to the physicochemical and structural characterization of the magnetic ionic liquids under controlled magnetic field conditions, developed along the first part of the PhD work.

Chapter 5 and 6 include the work developed in the second part of this thesis, about the design and characterization of supported magnetic ionic liquid membranes incorporating MILs as the liquid carrier. In particular, these chapters include studies which aimed to understand the ability to modulate the permeability of different model solutes contained in gas and liquid feed streams by adjustment of the magnetic field.

Chapter 5 is related with gas transport studies and Chapter 6 is dedicated to solute transport in liquid phase. Each chapter defines clearly the objectives, starting with the state of the art and motivation, followed by a detailed description of the experimental methods used, with a specific analysis and interpretation of the results and the respective conclusions. This PhD work has led, so far to the publication of four scientific papers, referred in the ISI Web of Science which include the work described in the Chapters 2, 3, 4 and 5 and one additional paper submitted, containing the work presented in Chapter 6.

Chapter 1 presents the background, the motivation and the strategy used to accomplish the main goals of this thesis.

Chapter 2 and 3 include the description of the ^1H -NMR relaxometry technique used to characterize the self-diffusion mechanism of the MILs under magnetic field, with a molecular interpretation of their behavior when distinct magnetic stimuli are applied. It was explored the molecular dynamics of the MILs through the study of a relaxation model with different contributions to explain the magnetic behavior, the translation and rotation mechanisms and the self-diffusion contribution. This molecular interpretation was related with the rheological behavior of the MILs, trying to obtain an explanation of the response of MILs under the magnetic field.

Following the viscosity study of MILs, Chapter 4 is focused on the application of a model based on the group contribution method in order to estimate the contribution of the cationic and anionic counter-parts in MILs viscosity at different temperatures. This study was developed using four different MILs containing distinct magnetic anions and the same phosphonium cation. The chance of modeling the physicochemical properties of MILs represents an advantage to the design of new MILs since it allows an a priori selection of the most suitable combination of cations and anions, leading MILs with the desired properties.

Chapter 5 and 6 describe the work about the development and the characterization of the magnetic responsive supported liquid membranes and evaluate the possibility to modulate the transport of solutes using these membranes. Chapter 5 is dedicated to gas permeation studies using CO_2 , N_2 and air as model gas streams whereas Chapter 6 is focused on the transport of α -pinene and ibuprofen between organic liquid solutions.

Chapter 7, includes an overview of the main conclusions of the work. Chapter 8 describes suggestions of future work aiming at gathering additional studies which may bring complementary information about the magnetic characterization of MILs. New challenges concerning different uses of MILs as responsive materials are identified and illustrated by a brief description of the results obtained in studies developed to conclude about the potential use of MILs as magnetic surfactants/micelles.

¹H-NMR RELAXOMETRY, VISCOMETRY, AND PFG NMR STUDIES OF MILS AND ILs

Published as: Carla I. Daniel, Fabián Vaca Chávez, Gabriel Feio, Carla A.M. Portugal, João G. Crespo, Pedro J. Sebastião “¹H-NMR Relaxometry, Viscometry, and PFG NMR Studies of Magnetic and Non-magnetic Ionic Liquids”, Journal of Physical Chemistry B, 117 (2013) 11877–11884.

2.1 Summary

A study is presented of the molecular dynamics and of the viscosity in pure [Aliquat][Cl] ionic liquid and in a mixture of [Aliquat][Cl] with 1% (v/v) of [Aliquat][FeCl₄]. The ¹H spin-lattice relaxation rate, R_1 , was measured by NMR relaxometry between 8 kHz and 300 MHz. In addition, the translation self-diffusion, D , was measured by pulse field gradient NMR. The ILs' viscosity was measured as a function of an applied magnetic field, B , and it was found that IL mixture's viscosity decreased with increasing B , whereas the [Aliquat][Cl] viscosity is independent of B . All experimental results were analyzed taking into account the viscosity's magnetic field dependence, assuming a modified Stokes-Einstein diffusion/viscosity relation.

The main difference between the relaxation mechanisms responsible for R_1 in the two IL systems is related with the additional paramagnetic relaxation contribution associated to the ¹H spins – [FeCl₄] paramagnetic moments' interactions. Cross-relaxation cusps in the R_1 dispersion, associated with ³⁵Cl and ¹H nuclear spins in the IL systems, were detected. The R_1 model considered was successfully fitted to the experimental results and it was possible to estimate the value of D at zero field in the case of the IL mixture which was consistent with the values of D measured at 7 Tesla and 14.1 T and with the magnetic field dependence estimated from the viscosity measurements. It was observed that a small concentration of [Aliquat][FeCl₄] in the [Aliquat][Cl] was enough to produce

a "super-paramagnetic"-like effect and to change the IL mixture's molecular dynamics and viscosity and to allow for their control with an external magnetic field.

2.2 Introduction

Ionic Liquids (ILs) belong to a class of liquids comprised by ions, recognized as novel solvents. The ILs are liquid salts over a wide range of temperatures, usually lower than 100 °C. In particular, those that are liquids at room temperature are designated Room Temperature Ionic Liquids (RTILs). ILs have extreme low volatility and are thermal stable, non-flammable and reusable. They have gained interest for various applications in separation, electrochemistry, material science as well as in organic synthesis and catalysis, and it is expected that they can contribute to reduce or eliminate the hazards associated with the use of organic solvents. Depending on the application, ILs can be composed by different cation – anion combinations, and for this reason are called by "designer solvents" [22].

A new class of magnetic sensitive ionic liquids – magnetic ionic liquids (MILs) has been recently synthesized and have gained interest due to their strong response to external magnetic fields [19, 34, 35]. MILs are ionic liquids comprised by metal anion complexes having physical properties such as: solubility, viscosity, surface tension and/or molecular orientation that may be influenced by applied magnetic fields [19, 20, 34, 35]. Actually, the magnetic field influence on the IL solubility was confirmed by the dependence found between the concentration of MILs in binary water mixtures and the applied magnetic field strength [19]. The potential applications of MILs that have been presented recently include the development of magnetic fluids based on nanoparticles, the use of MILs in transport and separation of different solutes, in catalysis, in extraction processes, and in electrochromic devices [21, 36, 37, 38, 39, 40, 41].

The dependence between the magnetic field intensity and molecular orientation of MILs also suggests that the magnetic field can be used to control the distribution of charge density, solubility or capacity to solvate different chemical species within the ILs, causing a significant impact in the solute transport through the IL media. For this, it is important to acquire a better comprehension about the influence of the magnetic field on the MILs magnetic behavior and how it should be tuned in order to get the adequate MILs properties. Since the macroscopic properties of MILs are related with the microscopic structure it is expected that the local magnetic structures play a key role in the MILs response to magnetic fields [20].

The viscosity, η , which is larger in ILs than that of most common organic solvents, is one of the most important macroscopic properties of these materials. The ILs viscosity depends essentially on the nature and combinations of cations and anions comprising ILs structure. Since the viscosity is directly related with the relative diffusion of ionic species comprising ILs network, self-diffusion, it is important to study the dependence

of both physical properties with the magnetic field and to get a better knowledge about their mutual relation in order to understand and optimize these systems for applications.

Nuclear Magnetic Resonance (NMR) is a well known experimental technique used to study the molecular order and dynamics in different materials. In particular, the self-diffusion coefficient, D , can be measured directly by pulse field-gradient (PFG) NMR methods [31].

It was reported that for ionic liquids the viscosity and translational self-diffusion relationship given by the Stokes-Einstein expression for conventional fluids is still valid provided some corrections to the original expression are considered [32]. In particular, molecular polar interactions also determine the D vs. η dependence [33].

In view of the fact that in MILs, the viscosity and the intrinsic diffusion of their ionic component species can be affected by external magnetic fields, a coherent estimate of both parameters requires the use of different experimental techniques to independently access each one of them. In fact, viscosity measurements using classical capillary viscometers can be made in the presence of magnetic fields up to 2 Tesla, however, D is mostly measured directly by PFG NMR at much higher magnetic fields. Therefore, the D vs. η dependence for the same magnetic field requires the estimation of D at low magnetic fields. As the spin-lattice relaxation time is sensitive to molecular motions, by using ^1H NMR relaxometry it is possible not only to characterize the system from the molecular motions point of view but also to obtain the value of D at low magnetic fields.

The aim of this work is to study the influence of external magnetic fields on the molecular dynamics and on the viscosity of [Aliquat][Cl] and on a mixture [Aliquat][Cl]/[Aliquat][FeCl₄]. Viscosity measurements as a function of the magnetic field and proton spin-lattice relaxation measurements for the frequency range 10 kHz - 300MHz (^1H -NMRD) were complemented by direct measurements of the self-diffusion coefficient by PFG NMR at magnetic fields of 7 Tesla and 14.1 T.

2.3 Experimental

2.3.1 Materials

The ILs selected for this study were the non-magnetic [Aliquat][Cl] and its magnetic analogue [Aliquat][FeCl₄], where the [Cl] anions are substituted by iron anions [FeCl₄]. The IL and MIL were synthesized at the Faculdade de Farmácia, Universidade de Lisboa, according to the experimental procedure reported in literature [36, 39]. Their molecular weight, density, water content and concentration of magnetic particles, at room temperature, are listed in Table 2.1. The ILs density was determined gravimetrically with a pycnometer, the water content was measured by thermogravimetry, and the concentration of magnetic particles by Inductively coupled plasma (ICP). Two samples were prepared: a sample of [Aliquat][Cl] and a mixture of [Aliquat][Cl]/[Aliquat][FeCl₄] 1% (v/v). The molecular structure of the Aliquat cation is presented in the Figure 2.1.

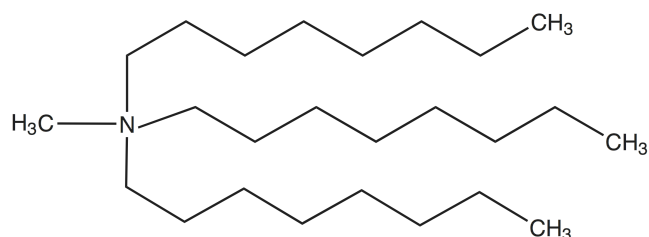


Figure 2.1: Molecular structure of the [Aliquat] cation.

Table 2.1: IL physical parameters. The molar concentration of [Aliquat][FeCl₄] in the [Aliquat][Cl]/[Aliquat][FeCl₄] mixture is 0.012 mol/L.

IL	Molecular Weight (g mol ⁻¹)	Density (g cm ⁻³)	Water Content (% wt)
[Aliquat][Cl]	404.16	0.88	5.8
[Aliquat][Cl]/ [Aliquat][FeCl ₄]	405.8	1.03	5.5

2.3.2 Methods

2.3.2.1 Viscosity measurements

The viscosity of the two IL systems was measured by capillary viscometry following the procedure reported in the literature [42]. The capillar used was manufactured and calibrated by Cannon – Instrument Company. The influence of an external magnetic field on the MIL viscosity was evaluated using a glass capillary viscometer Ubbelohde Viscometer – 3C and a GMW Dipole Electromagnet 3473-70 with a 75 mm poles gap by GMW Associates, USA.

The measurements were carried out with a capillar viscometer placed between the electromagnet poles. The viscosity was measured for magnetic fields between 0 and 2 Tesla. In order to decrease the experimental uncertainty, averages of six measurements were obtained with deviations from the mean smaller than $\pm 0.2\%$ at a room temperature of 22 °C.

2.3.2.2 Nuclear Magnetic Resonance

The proton spin-lattice relaxation rate, $R_1 (\equiv 1/T_1)$, was measured as a function of the Larmor frequency, $\nu_L = \gamma B / (2\pi)$, on the range 10 kHz to 300 MHz, using three different NMR equipments. In the range 10 kHz – 8.9 MHz the data were obtained with a home developed fast field-cycling (FFC) spectrometer [43] operating with a polarization and detection fields of 0.215 T and a switching time less than 3 ms. Between 10 and 91 MHz a variable-field iron-core magnet equipped with a Bruker Avance II console was used. Bruker Avance II spectrometers were used for the self-diffusion and spin-lattice

relaxation measurements at 300 MHz. For frequencies above 10MHz R_1 was measured using the inversion recovery $((\pi)_x - \tau - (\frac{\pi}{2})_{x,-x} - \text{Acq})$ sequence. All R_1 measurements were performed at 22 °C and the experimental error for the each R_1 was $\pm 10\%$.

The diffusion coefficient, D , was measured using the stimulated spin-echo sequence [44] and a Bruker Diff 30 gradient unit at 7 T and a Bruker TCI CryoProbe at 14.1 T. D was obtained from the echo decay according to

$$I = I_o \exp[-\gamma^2 g^2 \delta^2 D(\Delta - \frac{\delta}{3})] \quad (2.1)$$

where γ is the ^1H gyromagnetic ratio, g is the gradient strength, δ is the gradient length, and Δ is the delay between the gradients experiment. The values $\delta = 2$ ms and $\Delta = 50$ ms for the measurements at 7 T and $\delta = 6$ ms and $\Delta = 500$ ms in the case of 14.1 T were used.

2.4 Results

The ^1H -NMR relaxometry results are represented in the Figure 2.2 for the two IL systems. Obviously the ^1H NMR signal comes only from the cations since the anions do not contain protons. The proton spin-lattice relaxation rate is presented, in a log-log scale, as a function of the Larmor frequency in the range 10 kHz – 300 MHz.

For both samples, a bi-exponential decay of the time recovery of the longitudinal magnetization was observed, with two relaxation rates $R_{11} \equiv T_{11}^{-1}$ and $R_{12} \equiv T_{12}^{-1}$, in the whole frequency range. The two relaxation rates, R_{11} and R_{12} were attributed to the CH_3 and CH_2 groups in the aliphatic chains, respectively. This assumption is reasonable in view of the fact that the interdigitation of aliphatic chains of different [Aliquat] cations might reduce significantly the mobility of the ethyl groups in comparison with the terminal methyl groups. The weighting factor for each component was fixed depending on the corresponding number of protons.

In the case of the [Aliquat][Cl], the two relaxation rates are very close at high frequencies and quite different at low frequencies. In view of the log-log scale used to represent the data in Figure 2.2a) it is clear that R_{11} is not simply proportional to R_{12} , but is the result of a different combination of relaxation contributions. In Figure 2.2a), an enhancement on the proton relaxation rate can be also observed at frequencies around 20 and 30 MHz. This behavior was consistently observed for both IL systems and can not be associated with an increased scattering of data at these frequencies. In fact, it can be interpreted in terms of a cross-relaxation process between the ^1H and the ^{35}Cl spins systems [45].

In the case of the [Aliquat][Cl]/[Aliquat][FeCl_4] system it is clear that for frequencies above 9 MHz the increase of R_1 with frequency is more pronounced than that observed for the [Aliquat][Cl] IL, meaning that, for this system, the spin-lattice relaxation is affected by additional relaxation mechanisms. The broad frequency peak observed in the relaxation rate (see Figure 2.2b) is similar to the ones reported for systems of aqueous

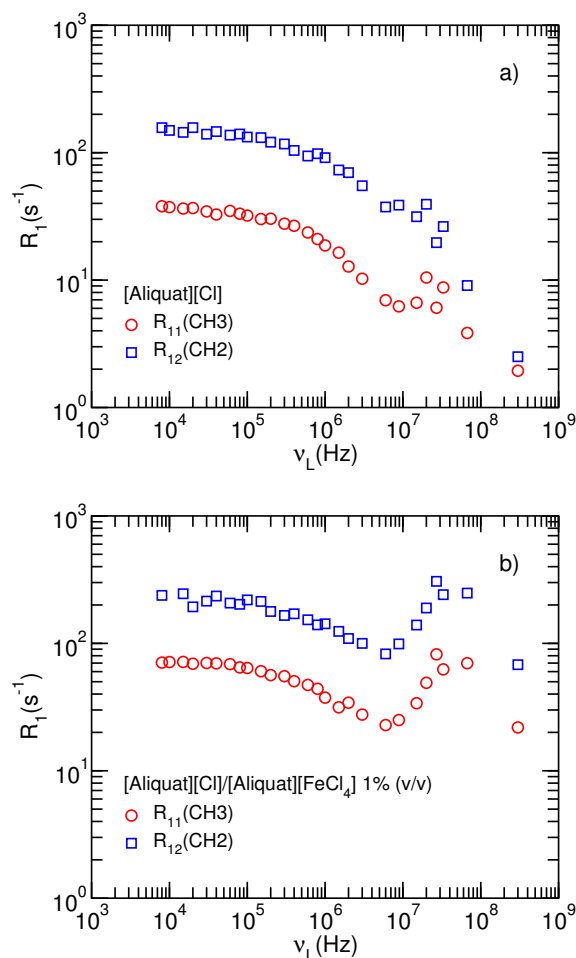


Figure 2.2: Larmor dependence of the proton spin lattice relaxation rate R_1 for the studied systems: non-magnetic ionic liquid [Aliquat][Cl], a) and MIL [Aliquat][Cl]/[Aliquat][FeCl₄] 1% (v/v) mixture, b).

colloidal suspensions of super-paramagnetic particles. In systems of this type, the relaxation is induced by the local magnetic field gradient associated with the presence of the paramagnetic species and is called Curie relaxation [46]. This relaxation process becomes quite important in the high frequency range. The relaxation profiles presented here for the magnetic ionic liquid are consistent with those reported by *Roch et al.* in a suspension of magnetic particles [47].

The additional increase of R_1 at specific Larmor frequencies in the range 20–30 MHz is also observed in the MIL system.

In Table 2.2 are presented the values measured for the viscosity, η , and the diffusion coefficients for the two IL systems. For sake of simplicity, the values for the [Aliquat][Cl] are presented in parentheses. Due to experimental constraints it was not possible to measure the viscosity for magnetic fields above 2 T. In addition, it was not possible to measure the diffusion coefficient magnetic fields below 7 T. It is interesting to note that η decreases with increasing magnetic field for the MIL system. As expected the viscosity of

[Aliquat][Cl] does not change with the applied magnetic field. The viscosities of both IL systems at the earth magnetic field are similar.

Table 2.2: Viscosity and diffusion experimental results for the [Aliquat][Cl]/[Aliquat][FeCl₄] 1% (v/v) MIL (in parenthesis the values for the [Aliquat][Cl] IL).

B(T)	η (Pa.s)	D ($10^{-12}m^2s^{-1}$)
$\sim 45 \times 10^{-6}$	1.26 (1.33)	–
0.47	1.24 (1.33)	–
1	1.22 (1.33)	–
1.3	1.20 (1.33)	–
1.8	1.17 (1.33)	–
7	–	3.0 (1.3)
14.1	–	4.7

2.5 Analysis and discussion

It is known that the frequency dependence of the proton nuclear magnetic spin-lattice relaxation rate is related with different molecular dynamic processes, such as rotational and translational diffusional mechanisms in isotropic fluids, and also with slow molecular motions in the case of mesomorphic materials [48, 49, 50]. In the case of isotropic fluids, rotations/reorientations of the molecules and translational self-diffusion are the motions that effectively modulate the dipolar spin interactions in the frequency range accessible by NMR. In particular, translational diffusion can become more important than molecular rotations/reorientations in the case of viscous fluids. In this case, the correlation times of the translational diffusion processes become larger than the correlation times of the rotational motions. This difference can be noticed in the R_1 dispersion, since at high frequencies R_1 is influenced more by the faster motions and at low frequencies R_1 is more sensitive to slow motions.

The ¹H-NMR R_1 dispersions observed for the studied IL systems are dominated mainly by the relaxation mechanisms associated with the motions of the protonated cations, rotations/reorientations and translational diffusion. Due to the presence of Cl in the IL anions, cross relaxation between ¹H and ³⁵Cl might also be detected. In the case of magnetic ionic liquid the [FeCl₄][–] anions might influence the proton spin-lattice relaxation through the coupling between the ¹H nuclear spin moment and the paramagnetic anions' magnetic moment. A contribution associated with this specific relaxation processes was detected in the high frequency range, as it was observed for aqueous colloidal suspensions of paramagnetic particles [47].

2.5.1 Theoretical models

2.5.1.1 Translational self-diffusion

In the case of isotropic liquids or isotropic phases of liquid crystal compounds, the contribution of translational self-diffusion (SD) to the relaxation can be expressed by the Torrey's model [51] with:

$$\left(\frac{1}{T_1}\right)_{\text{SD}} = C_d \frac{n\tau_D}{d^3} [T(\omega\tau_D) + 4T(2\omega\tau_D)], \quad (2.2)$$

where $\omega = 2\pi\nu_L$, $C_d = (1/2)(3\mu_0\gamma^2\hbar/(8\pi))^2$ is the strength of the dipolar interaction and $T(\omega\tau_D)$ is a dimensionless analytical function that depends on the average time between diffusion jumps τ_D , the mean-square jump distance $\langle r^2 \rangle$, and the molecular width d . τ_D is related with the self-diffusion constant D by the relation $\langle r^2 \rangle = 6\tau_D D$. n is the density of ^1H spins.

2.5.1.2 Rotations/reorientations

Molecular rotations/reorientations (Rot) may be characterized by one or more correlation times according to the number of independent rotational axes considered to describe this motion. Usually, rotations along the molecular long axis and rotations/reorientations along a molecular transverse axis have different correlations times and the most simple model used to describe this relaxation process is given a $\text{Rot}_1 + \text{Rot}_2$, where Rot_i is given by the Bloemberger, Purcel and Pound (BPP) relaxation model:

$$\left(\frac{1}{T_1}\right)_{\text{Rot}_i} = A_{\text{Rot}_i} \left[\frac{\tau_{\text{Rot}_i}}{1 + \omega^2\tau_{\text{Rot}_i}^2} + \frac{4\tau_{\text{Rot}_i}}{1 + 4\omega^2\tau_{\text{Rot}_i}^2} \right] \quad (2.3)$$

with $A_{\text{Rot}_i} = 9\mu_0^2\gamma^4\hbar^2/(128\pi^2r_{i_{\text{eff}}}^6)$ where $r_{i_{\text{eff}}}$ is an effective inter-spin distance [52] and τ_{Rot_i} is the correlation time related with the rotations/reorientations.

2.5.1.3 Cross-relaxation

^{35}Cl has nuclear spin 3/2 and cross-relaxation CR between the proton spins and ^{35}Cl nuclear spins can occur. Cross-relaxation has indeed been observed between proton spins and nitrogen and also between proton spins and ^{35}Cl spins [45, 53, 54]. Cross-relaxation may become significant when the proton's Larmor frequency is close to each one of the quadrupole frequencies of the other nucleus. The relaxation rate can be expressed by [53]

$$\left(\frac{1}{T_1}\right)_{\text{CR}_i} = A_{\text{CR}_i} \frac{\tau_{\text{CR}_i}}{1 + (\omega - \omega_i)^2\tau_{\text{CR}_i}^2} \quad (2.4)$$

where ω_i , with $i = 1, 2, \dots$, are the frequencies that correspond to the ^{35}Cl spin energy levels and A_{CR_i} are parameters related with the strength of the interaction and τ_{CR_i} is the correlation time of the cross relaxation contribution at different frequencies.

2.5.1.4 Paramagnetic relaxation

Proton spin-lattice relaxation can be affected by the presence of magnetic ions in two ways: i) the so-called *inner-sphere* relaxation, which occurs when relaxing protons bind temporarily to ions or ion complexes, and ii) the *outer-sphere* relaxation, which applies to protons that do not bind but move or diffuse close to magnetic ions or particles [55]. This paramagnetic relaxation PM mechanism is here described using the outer-sphere approach whose relaxation equation is:

$$\left(\frac{1}{T_1}\right)_{PM} = 6\tau_d c \left\{ S_c^2 j_1(\omega, \tau_d, \tau_s \rightarrow \infty) + \left[S_1(S_1 + 1) - S_c \cotg \frac{x}{2S_1} - S_c^2 \right] j_1(\omega, \tau_d, \tau_s) \right\} \quad (2.5)$$

where S_1 is the electronic spin along the applied magnetic field and c is a quantity proportional to the molar concentration of magnetized particles, [M]. r is the distance of closest approach between the anion and the protonated cation, $\tau_d = \langle r^2 \rangle / D$, D is the diffusion time constant, τ_s is the longitudinal electronic relaxation time and ω is the proton Larmor frequency. S_c is given by

$$S_c = \frac{2S_1 + 1}{2} \tanh^{-1} \left((2S_1 + 1) \frac{\omega}{\omega_r} \right) - \frac{1}{2} \tanh^{-1} \left(\frac{\omega}{\omega_r} \right) \quad (2.6)$$

where $\omega_r = 2\gamma kT / (\hbar \gamma_S)$ and γ_S is the electron's gyromagnetic ratio. The corresponding spectral density for outer-sphere relaxation is [55]

$$j_1(\omega, \tau_d, \tau_s) = \text{Re} \left\{ \frac{1 + \Omega^{1/2}/4}{1 + \Omega^{1/2} + 4\Omega/9 + \Omega^{3/2}/9} \right\} \quad (2.7)$$

where $\Omega = (i\omega + 1/\tau_s)\tau_d$.

2.5.2 Model fits to the experimental results

The model used to analyze the R_1 experimental results can be expressed by a sum of different contributions: rotations/reorientation, self-diffusion, cross-relaxation, and paramagnetic relaxation, depending on the IL system:

$$R_1(\nu_L) = R_1^{SD}(\nu_L) + \left[R_1^{\text{Rot}_1}(\nu_L) + R_1^{\text{Rot}_2}(\nu_L) \right] + R_1^{\text{CR}}(\nu_L) + \left[R_1^{\text{PM}}(\nu_L) \right]_{\text{MIL}} \quad (2.8)$$

This model assumes that the relaxation mechanisms are statistically independent, as is often the case [48, 49]. When fitting eq. 2.8 to the experimental results it was considered that $M \simeq 1.2 \times 10^{-2}$ mol/L, estimated by ICP and $n \simeq 8 \times 10^{28}$ spins/m³, estimated from the values of Table 2.1. d , τ_D , r , τ_d , τ_s , τ_1, τ_2 , $A_{\text{Rot}_1}, A_{\text{Rot}_2}$, and a pair of $\tau_{\text{CR}_i}, A_{\text{CR}_i}$ for each cross-relaxation cusp in the R_1 dispersion, were considered free fitting parameters.

Since for the [Aliquat][Cl]/[Aliquat][FeCl₄] system the viscosity depends on the magnetic field, as observed in Table 2.2, the diffusion coefficient is expect to be also field

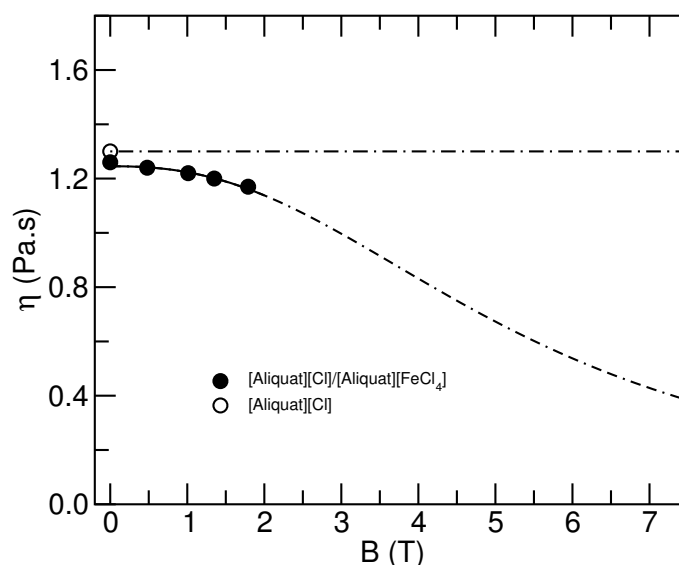


Figure 2.3: Viscosity measured for the [Aliquat][Cl] and [Aliquat][Cl]/ [Aliquat][FeCl₄] systems. The solid line corresponds to the fit using eq. 2.9. Dashed curves correspond to the extrapolated values of viscosity as a function of the magnetic field estimated using also eq. 2.9.

dependent. Therefore, $\tau_d = \langle r^2 \rangle / (D)$ is also field dependent. In order to include this field dependence on the theoretical R_1 model, it is convenient to have an analytical interpolating equation.

In Figure 2.3 are presented the viscosity values of Table 2.2 as a function of the magnetic field for the two ILS. η is independent of the B in the case of [Aliquat][Cl]. In view of the field dependence of η for the [Aliquat][Cl]/[Aliquat][FeCl₄] system, the empirical model

$$\eta = \frac{\eta_0}{1 + (\gamma B \tau_{v_1})^{p_1}} \quad (2.9)$$

was considered to fit the available experimental results. η_0 is the viscosity at zero field and τ_{v_1} and p_1 are the parameters that explained the decay of viscosity with B . Values of $\eta_0 = 1.26 \text{ Pa.s}$, $\tau_{v_1} \simeq 7 \times 10^{-10} \text{ s}$, and $p_1 \simeq 2.4$ were determined.

The viscosity and self-diffusion coefficients are commonly related by the Stokes-Einstein equation. In the case of ionic liquids, it was found that this equation can be expressed as [32, 33]

$$D = C \frac{T \sqrt{\alpha_1}}{\eta} \quad (2.10)$$

where $C = 7.48 \times 10^{-8} M_w^{1/2} / V^{0.6}$ depends on the MIL molar mass M_w and the molar volume V . α_1 is an association degree often considered when relating the viscosity and diffusion in polar liquids. Assuming that α_1 might depend on the magnetic field and combining eqs. 2.9 and 2.10 we consider here that

$$D = D_0 [1 + (\gamma B \tau_{v_2})^{p_2}] \quad (2.11)$$

where D_0 is the diffusion coefficient at zero magnetic field. Since $\nu_L = \gamma B / (2\pi)$ it is possible to include the field dependence of D in the relaxation model of eq. 2.8.

Also, the model fitting parameters τ_d and τ_D must be expressed in terms of D_0 , p_2 , and τ_{v_2} : $\tau_D = \tau_{D_0} / [1 + (\gamma B \tau_{v_2})^{p_2}]$ and $\tau_d = \tau_{d_0} / [1 + (\gamma B \tau_{v_2})^{p_2}]$

In view of the fact that the measured spin-lattice relaxation rate reflects the molecular dynamics of the IL cations, some of the physical parameters considered in the relaxation model of eq. 2.8 must be the same for both IL studied. Therefore, eq. 2.8 was fitted simultaneously to all experimental relaxation results using a non-linear least-square minimization procedure [56, 57], with a global minimum target. In this procedure the values of the self-diffusion coefficients were also taken into account in order to obtain the values of τ_{v_2} and p_2 . The fitting parameters obtained for the best fit of eq. 2.8 to the experimental results are presented in Table 2.3.

Table 2.3: Relaxation model parameters obtained for the best fit of eq. 2.8 to the R_1 experimental results for the [Aliquat][Cl] and [Aliquat][Cl] / [Aliquat][FeCl₄] 1% (v/v) IL systems, as explained in the text. The follow fitting parameters are common for both IL systems: $\tau_{D_0} = (2.8 \pm 0.2) \times 10^{-9} s$, $d \simeq 7.3 \times 10^{-10} m$, $M \simeq 0.012 mol/L$, $S_1 \simeq 370 \pm 10$, $n = 8 \times 10^{28} spins/m^3$, $p_1 \simeq 2.4$, and $\tau_{v_1} \simeq 7 \times 10^{-10} s$, $p_2 \simeq 1.2$, and $\tau_{v_2} \simeq 9.3 \times 10^{-10} s$, $\omega_1 / (2\pi) \simeq 33 MHz$, and $\omega_2 / (2\pi) \simeq 18 MHz$

	[Aliquat][Cl] / [Aliquat][FeCl ₄]			
	[Aliquat][Cl]		[Aliquat][FeCl ₄]	
	CH ₂	CH ₃	CH ₂	CH ₃
$\sqrt{\langle r^2 \rangle} (10^{-10} m)$	1.3 ± 0.2	1.9 ± 0.2	1.3 ± 0.2	1.9 ± 0.2
$\tau_{d_0} (10^{-8} s)$	–		2.5 ± 0.2	2.8 ± 0.2
$\tau_s (10^{-10} s)$	–		1.3 ± 0.1	
$A_{Rot_1} (10^9 s^{-2})$	3.0 ± 0.3	2.7 ± 0.2	3.0 ± 0.3	2.7 ± 0.2
$\tau_1 (10^{-10} s)$	4.9 ± 0.5	2.4 ± 0.4	4.9 ± 0.5	2.4 ± 0.4
$A_{Rot_2} (10^9 s^{-2})$	0.4 ± 0.1	–	0.4 ± 0.1	–
$\tau_2 (10^{-8} s)$	3.2 ± 0.2	–	3.2 ± 0.2	–
$A_{CR1} (10^7 s^{-2})$	2.5 ± 0.5		–	
$\tau_{CR1} (10^{-7} s)$	3.9 ± 1.0	1.9 ± 0.3	–	
$A_{CR2} (10^8 s^{-2})$	2.6 ± 0.2	~ 0.2	–	
$\tau_{CR2} (10^{-8} s)$	9.2 ± 1.1	~ 80	–	

In Figure 2.4 are presented the best model fitting curves to the experimental spin-lattice relaxation results.

It is clear that for [Aliquat][Cl] the R_1 dispersion is well explained by the proposed

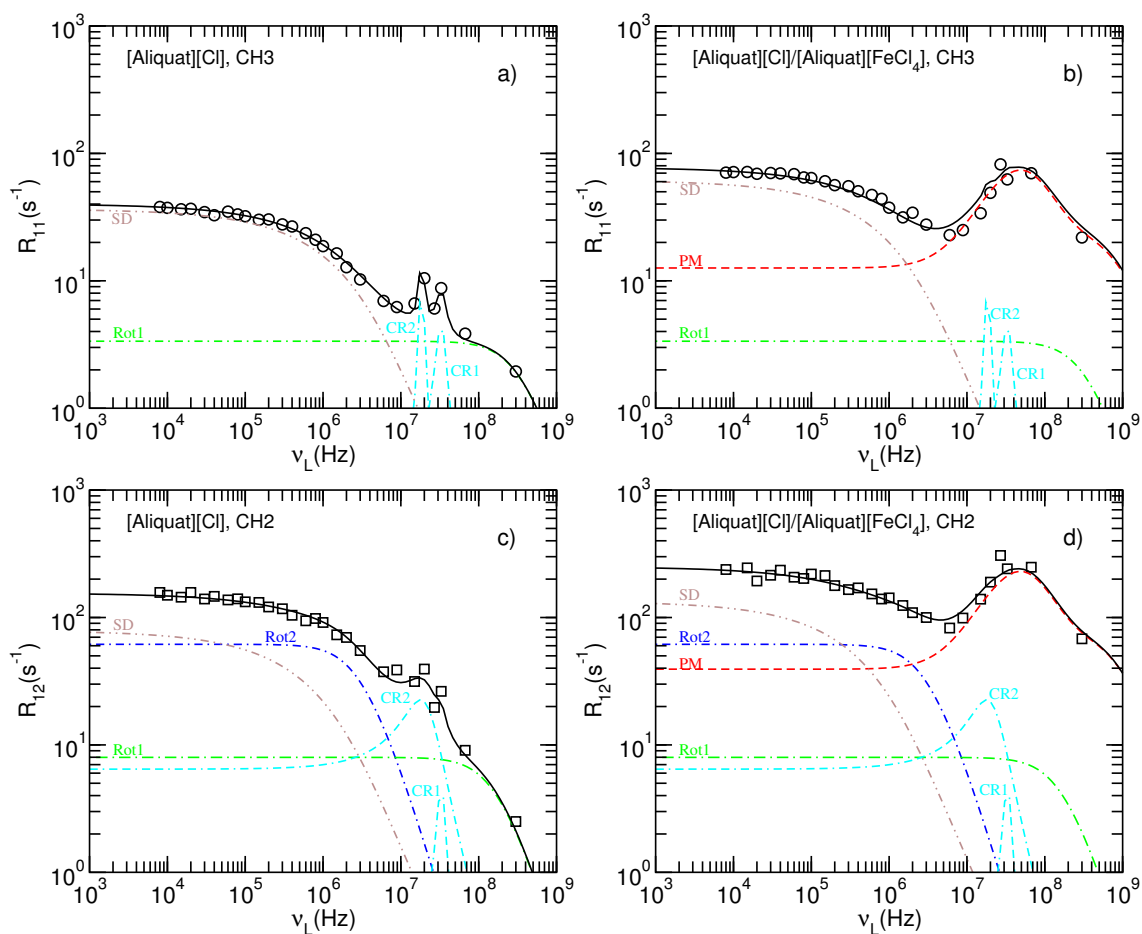


Figure 2.4: Experimental results and model fitting curves for the two spin-lattice relaxation rates as a function of frequency for the IL systems, as explained in the text.

relaxation model used. The R_{11} dispersion in Figure 2.4a) is mainly described by a relaxation contribution with a short correlation time associated with rotations/reorientations of the $[\text{Aliquat}][\text{Cl}]$ cations for frequencies above 10 MHz and by the translational self-diffusion relaxation contribution at lower frequencies. Clearly, the sharp cusps observed in the 10–40 MHz range are explained by the localized relaxation processes associated with the cross-relaxation mechanism between the ^1H and ^{35}Cl nuclear spins.

The same basic relaxation features are present in the $[\text{Aliquat}][\text{Cl}]$ R_{12} dispersion fit of Figure 2.4c). The main difference is the inclusion of a second rotations/reorientations contribution (Rot2) with a much large correlation time than that of (Rot1). These features are compatible with the original assignment of R_{11} and R_{12} with the CH_3 and CH_2 cation groups, as it is reasonable to assume that the former groups can rotate faster than the latter ones. In fact, the interdigitation of the cations' chains might hinder conformational changes and restrict the CH_2 motions.

Also, the CH_2 group motions might reflect overall molecular motions, necessarily slower than the motions of the methyl groups. It is also interesting to note that the mean-square jump distance associated to the translational displacements is small for both R_{11}

and R_{12} , but it is larger in the case of the CH_3 groups. The translational diffusion seems to be an almost continuous process in both cases, but it reflects an additional mobility of the chains end groups. The cross-relaxation process between ^1H and ^{35}Cl nuclear spins is also localized in the frequency range 10–40 MHz but the R_{12} cusps are worst resolved that in the case of R_{11} . From this point of view it is possible to assume that R_{11} has an important contribution from the ^1H spins of the methyl group bonded to the nitrogen that are perhaps more spatially correlated with the ^{35}Cl spins in the anions.

The main difference between the R_1 model fits of $[\text{Aliquat}][\text{Cl}]$ and $[\text{Aliquat}][\text{Cl}]/[\text{Aliquat}][\text{FeCl}_4]$ observed in Figure 2.4 is the notable presence of the paramagnetic relaxation mechanism dominant in the high frequency region. This relaxation mechanism is characterized by the existence of a maximum relaxation rate in the frequency region above 1 MHz. It was possible to fit R_{11} for both $[\text{Aliquat}][\text{Cl}]$ and $[\text{Aliquat}][\text{Cl}]/[\text{Aliquat}][\text{FeCl}_4]$ using the same Rot1, Rot2, and CR relaxation contributions. However, the translational self-diffusion presented slightly different contributions in the two IL systems. It is clear that the cross-relaxation is masked by the strong dominating PM contribution. Nevertheless, this contribution was also considered in the $[\text{Aliquat}][\text{Cl}]/[\text{Aliquat}][\text{FeCl}_4]$ model fit to the R_{11} and R_{12} experimental results. Therefore, the effect of local order changes due to the presence of magnetic anions is detected mainly in the cations' self-diffusion, in comparison with dynamics in the $[\text{Aliquat}][\text{Cl}]$.

One important aspect of the model fit analysis is the fact that the SD contribution to the relaxation rate is approximated by $R_1(\nu_L) \sim \nu_L^{-2}$ for frequencies above 2 MHz and becomes negligible for frequencies above 10 MHz in comparison with the dominant contributions of the other relaxation mechanisms. Therefore, the magnetic field effect on the $[\text{Aliquat}][\text{Cl}]/[\text{Aliquat}][\text{FeCl}_4]$ viscosity and consequently on the diffusion coefficient is not important for the SD relaxation contribution for frequencies above 2 MHz. For lower frequencies the magnetic field effect on D is expected to be small in view of the small effect on the measured viscosity in the range 0-0.5 T (i. e. between 0-20 MHz), as it can be observed in Figure 2.3.

It is interesting to observe that from the values of A_{Rot} it is possible to estimate the two values of r_{eff} , $r_{eff1} \simeq 2.5 \times 10^{-10}$ associated with a correlation time τ_1 of the order of 10^{-10} s and $r_{eff2} \simeq 3.4 \times 10^{-10}$ associated with a correlation time τ_2 of the order of 10^{-8} s and present only in the analysis of the spin-lattice relaxation rate associated with the CH_2 $[\text{Aliquat}]$ chain protons. τ_2 might therefore be related with rotations/reorientations involving the $[\text{Aliquat}]$ chains as a whole, since r_{eff2} is larger than r_{eff1} , which is associated to the faster moving CH_3 groups.

The value of the paramagnetic spin S_1 obtained from the model fit, presented in Table 2.3, is considerable larger than the value of the $[\text{FeCl}_4]$ anion spin $S_1 = 5/2$ associated to the Fe^{3+} ion [46]. Large values of S_1 ($S_1 > 25$) are usually associated to super-paramagnetic particles, with dimensions much larger than ~ 5 nm. The spin-lattice relaxation rate dispersions obtained for the $[\text{Aliquat}][\text{Cl}]/[\text{Aliquat}][\text{FeCl}_4]$ system are similar to the ones observed for aqueous solutions of super paramagnetic particles in what concerns the

broad peak in the high frequency region [47]. Therefore, it is reasonable to conclude that the collective alignment process of the paramagnetic spins, associated with the super-paramagnetic spin's concept, is also observed in the $[\text{Aliquat}][\text{Cl}]/[\text{Aliquat}][\text{FeCl}_4]$ system. Indeed, domains formed by the ensemble of $[\text{Aliquat}][\text{Cl}]/[\text{Aliquat}][\text{FeCl}_4]$ iron anions, required to produce a super-paramagnetic spin $S_1 \approx 370$, might exist and influence the cations' ^1H spin-lattice relaxation including those within these regions. In the $[\text{Aliquat}][\text{Cl}]/[\text{Aliquat}][\text{FeCl}_4]$ system, we found that the process of paramagnetic relaxation depends only the value of S_1 , in contrast with the paramagnetic relaxation in aqueous solutions of super-paramagnetic particles where both the radius of the particles and S_1 are important [47].

The large effective paramagnetic spin estimated might also be associated with the noticeable viscosity's magnetic field dependence observed for the MIL mixture system. The decrease of viscosity with increasing magnetic field might be a consequence of the interaction between the magnetic field and the delocalized charge in the $[\text{FeCl}_4]$ anion, which might weaken the average ionic interaction, thus favoring the molecular diffusion.

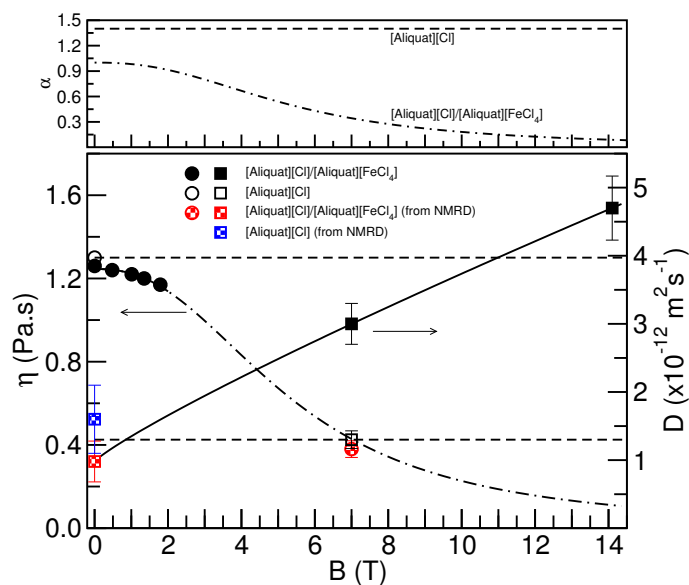


Figure 2.5: Viscosity [full and empty black circles] and translational self-diffusion [full and empty black squares] measured for the $[\text{Aliquat}][\text{Cl}]$ and $[\text{Aliquat}][\text{Cl}]/[\text{Aliquat}][\text{FeCl}_4]$ systems. The patterned squares (red and blue online only) refer to the estimated diffusion values from the model fit of eq. 2.8, as explained in the text. Flat dashed curves correspond to the extrapolated values of viscosity and diffusion as a function of the magnetic field. The dashed-dot curve and the red (online only) patterned circle were obtained using eq. 2.9. The self-diffusion coefficient measured at 7T and 14.1 T were fitted together with the value at zero field obtained from NMRD. The phenomenological magnetic field dependence of α_1 for both $[\text{Aliquat}][\text{Cl}]$ and $[\text{Aliquat}][\text{Cl}]/[\text{Aliquat}][\text{FeCl}_4]$ are also plotted.

From the values of the τ_{D_0} and τ_{d_0} in Table 2.3 it is possible to estimate the values of D_0 for the IL systems using the expressions $\tau_{D_0} = \langle r^2 \rangle / (6D_0)$ and $\tau_{d_0} = \langle r^2 \rangle / (D_0)$, respectively.

The values $D_0 = (1.6 \pm 0.5) \times 10^{-12} \text{ m}^2 \text{ s}^{-1}$ and $D_0 = (1.0 \pm 0.3) \times 10^{-12} \text{ m}^2 \text{ s}^{-1}$ corresponding to [Aliquat][Cl] and [Aliquat][Cl]/[Aliquat][FeCl₄] ILs, respectively, are presented in Figure 2.5. In this figure are also presented the values of the D measured by PFG NMR at of 7 T and 14.1 T. The fitting $D(B)$ curve obtained using eq 2.11 is also shown. On the basis of the founding that τ_{v_1} and p_1 are different from τ_{v_2} and p_2 it can be inferred from eq. 2.9 to eq. 2.11 that the association parameter is also magnetic field dependent. The phenomenological dependence obtained for α_1 is shown on the top of Figure 2.5.

The values of α_1 estimated for [Aliquat][Cl] and [Aliquat][Cl]/[Aliquat][FeCl₄] at zero field, using eq. 2.10, were $\alpha_1 = 1.4 \pm 0.3$ and $\alpha_1 = 1.0 \pm 0.2$, respectively. The difference between these two values might be due to different nature of the [Cl] and [FeCl₄] anions. In Figure 2.5 are presented the phenomenological magnetic field dependence of α_1 for the two IL systems.

With the values of η_0 , D_0 , and D at 7 T it is possible to estimate the value of viscosity at 7 T. The value obtained: $\eta_{7T} \simeq 0.38 \text{ Pa.s}$, is coherent with the extrapolated values obtained from the phenomenological model fitting curve of the viscosity measured between 0 and 2 T.

2.6 Conclusions

This work presents a molecular dynamics study of two ionic liquids: a non-magnetic ionic liquid, [Aliquat][Cl] and an ionic liquid mixture of [Aliquat][Cl] with its analogue [Aliquat][FeCl₄]. The two systems were studied by viscometry, ¹H NMR relaxometry, and pulse field gradient NMR.

The viscosity results showed that at zero magnetic field both IL system presented basically the same viscosity, although the [Aliquat][Cl] viscosity was slightly larger that of [Aliquat][FeCl₄]. For increasing magnetic fields the viscosity of [Aliquat][Cl] remained constant. However, for the [Aliquat][Cl]/[Aliquat][FeCl₄] a clear viscosity decrease for increasing magnetic fields was observed.

The spin-lattice relaxation time was measured over a broad frequency range from 10 kHz – 300 MHz at 22 °C. A bi-exponential decay in the time recovery of the longitudinal magnetization was detected for both IL systems, revealing the presence of two spin sub-systems in the samples. One spin-lattice relaxation rate, R_{11} , was associated to the CH₃ and the other, R_{12} , to the CH₂ groups.

Both R_{11} and R_{12} relaxation rates revealed a peculiar frequency dependence in the case of the [Aliquat][Cl]/[Aliquat][FeCl₄] ionic liquid with a broad peak in the high frequency region between 10–300 MHz. In the case of [Aliquat][Cl] these broad peaks where not observed, but in frequency region 20–30 MHz, some sharp cusps where detected.

The experimental viscosity results obtained as a function of the magnetic field were analyzed in terms of a phenomenological curve that considers a maximum value for zero field and a Lorentzian-like decay with the magnetic field. The viscosity and diffusion

coefficients were assumed to be inversely proportional according to a modified Stokes–Einstein relation that considers an association degree in order to take into account the polar character of the fluids. The diffusion coefficient magnetic field dependence was introduced in the relaxation model used to analyze the spin-lattice relaxation results.

The relaxation model considered includes the contributions of rotations/reorientations, translational self-diffusion and cross-relaxation between the ^1H and the ^{35}Cl nuclear spins. In the case of $[\text{Aliquat}][\text{Cl}]/[\text{Aliquat}][\text{FeCl}_4]$ system the broad relaxation peak in the frequency range 10–300 MHz was interpreted in terms of a relaxation mechanism associated with the paramagnetic relaxation involving the ^1H spins and the paramagnetic $[\text{FeCl}_4]$ magnetic moments. The model fit to all experimental relaxation rate results is very good. The values of the diffusion coefficient corresponding to zero magnetic field were obtained from the fits and were compatible with the diffusion coefficients measured by PFG NMR at 7 T and 14.1 T within the frame of the magnetic field dependence used for the viscosity/diffusion.

In view of the independent measurements of viscosity and self-diffusion it is concluded that the modified Stokes-Einstein, which considered a molecular association factor, is needed to relate both quantities. Moreover, it was found that this association factor is also magnetic field dependent for the $[\text{Aliquat}][\text{Cl}]/[\text{Aliquat}][\text{FeCl}_4]$ system.

It was possible to estimate the viscosity for the magnetic field of 7 T, that otherwise would be difficult to obtain with the available experimental setups.

In spite the small concentration of $[\text{Aliquat}][\text{FeCl}_4]$ in the $[\text{Aliquat}][\text{Cl}]/[\text{Aliquat}][\text{FeCl}_4]$ mixture it was enough to change its molecular dynamics and viscosity and to control both with an external magnetic field.

It can be concluded that the MIL mobility can be modulate by the presence of a magnetic field. The tuning of the MILs properties and the increase of the diffusion in the presence of a magnetic field might be an advantage, for example in the case of transport of molecular species across the MILs.

¹H-NMR RELAXATION STUDY OF A MAGNETIC IONIC LIQUID AS A POTENTIAL CONTRAST AGENT

Published as: Carla I. Daniel, Fabián Vaca Chávez, Carla A.M. Portugal, João G. Crespo, Pedro J. Sebastião “¹H-NMR Relaxation Study of a Magnetic Ionic Liquid as a Potential Contrast Agent”, Journal of Physical Chemistry B, 119 (2015), 11740–11747.

3.1 Summary

A proton nuclear magnetic relaxation dispersion ¹H NMRD study of the molecular dynamics in mixtures of magnetic ionic liquid [P₆₆₆₁₄][FeCl₄] with [P₆₆₆₁₄][Cl] ionic liquid and mixtures of [P₆₆₆₁₄][FeCl₄] with Dimethyl sulfoxide (DMSO) is presented. The proton spin lattice relaxation rate, R_1 , was measured in the frequency range of 8kHz-300MHz.

The viscosity of the binary mixtures was measured as a function of an applied magnetic field, B , in the range of 0 - 2T. In the case of DMSO/[P₆₆₆₁₄][FeCl₄] the viscosity was found to be independent from the magnetic field, while in the case of the [P₆₆₆₁₄][Cl]/[P₆₆₆₁₄][FeCl₄] system viscosity decreased with the increase of the magnetic field strength.

The spin-lattice relaxation results were analyzed for all systems taking into account the relaxation mechanisms associated to the molecular motions with correlation times in a range between 10^{-11} and 10^{-7} s, usually observed by NMRD, and the paramagnetic relaxation contributions associated with the presence of the magnetic ions in the systems.

In the case of DMSO/[P₆₆₆₁₄][FeCl₄] system the R_1 dispersion shows the relaxation enhancement due to the presence of the magnetic ions, similar to that reported for contrast agents. For the [P₆₆₆₁₄][Cl]/[P₆₆₆₁₄][FeCl₄] system, the R_1 dispersion presents a much larger paramagnetic relaxation contribution, in comparison with that observed for the DMSO/[P₆₆₆₁₄][FeCl₄] mixtures, but different from that reported for other magnetic

ionic liquid system. In the $[\text{P}_{66614}][\text{Cl}]/[\text{P}_{66614}][\text{FeCl}_4]$ system the relaxation enhancement associated to the paramagnetic ions is clearly not proportional to the concentration of magnetic ions, in contrast with what is observed for the $\text{DMSO}/[\text{P}_{66614}][\text{FeCl}_4]$ system.

3.2 Introduction

Proton Nuclear Magnetic Resonance (^1H -NMR) is a widely known non-invasive experimental technique used to characterize molecular order/structure and dynamics in a large variety of systems [31, 58]. In particular, ^1H -NMR imaging is a powerful tool to obtain information on the morphology, function and metabolism of complex systems like porous materials, composites, biological systems among many others.

Magnetic nanoparticles as contrast agents for NMR imaging have been the target of numerous research works due to their unique magnetic properties and the ability to contribute to probe molecular interactions at cellular and molecular level [59, 60, 61]. The paramagnetic metal ions present in magnetic contrast agents, possess permanent magnetic moments that contribute to strongly increase the local magnetic field in the vicinity of each ion. Through paramagnetic relaxation they produce a decrease of spin lattice (T_1) and spin-spin (T_2) relaxation times of neighboring hydrogen nuclei, a phenomenon called "Proton relaxation enhancement (PRE)" [62].

Therefore, in medical NMR imaging tissues with different concentrations of paramagnetic ions will have distinct spin lattice relaxation times which can be used to produce images with higher contrast [63]. The PRE effect can be useful not only for clinical diagnosis but also to increase contrast in NMR imaging in general as in the case of the study of chemical reactions and processes [64]. Magnetic colloids, magnetic nanoparticles, paramagnetic and super paramagnetic compounds, magnetic ionic liquids are systems of high interest for the enhancement of NMR imaging quality.

The development and characterization of new magnetic compounds has been an important research subject [59, 60, 61, 65, 66]. The magnetic behavior of the metal ions make these compounds effective proton relaxation agents because the contrast effect is produced indirectly by the changes in the local magnetic environment [62, 67]. Different paramagnetic metal ions can be used: Fe(III), Gd(III), Mn(II) and Dy(III), according to their magnetic susceptibilities and levels of toxicity for specific applications [68].

The effect of paramagnetic relaxation can be described by the so-called Curie relaxation that considers fluctuations of the dipolar interactions between the paramagnetic particles' global magnetic moments and the proton nuclear magnetic moments of neighbor hydrogen nuclei either temporary bounded to the magnetic particle or within the first neighbor layer spheres (inner-spheres) or in outer layer spheres. [47, 49, 62, 69, 70]

Nowadays, the commercial contrast agents are based on Gd (III) paramagnetic ion, due to high magnetic response in comparison with the other metal ions described before [68]. However, the toxicity of these compounds as contrast agents is high. In particular the Gd (III) toxicity is higher than Fe (III) [68]. To reduce the levels of cells toxicity, the

paramagnetic ions may be used as contrast agents, in the form of complexes (or chelates) with organic ligands [71, 72]. The toxicity of Gd(III) and Fe(III) is identical when these elements are used as members of complexes or chelate systems. In this case, Gd(III) based contrast agents are preferred due to their high magnetic relaxivities values observed in the magnetic resonance applications [71, 72, 73].

Besides the magnetic behavior of magnetic nanoparticles and magnetic colloids, new magnetic ionic liquids (MILs) have been explored due to their particular magnetic features. In MILs, usually the anionic counterparts is replaced by others containing a paramagnetic metal complex. Recent studies of different magnetic ionic liquids have shown that the MILs physicochemical properties might change when submitted to different magnetic field conditions [19, 20, 34, 35]. The influence of the magnetic field on the physicochemical properties of MILs might be explained by the dependence between the magnetic field intensity and the structural arrangement of the ionic paramagnetic network and a peculiar coupling between magnetic moments of the paramagnetic ions [74].

The previous ^1H -NMR study, by Daniel *et al.* [74] described in Chapter 2, of the molecular dynamics of a magnetic ionic liquid system comprising a mixture of [Aliquat][Cl]/[Aliquat][FeCl₄], showed the relation between the viscosity and the self-diffusion of the studied ionic liquid systems in the presence of different magnetic fields. The results of the proton spin-lattice relaxation rate (T_1^{-1}) revealed a strong enhancement of T_1^{-1} at Larmor frequencies higher than 10 MHz (magnetic fields larger than 0.2 T) as observed for contrast agent systems with super-paramagnetic particles [47].

Also, it was observed that the MILs viscosity decreased with increasing magnetic field intensity consistent with an increase of the MILs self-diffusion coefficient. The specific MIL behavior was analyzed and related to the paramagnetic moments of the anion [FeCl₄], to the particular molecular arrangement and to the electrostatic equilibrium between the ionic species [74].

Some recent works have reported the possibility of using magnetic ionic liquids as potential contrast agents [25, 38]. In fact, ionic liquids can be designed by changing both cations and anions [24] and offer the possibility to adjust their physicochemical properties for specific applications [21, 75], taking into account eventual limitations due to toxicity effects in the case of medical applications. Studies were published concerning the understanding about factors that influence toxicity. In terms of the magnetic anion toxicity, a study in human cells [76], demonstrated that iron complexes are preferable to gadolinium ones.

Along with this finding, some works have shown that long aliphatic chains in the cations can also contribute to an increase of toxicity of the paramagnetic ionic liquids, depending on the medium of application (bacterias, human cells) [76, 77]. Since the magnetic ionic liquids properties are magnetic field dependent, a new ionic liquid/magnetic ionic liquid pair, [P₆₆₆₁₄][Cl]/[P₆₆₆₁₄][FeCl₄], was selected to be studied, aiming at understanding how the magnetic field influences the molecular structure and molecular packing of the cations and its subsequently impact on the properties of the ionic system.

Considering the cations of $[\text{P}_{66614}][\text{FeCl}_4]$ and $[\text{Aliquat}][\text{FeCl}_4]$, it is reasonable to expect that the molecular packing of phosphonium salt $[\text{P}_{66614}]^+$ molecules (which have four long chains) might be different from that of the quaternary ammonium $[\text{Aliquat}]^+$ molecules (which have three long chains and one methyl group), the latter favoring a closer approach between the ions pairs in the ionic liquid. These differences may possibly translate into different magnetic induced molecular dynamics and structural rearrangements.

Here is presented a study of the molecular dynamics by ^1H -NMR relaxation and a study of the physicochemical properties as a function of the magnetic field of the ionic liquid systems: $[\text{P}_{66614}][\text{Cl}]$, a mixture $[\text{P}_{66614}][\text{Cl}]/[\text{P}_{66614}][\text{FeCl}_4]$ and also a mixture of $[\text{P}_{66614}][\text{FeCl}_4]$ with Dimethyl sulfoxide (DMSO). The proton spin-lattice relaxation measurements were done between 8kHz-300MHz and the self-diffusion, D , was determined directly using PFG (Pulse Field Gradient) NMR technique at a magnetic field intensity of 7 T. Due to the relation between the diffusion and viscosity, studies were performed to find a correlation between the viscosity and magnetic relaxation behavior. A comparison between the relaxation profiles obtained in this work for the $[\text{P}_{66614}][\text{Cl}]/[\text{P}_{66614}][\text{FeCl}_4]$ system and DMSO/ $[\text{P}_{66614}][\text{FeCl}_4]$ solutions and the profiles reported for other contrast agents systems is presented.

3.3 Experimental

3.3.1 Materials

The ionic systems selected for this study are based on phosphonium salts where the cation has the structure presented in the Figure 3.1 and is hereafter referred to as $[\text{P}_{66614}]^+$. Two ionic liquids were considered, $[\text{P}_{66614}][\text{Cl}]$ and the mixture of $[\text{P}_{66614}][\text{Cl}]/[\text{P}_{66614}][\text{FeCl}_4]$ 1% (v/v), where chloride anions were partially replaced by magnetic $[\text{FeCl}_4]^-$ anions.

The ILs systems were synthesized by Afonso *et al.*, from Faculdade de Farmácia, Universidade de Lisboa, according to the experimental procedure described in the references [36, 39]. The density of the ILs systems was measured gravimetrically using a pycnometer and the percentage of the magnetic element, Fe^{3+} , in each sample was determined by Inductively coupled plasma (ICP). The molecular weight and density of the two ionic liquid systems are presented in Table 3.1.

3.3.2 Methods

3.3.2.1 ^1H -NMR assays

The assays of ^1H -NMR were performed following a procedure previously described for similar systems [50, 74]. The proton spin-lattice relaxation rates R_1 ($\equiv 1/T_1$) were measured at 22 °C for a broad Larmor frequency range between 8 kHz and 300 MHz. Three complementary NMR set up were used for the measurements: a conventional Bruker

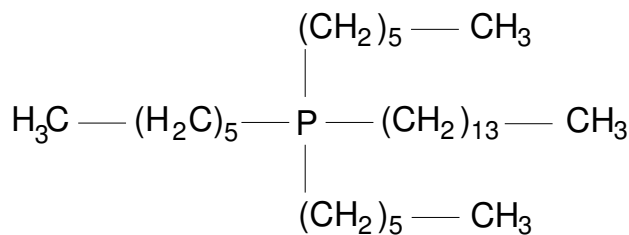


Figure 3.1: Molecular structure of the $[\text{P}_{66614}]^+$ cation. The charge is localized at the phosphorous atom.

Table 3.1: Physical parameters of the ionic liquid systems used. The molar concentration of $[\text{P}_{66614}][\text{FeCl}_4]$ in the $[\text{P}_{66614}][\text{Cl}]/[\text{P}_{66614}][\text{FeCl}_4]$ mixture is 0.014 mol/L.

IL	Molecular Weight (g mol^{-1})	Density (g cm^{-3})
$[\text{P}_{66614}][\text{Cl}]$	518.3	0.891
$[\text{P}_{66614}][\text{Cl}]/[\text{P}_{66614}][\text{FeCl}_4]$	519.9	1.11

Avance II NMR console operating either a 7T superconductor electromagnet or a variable field (0.2T - 2T) electromagnet and a Fast Field-Cycling NMR relaxometer [78]. The details of the experimental techniques used with each equipment can be found in the literature [50, 74, 79, 80, 81].

3.3.2.2 Viscosity measurements

The measurements of viscosity were carried out in a capillary viscometry set up using the conventional protocol described in the literature [74, 75]. The experiments were conducted with and without applied magnetic field to analyze the influence of the magnetic field on the ionic liquids' viscosity.

3.4 Results

For both ionic liquid systems it was found that the spin-lattice relaxation was described by a two components exponential decay. Two spin-lattice relaxation rates R_{11} and R_{12} were determined considering a relative weight of the two relaxation components that was attributed to the number of hydrogen protons of the CH_3 (terminal methyl groups) and CH_2 (ethyl groups) groups of the carbonated chains. In Figure 3.2 are presented the proton spin-lattice relaxation rates for the two ionic liquid systems. In Figure 3.2a) are presented the values of R_{12} and in Figure 3.2b) are presented the values of R_{11} , in the Larmor frequency range between 8 kHz–300 MHz.

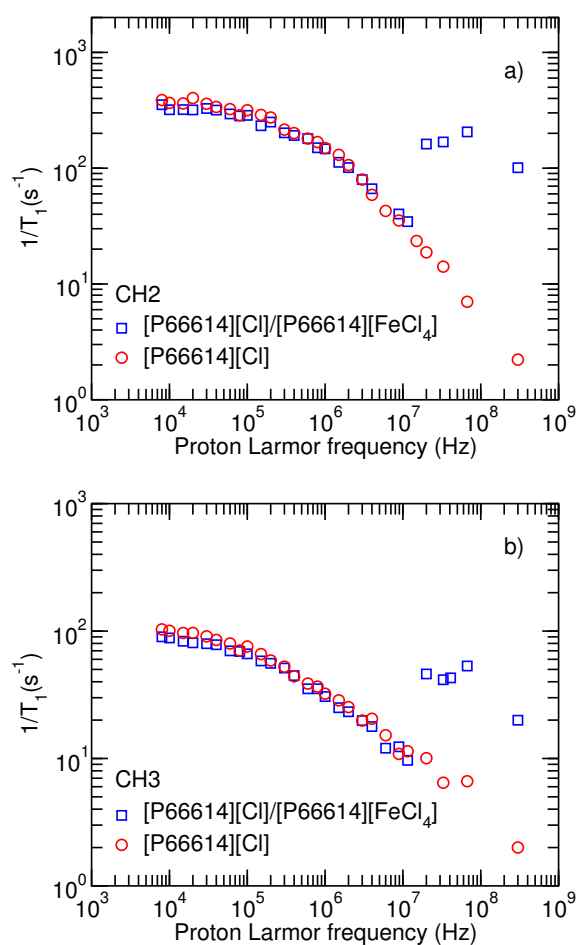


Figure 3.2: Larmor frequency dependence of proton spin lattice relaxation rates for the systems $[\text{P}_{66614}][\text{Cl}]$ and MIL $[\text{P}_{66614}][\text{Cl}]/[\text{P}_{66614}][\text{FeCl}_4]$ 1% (v/v) mixture: R_{12} , a) and R_{11} , b).

As can be observed in both Figures 3.2a) and 3.2b) the values of R_{11} and R_{12} for the two ionic liquid systems are quite similar for frequencies below 10 MHz but differ significantly for higher frequencies. The difference between IL and MIL R_{11} and R_{12} behaviors at high frequencies is similar to that reported previously for the IL/MIL [Aliquat][Cl] based system [74]. In that work this difference was possibly associated to the paramagnetic relaxation contribution due to the presence of the magnetic ions in the MIL system. Such strong spin-lattice relaxation increase at high frequencies due to paramagnetic relaxation was also reported for liquid mixtures with contrast agents of super-paramagnetic particles [47].

However, the similarity between the IL and MIL R_{11} and R_{12} behaviors at frequencies below 10 MHz is quite unexpected in view of the results reported for the [Aliquat][Cl] IL systems [74] and taking into account the usually observed linear dependence of the relaxation rate on the concentration of paramagnetic particles [63]. Additionally for the MIL is observed an enhancement of the R_1 at 20 and 33 MHz which can be associated

with the cross relaxation among ^1H and ^{35}Cl spins [45].

The values of viscosity of both ionic liquid systems are presented in Table 3.2. As expected the viscosity of the non-magnetic ionic liquid is independent of the magnetic field. As can be observed the viscosity of the $[\text{P}_{66614}][\text{Cl}]/[\text{P}_{66614}][\text{FeCl}_4]$ decreases with the increase of the magnetic field as reported in the literature for different magnetic ionic liquids [74, 75].

Table 3.2: Viscosity determined experimentally as a function of applied magnetic field for the $[\text{P}_{66614}][\text{Cl}]/[\text{P}_{66614}][\text{FeCl}_4]$ 1% (v/v) solution (in parenthesis the values for the $[\text{P}_{66614}][\text{Cl}]$ IL). The viscosity of $\text{DMSO}/[\text{P}_{66614}][\text{FeCl}_4]$ 1% (v/v) was $\eta_{\text{DMSO}} = 2.15$ Pa.s, independent of the applied magnetic field.

B(T)	η (Pa.s)
$\sim 45 \times 10^{-6}$	1.97 (2.06)
0.47	1.93 (2.06)
1	1.81 (2.06)
1.3	1.73 (2.06)
1.8	1.71 (2.06)

3.5 Analysis and Discussion

The ^1H -NMR R_1 dispersions presented in Figure 3.2 were analyzed taking into account the relaxation processes associated with the molecular motions usually found in low molecular mass organic materials like liquid crystals and ionic liquids [49, 74, 79, 81]. The presence of paramagnetic ions adds an additional degree of complexity on the analysis of R_1 dispersion data as the coupling between the magnetic moment of the paramagnetic ions with proton's magnetic moment leading to the inclusion of an additional relaxation process parameter in the analysis [74]. In the case of the phosphonium salt based systems only the cations possess hydrogen protons, therefore, the relaxation information regarding molecular motions that is obtained reflects mainly the global motions of the cations and the alkyl chain dynamics.

The relaxation model considered here follows that presented previously for a similar system where the cations possessed a nitrogen central atom bounded with just three long aliphatic chains and a methyl group. The total relaxation rate is the sum of the relaxation contributions: translational and rotational self-diffusion, chain dynamics, paramagnetic relaxation and cross relaxation between the hydrogen protons ^1H system and the chloride ^{35}Cl spins system [74]. Given the complexity of the molecular system and the presence of a molecular packing with the strong interdigitation of the molecular chains of different cations, the use of the relaxation models considered for liquid crystals and simpler ionic

liquids [49, 50, 74] must be considered as a first approximation.

The model considered for the analysis of the R_1 experimental results can be expressed by the sum of the contributions mentioned before. In the case of the MIL system the contribution corresponding to the paramagnetic relaxation was also included.

$$R_1(\nu_L) = R_1^{\text{SD}}(\nu_L) + [R_1^{\text{Rot}_1}(\nu_L) + R_1^{\text{Rot}_2}(\nu_L)] + R_1^{\text{CR}}(\nu_L) + [R_1^{\text{PM}}(\nu_L)]_{\text{MIL}} \quad (3.1)$$

The cross terms contributions in eq. 3.1 were neglected assuming that the relaxation mechanisms are statistical independent. The theoretical details of each relaxation model are presented in the Appendix A of this thesis. The model fitting parameters were: d , τ_D , $\langle r^2 \rangle$, τ_d , τ_{d1} , τ_s , τ_1 , A_{Rot_1} , τ_2 , A_{Rot_2} , and a pair of $\tau_{\text{CR}i}$, $A_{\text{CR}i}$ for each cross-relaxation peak, where d is an average width associated with the volume defined by the aliphatic chains, $\langle r^2 \rangle$ is the mean-square jump distance, τ_s is the longitudinal electronic relaxation time, τ_1 and τ_2 are correlation times associate with the rotations of the aliphatic chains, A_{Rot_1} and A_{Rot_2} depend on the protons spins dipolar coupling constant and effective inter-spins distance. $\tau_{\text{CR}i}$, $A_{\text{CR}i}$ are parameters associated to the width and amplitude of the cross relaxation process.

Due to the differences in the relaxation of the IL systems, two correlation times for the translation diffusion processes had to be considered: τ_D for the non-magnetic IL system, τ_d and τ_{d1} for the MIL system. In the case of the MIL system the viscosity dependence on the magnetic field was considered in the fits assuming an empirical model previously introduced for the [Aliquat][FeCl₄] system [74]. In addition the iron molar concentration measured by ICP was $M = 1.4 \times 10^{-2} \text{ mol/L}$ and the ¹H spins density $n = 7 \times 10^{28} \text{ spins/m}^3$ was estimated taking into account the IL and MIL molecular structures and the values of Table 3.1.

The model was fitted to the experimental results using a non-linear least-squares minimization procedure with a global minimum target [56, 57]. The [P₆₆₆₁₄][Cl] and [P₆₆₆₁₄][Cl]/[P₆₆₆₁₄][FeCl₄] relaxation results were fitted simultaneously in two sub-processes: the R_{11} and R_{12} fits. In Figure 3.3 are presented the plots corresponding to the best global fit, whereas the fitting parameters are listed in Table 3.3.

In general terms the fits results obtained for the [P₆₆₆₁₄][Cl] based systems are similar to the ones found for the [Aliquat][Cl]. However, a closed analysis reveals some interesting differences. In fact, the model fit quality for the [P₆₆₆₁₄][Cl]/[P₆₆₆₁₄][FeCl₄] system is worse than that obtained for the [Aliquat][FeCl₄], in particular, in what concerns the description of the slower rotations and the paramagnetic relaxation contributions. Also, the small difference observed in the values of R_{11} and R_{12} of [P₆₆₆₁₄][Cl]/[P₆₆₆₁₄][FeCl₄] for frequencies below 1 MHz could not be explained by the same values of d and τ_d . As a consequence it was not possible to fit the paramagnetic relaxation contribution with the same quality as for the [Aliquat][FeCl₄] system. The presence of [FeCl₄]⁻ in the mixture of [P₆₆₆₁₄][Cl] is not only associated with the additional paramagnetic relaxation contribution to the proton spin-lattice relaxation but also seems to affect the molecular

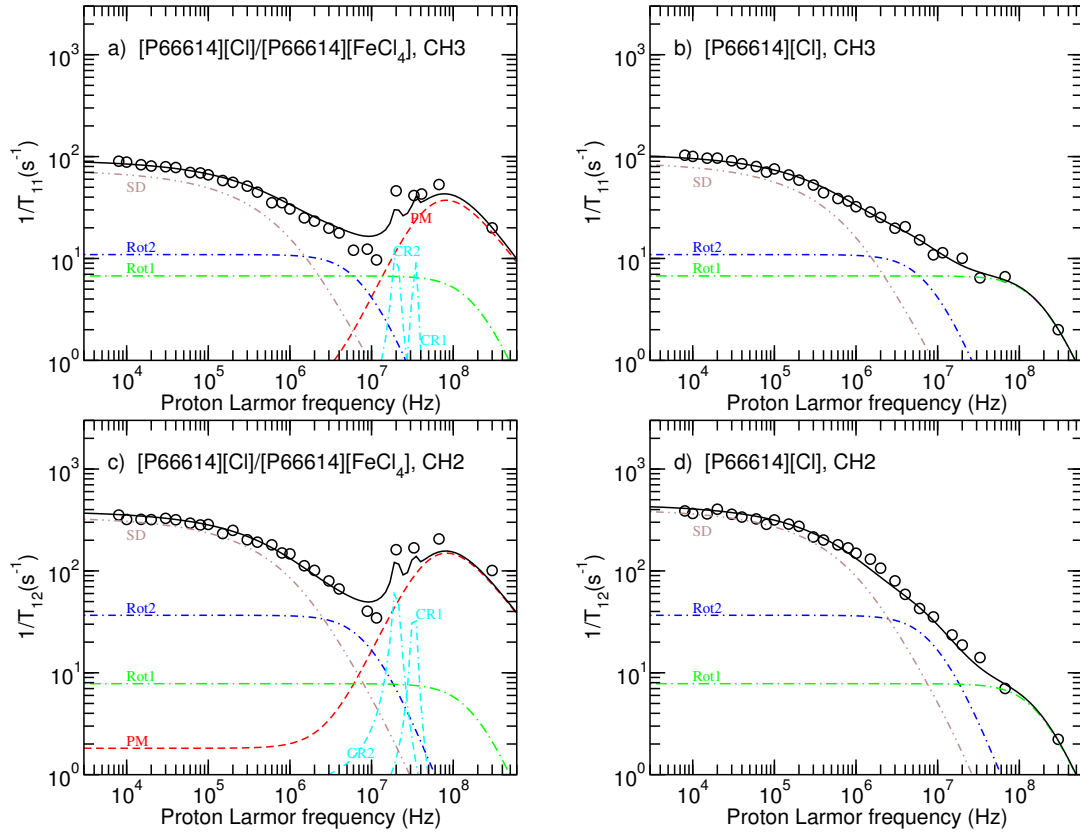


Figure 3.3: Experimental results and model fitting curves for the two spin-lattice relaxation rates as a function of frequency for the IL systems, as explained in the text.

dynamics of the cations in a way that was not observed for the $[\text{Aliquat}][\text{FeCl}_4]$ system previously studied.

The values obtained for the fitting parameters present in Table 3.3 are consistent with those found for the quaternary ammonium magnetic ionic liquid system $[\text{Aliquat}][\text{FeCl}_4]$ mixtures [74], taking into account the differences observed in the relaxation dispersion. In particular, the cross-relaxation contributions are less important than for the $[\text{Aliquat}][\text{Cl}]$ mixtures.

It is interesting to note that the expression usually considered to estimate the concentration effect of a contrast agent in a solution:

$$\frac{1}{T_1} = \left[\frac{1}{T_1} \right]_{\text{Solvent}} + r_1[C], \quad (3.2)$$

where $[C]$ is the concentration of the paramagnetic particles, $[1/T_1]_{\text{Solvent}}$ is the relaxation rate without the presence of the contrast agent and r_1 is the relaxivity of the contrast agent, seems not to be valid in the case of the $[\text{P}_{66614}][\text{Cl}]/[\text{P}_{66614}][\text{FeCl}_4]$ system, as it can be understood from the data in Figure 3.2, assuming that $[\text{P}_{66614}][\text{Cl}]$ acts as a solvent of $[\text{P}_{66614}][\text{FeCl}_4]$.

In order to test the properties of the $[\text{P}_{66614}][\text{FeCl}_4]$ as a contrast agent and to check if

Table 3.3: Relaxation model parameters obtained for the best fit of eq 3.1 to the R_1 experimental results for the $[\text{P}_{66614}][\text{Cl}]$ and $[\text{P}_{66614}][\text{Cl}]/[\text{P}_{66614}][\text{FeCl}_4]$ systems. The follow fitting parameters are common for both systems: $\tau_{D_0} = (1.46 \pm 0.06) \times 10^{-8} \text{ s}$, $d \simeq 7.3 \times 10^{-10} \text{ m}$, $M \simeq 0.014 \text{ mol/L}$, $S_1 \simeq 400$, $n = 7 \times 10^{28} \text{ spins/m}^3$, $p \simeq 1.13$, and $\tau_v \simeq 3.85 \times 10^{-10} \text{ s}$, $\omega_1/(2\pi) \simeq 33 \text{ MHz}$, and $\omega_2/(2\pi) \simeq 20 \text{ MHz}$

	[P ₆₆₆₁₄][Cl]		[P ₆₆₆₁₄][Cl]/ [P ₆₆₆₁₄][FeCl ₄]	
	CH ₂	CH ₃	CH ₂	CH ₃
$\sqrt{\langle r^2 \rangle} (10^{-10} \text{ m})$	1.6 ± 0.027	2.5 ± 0.014	1.6 ± 0.027	2.5 ± 0.014
$\tau_{d_1} (10^{-9} \text{ s})$	–	–	6.02 ± 0.73	6.35 ± 0.59
$\tau_s (10^{-11} \text{ s})$	–	–	1.0 ± 0.064	–
$\tau_{d_0} (10^{-8} \text{ s})$	–	–	7.34 ± 0.35	–
$A_{Rot_1} (10^8 \text{ s}^{-2})$	7.33 ± 0.3	1.85 ± 0.2	7.33 ± 0.3	1.85 ± 0.2
$\tau_1 (10^{-8} \text{ s})$	1.0 ± 0.1	1.18 ± 0.1	1.0 ± 0.1	1.18 ± 0.1
$A_{Rot_2} (10^9 \text{ s}^{-2})$	3.03 ± 0.1	2.81 ± 0.1	3.03 ± 0.1	2.81 ± 0.1
$\tau_2 (10^{-10} \text{ s})$	5.16 ± 0.2	4.8 ± 0.1	5.16 ± 0.2	4.8 ± 0.1
$A_{CR1} (10^7 \text{ s}^{-2})$	–	–	1.3 ± 0.4	2.5 ± 0.11
$\tau_{CR1} (10^{-7} \text{ s})$	–	–	5.0 ± 3.2	5.0 ± 3.2
$A_{CR2} (10^8 \text{ s}^{-2})$	–	–	1.5 ± 0.3	2.5 ± 0.9
$\tau_{CR2} (10^{-7} \text{ s})$	–	–	5.0 ± 0.2	–

the superparamagnetic-like relaxation effect observed for the $[\text{P}_{66614}][\text{Cl}]/[\text{P}_{66614}][\text{FeCl}_4]$ system can be observed using a non ionic liquid solvent, additional measurements were made using solutions of $[\text{P}_{66614}][\text{FeCl}_4]$ in DMSO. The viscosity measurements showed that viscosity was independent of the magnetic field for DMSO/ $[\text{P}_{66614}][\text{FeCl}_4]$ 1% (v/v) (See Table 3.2). In Figure 3.4 are presented the relaxivity results according to eq. 3.2, as a function of the proton Larmor frequency for a 10mM sample DMSO/ $[\text{P}_{66614}][\text{FeCl}_4]$.

The measured R_1 corresponds to the DMSO protons in the view of small concentration of the ionic liquid. The R_1 0.52 s^{-1} of the pure DMSO was frequency independent in the range of 8 kHz to 300 MHz. As it can be noticed, the relaxivity dispersion presents a much less pronounced paramagnetic contribution in comparison with the relaxation enhancement effect observed for the $[\text{P}_{66614}][\text{Cl}]/[\text{P}_{66614}][\text{FeCl}_4]$ system with a close molar concentration (14 mM). The relaxivity dispersion is described by the sum of *inner*-sphere, $(T_1^{-1})_{is}$, and *outer*-sphere, $(T_1^{-1})_{os}$, relaxation contributions.

$$r_1 = (T_1^{-1})_{is} + (T_1^{-1})_{os} \quad (3.3)$$

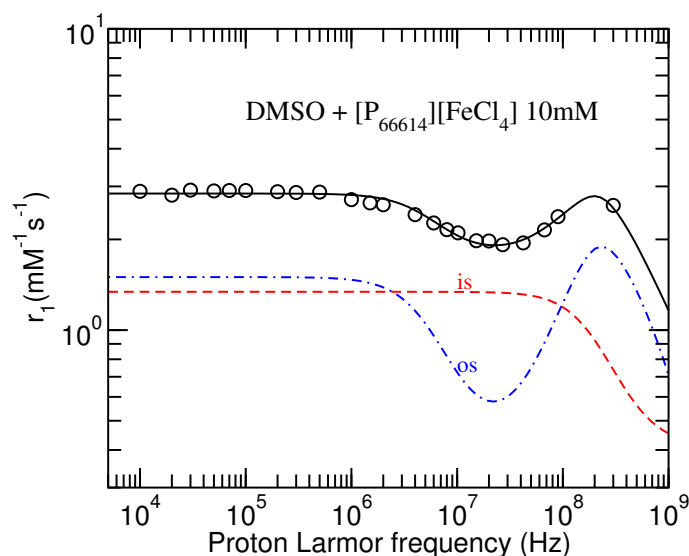


Figure 3.4: Experimental results and model fitting curves for the relaxivity as a function of frequency for the 10mM DMSO/[P₆₆₆₁₄][FeCl₄] system, as explained in the text.

The details of the models used for these two relaxations mechanisms can be found in the Appendix A. The only free fitting parameters were the distance between the FeCl₄⁻ ions and the DMSO molecules, r_{FeH} and R_{FeH} , for the *is* and *os* relaxation contributions, respectively, the correlation time τ_{mH} for the *is* inner relaxation, and the correlation time τ_v and the mean square fluctuations Δ^2 of the electronic zero-field-splitting (ZFS) relaxation contribution. The values obtained from the fit were: $r_{\text{FeH}} = (3.5 \pm 0.2)\text{\AA}$, $R_{\text{FeH}} = (8.0 \pm 0.3)\text{\AA}$, $\tau_{mH} = (1.12 \pm 0.007) \times 10^{-12} \text{ s}$, $\tau_v = (2.6 \pm 0.25) \times 10^{-12} \text{ s}$, and $\Delta^2 = (2.9 \pm 0.3) \times 10^{10} \text{ s}^{-2}$.

During the mixing process of [P₆₆₆₁₄][FeCl₄] MIL with DMSO no chemical reaction was observed involving the FeCl₄⁻. This observation was further confirmed by preparing a 10mM solution of FeCl₃ hexahydrate and DMSO. The relaxivity results obtained for this system can be found in the Appendix A for comparison. It is worthwhile to mention that the physically consistent fits could only be obtained considering that the FeCl₄⁻ ions were surrounded by around 8 DMSO molecules with very short resident times.

In view of the fact that the chlorine atoms remain covalently bounded to Fe there is no actual binding between DMSO molecules to Fe. Therefore, it is reasonable to obtain τ_{mH} values close to the characteristic times of methyl groups rotation [82], in contrast to the long resident times of water molecules in the case of conventional contrast agent paramagnetic complexes.

In Figure 3.5 are presented results of the proton spin-lattice relaxation rate as a function of the ionic liquid concentration in DMSO for three selected Larmor frequencies. As it can be observed, the spin-lattice relaxation of the DMSO/[P₆₆₆₁₄][FeCl₄] solutions is certainly well described by eq. 3.2 for concentration below $\sim 10\text{mM}$. The values of relaxivity depend on the frequency and vary in the range $2\text{--}3 \text{ mM}^{-1}\text{s}^{-1}$. These values

are higher than the iron(III) complexes recently reported which are good candidates for further development in order to be used as MRI contrast agents [83].

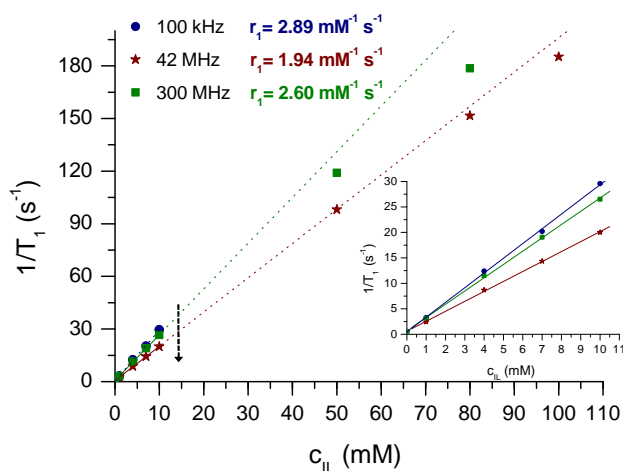


Figure 3.5: Experimental results of the DMSO spin-lattice relaxation as a function of $[\text{P}_{66614}][\text{FeCl}_4]$ concentration. Relaxivities were estimated for three selected Larmor frequencies, as explained in the text. The arrow in the inset figure represent the concentration corresponding to the mixture $[\text{P}_{66614}][\text{Cl}]/[\text{P}_{66614}][\text{FeCl}_4]$ studied here.

From the results obtained it is possible to conclude that $[\text{P}_{66614}][\text{FeCl}_4]$ acts as a typical contrast agent enhancing the spin-lattice relaxation rate with a relaxivity well described by the usually accepted paramagnetic relaxations mechanisms for *inner* sphere and *outer* sphere interactions. In contrast, in the mixture of $[\text{P}_{66614}][\text{FeCl}_4]$ with $[\text{P}_{66614}][\text{Cl}]$ ionic liquid the effect of the paramagnetic ions on the spin-lattice relaxation of the solvent molecules protons' spins system cannot be described by the linear combination of the non-paramagnetic and paramagnetic relaxation contributions (eq. 3.2) where the paramagnetic contribution is proportional to the concentration.

In fact, the relaxation enhancement effect due to the presence of $[\text{FeCl}_4]^-$ ions must be negligible for frequencies below 10MHz. Actually, a detailed observation of the experimental results (see Figures 3.2 and 3.3) reveals that at low frequencies the relaxation rate for the $[\text{P}_{66614}][\text{Cl}]/[\text{P}_{66614}][\text{FeCl}_4]$ system is smaller than that of $[\text{P}_{66614}][\text{Cl}]$. Therefore, it seems that the presence of the $[\text{FeCl}_4]^-$ ions, affects more the motions of the cations' aliphatic chains, more than Cl. Together with the paramagnetic relaxation it produces just a small change in the spin-lattice relaxation at low frequencies.

The super-paramagnetic relaxation observed for the $[\text{P}_{66614}][\text{Cl}]/[\text{P}_{66614}][\text{FeCl}_4]$ R_1 dispersion as well as the viscosity's dependence on the magnetic field, seems to be associated with ionic nature of the $[\text{P}_{66614}][\text{Cl}]$ solvent in comparison with the non ionic DMSO.

3.6 Conclusions

In this work is presented a ^1H Nuclear Magnetic Relaxation dispersion study of the molecular dynamics of the neat ionic liquid $[\text{P}_{66614}][\text{Cl}]$ and the binary mixtures of magnetic ionic liquid $[\text{P}_{66614}][\text{FeCl}_4]$ with $[\text{P}_{66614}][\text{Cl}]$ and with DMSO. The proton spin-lattice relaxation was measured over the broad frequency range between 8 kHz - 300 MHz at 22 °C. In addition, viscosity measurements were made as a function of an applied magnetic field in the range 0 - 2T. The longitudinal magnetization decay with time was found to be bi-exponential and characterized by relaxation rates R_{12} and R_{11} in consistency with the number of CH_2 and CH_3 groups in the cation molecules, respectively.

For both $[\text{P}_{66614}][\text{Cl}]$ and the mixtures DMSO/ $[\text{P}_{66614}][\text{FeCl}_4]$ it was observed that the viscosity was independent from the magnetic field. In the case of the mixtures of $[\text{P}_{66614}][\text{FeCl}_4]$ with $[\text{P}_{66614}][\text{Cl}]$ it was observed that the viscosity decreased with the magnetic field strength and at 2T the viscosity was 13% less than at 0T.

The spin-lattice relaxation results were analyzed for all MILs mixtures taking into account the relaxation mechanisms associated to the molecular motions typically observed for these systems. In the case of DMSO/ $[\text{P}_{66614}][\text{FeCl}_4]$ and $[\text{P}_{66614}][\text{Cl}]/[\text{P}_{66614}][\text{FeCl}_4]$ spin-lattice relaxation results additional paramagnetic relaxation contributions were considered due to the presence of the magnetic ions.

The spin-lattice relaxation dispersion observed for the DMSO/ $[\text{P}_{66614}][\text{FeCl}_4]$ was quite different from that detected for the pure DMSO as expected due to the presence of iron ions in the mixtures. In fact, the $[\text{FeCl}_4]^-$ anions constitute a paramagnetic relaxation agent increasing the proton spin-lattice relaxation rate with a paramagnetic contribution that depends linearly on the concentration of the $[\text{FeCl}_4]^-$ ions for small concentrations, as usually found for known iron based contrast agents.

The R_1 dispersions observed for the $[\text{P}_{66614}][\text{Cl}]/[\text{P}_{66614}][\text{FeCl}_4]$ system are significantly different from those where DMSO was the solvent. The R_1 dispersion obtained for systems using $[\text{P}_{66614}][\text{Cl}]$ as solvent evidences a combination of relaxation mechanisms associated with molecular motions obviously not found when it is replaced by DMSO, due to the considerable differences in the molecular structure, and consequently in the local molecular organization considering the ionic character of the phosphonium salt. In the case of $[\text{P}_{66614}][\text{Cl}]/[\text{P}_{66614}][\text{FeCl}_4]$ system, the paramagnetic relaxation contribution is dominant in high frequency range, as it was previously observed for a quaternarium ammonium magnetic ionic liquid system, but is negligible at lower frequencies. In this system, the proton spin-lattice relaxation clearly does not depend linearly on the concentration of $[\text{FeCl}_4]^-$ ions. The presence of the $[\text{FeCl}_4]^-$ ions in the $[\text{P}_{66614}][\text{Cl}]$ ionic medium seems to affect the local molecular organization and the relative contribution of molecular motions to the spin-lattice relaxation. The differences observed in the R_1 dispersion of $[\text{P}_{66614}][\text{Cl}]/[\text{P}_{66614}][\text{FeCl}_4]$ with respect to that of $[\text{P}_{66614}][\text{Cl}]$ reflect the contribution of a paramagnetic relaxation and the changes in the molecular order, dynamics and packing.

When comparing the paramagnetic relaxation contributions detected for the $[\text{P}_{66614}][\text{Cl}]$

/ $[\text{P}_{66614}][\text{FeCl}_4]$ and $\text{DMSO}/[\text{P}_{66614}][\text{FeCl}_4]$ the stronger enhancement of the R_1 dispersion due to the amplitude of this mechanism in the $[\text{P}_{66614}][\text{Cl}]/[\text{P}_{66614}][\text{FeCl}_4]$ system is perhaps due to the coupling between the magnetic moments of the $[\text{FeCl}_4]^-$ ions as the result of the ionic nature of the $[\text{P}_{66614}][\text{Cl}]$ acting as a solvent in comparison with an organic solvent such as DMSO.

The results obtained in this work suggest the possibility of using MILs as contrast agents, provided that their toxicity is reduced. One possibility, that requires future studies is the replacement of the ILs cations (ex. phosphonium or quaternary ammonium) by bio compatible water-soluble cations, like those present in several vitamin complexes, coordinated with a magnetic anion, such as $[\text{FeCl}_4]$.

A GROUP CONTRIBUTION METHOD FOR THE INFLUENCE OF THE TEMPERATURE IN THE VISCOSITY OF MAGNETIC IONIC LIQUIDS

Published as: C. I. Daniel, J. Albo, E. Santos, C.A.M. Portugal, J.G. Crespo, A. Irabien, "A group contribution method for the influence of the temperature in the viscosity of magnetic ionic liquids", Fluid Phase Equilibria, 360, (2013) 29-35.

4.1 Summary

Ionic liquids are widely under research due to their potential properties as solvents. The prediction of their physicochemical properties is an important strategy to achieve a better knowledge for further applications.

The present work applies a group contribution method to estimate the viscosity at different temperatures of a new generation of ionic liquids, magnetic ionic liquids (MILs), which are comprised by anions containing transition metal complexes. These new substances have received a high interest due to their response at the presence of a magnetic field. In this study the magnetic ionic liquids are based on the phosphonium cation $[P_{66614}]^+$ with different number of cations chains and on the magnetic anions: $[GdCl_6]^{3-}$, $[MnCl_4]^{2-}$, $[FeCl_4]^-$ and $[CoCl_4]^{2-}$.

The database covers a wide range of temperature, 293.15 - 373.15K, and viscosity 44 - 123500 cP. The modeling estimations show a good agreement with the experimental results, presenting a mean percentage deviation of 7.64%. These results confirm the interest of this model for the estimation of viscosity and the influence of the temperature, which can be extended for a large variety of group combinations in magnetic ionic liquids leading to different applications.

4.2 Introduction

Ionic liquids (ILs) have been receiving a high interest for their unique physicochemical properties. They may be regarded as organic solvents comprised entirely by ions in the liquid state over a wide temperature range including room temperature (RTILs - room temperature ionic liquids). These ILs show a low melting point, high thermal stability and thermal capacities, non-measurable vapor pressure and they are non-flammable, and reusable. Additionally, their physicochemical properties can be modified by changing their cationic and anionic composition according to their specific task, being recognized as “green and designer solvents” [24].

A new generation of magnetic sensitive ionic liquids - magnetic ionic liquids (MILs), exhibiting a response to the magnetic field has been developed [19, 34, 35]. MILs are comprised by anions containing transition metal complexes, having properties (solubility, viscosity, surface tension and molecular orientation), that may be influenced by the presence of an applied magnetic field [19, 20, 34, 35]. Actually, magnetically induced changes of IL solubility were confirmed by the dependence found between the concentration of binary MIL/water mixtures and the applied magnetic field strength [19].

A deeper knowledge about the fundamental properties of ILs is required, including: density, viscosity, solubility, surface tension, refractive index and speed of sound, in order to better understand their structure-properties relationships [84]. One of the important physical properties of ILs is viscosity [85], which is higher for most ILs than for common organic solvents. The viscosity of ILs may be adjusted by a judicious cation-anion combination leading to ILs with lower or higher viscosity depending on the requirements. ILs estimation models for the temperature influence in the viscosity are available in the literature supported in different assumptions. The widely used are: Arrhenius-like law [86], Vogel-Fulcher-Tamman (VFT) [87, 88, 89], modified Vogel-Fulcher-Tamman (mVFT) [90], Litovitz, fluidity equation [91] and Orrick-Erbar equation [92]. The group contribution methods are common to estimate the viscosity of complex molecules, such as: Orrick-Erbar equation [92], Sastry-Rao method [93] and the UNIFAC-VISCO method [94]. In this method it is assumed that the physicochemical properties of the molecules are the summation of the contribution of their atoms and /or fragments [95].

The Vogel-Fulcher-Tamman (VFT) has been used recently, [96] as a new correlation based on the group contribution model to predict the viscosity, electrical conductivity, thermal conductivity, refractive index, isobaric expansivity and isothermal compressibility of ILs. This correlation has been applied instead of the Orrick-Erbar equation to overcome the limitation of density data. The density is a fundamental property of the compounds and recent works are focused on energetic ILs/salts, since ionic compounds present many advantages over molecular species such as low vapor pressure and high density values [97].

The correlation of the IL density may be based on different models [84], [97]. Jenkins proposed an equation based on the contribution of the cation and anion volumes, where

the molar volume of the molecule is the summation of the two contributions [98]. The Ye and Shreeve method has followed this theory for RTILs and salts [97] and its extension from R. Gardas et al. [99] is based on the same assumptions, but including others parameters to estimate densities accurately.

The aim of the present work is the estimation of the viscosity at different temperatures of MILs using the Orrick-Erbar equation [92, 100] with the contribution of the MILs structure, considering the phosphonium cation $[P_{66614}]^+$ with different number of cations chains and the magnetic anions: $[GdCl_6]^{3-}$, $[MnCl_4]^{2-}$, $[FeCl_4]^-$ and $[CoCl_4]^{2-}$. The density is correlated using the model proposed by R.Gardas et al. [99] which is currently applied to describe the influence of the temperature in the viscosity of different compounds.

4.3 Experimental

4.3.1 Materials and Methods

The selected MILs based on the phosphonium cation were:

- Trihexyl(tetradecyl)phosphonium hexachlorogadolinium: $[P_{66614}]_3 [GdCl_6]$
- Trihexyl(tetradecyl)phosphonium tetrachloromanganate: $[P_{66614}]_2 [MnCl_4]$
- Trihexyl(tetradecyl)phosphonium tetrachloroferrate: $[P_{66614}] [FeCl_4]$
- Trihexyl(tetradecyl)phosphonium tetrachlorocobaltate: $[P_{66614}]_2 [CoCl_4]$

The MILs were prepared in the Faculdade de Farmácia, Universidade de Lisboa according to the experimental procedure reported elsewhere [36, 39]. Their properties, molecular weight, density and water content at room temperature are listed in Table 4.1. The density of MILs was determined gravimetrically with a pycnometer and their water content was measured using Karl-Fisher technique [36].

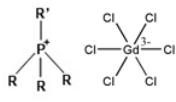
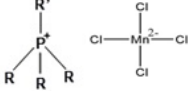
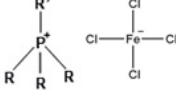
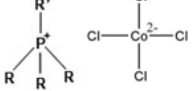
The experimental viscosities and densities were measured using a rheometer (Haake RS75), covering the range of temperature, 293.15 - 373.15K as presented in Table 4.2.

Table 4.2 shows the experimental results of viscosity with the temperature, which includes 20 experimental data points for MILs based on the same phosphonium cation and four magnetic anions. Comparing the present data with the literature [95], this study covers a wide range of viscosities, 44 - 123500 cP.

4.4 Results and Discussion

The group contribution method based on the Orrick-Erbar model [92], described by eq. 4.1, was applied to estimate the viscosity for different temperatures of these MILs. For the ionic liquids, the group contribution is due to the presence of cations and anions. In the present case the contribution is divided in the phosphonium cation $[P_{66614}]^+$ with different number of cations chains and in the four magnetic anions: $[GdCl_6]^{3-}$, $[MnCl_4]^{2-}$, $[FeCl_4]^-$ and $[CoCl_4]^{2-}$.

Table 4.1: Properties of the magnetic ionic liquids

MILs	Structure	Molecular Weight (g mol ⁻¹)	Density (g cm ⁻³)	Water content (% wt.)
[P ₆₆₆₁₄] ₃ [GdCl ₆]		1821.5	0.982	0.2
[P ₆₆₆₁₄] ₂ [MnCl ₄]		1103.0	0.956	0.35
[P ₆₆₆₁₄][FeCl ₄]		681.5	1.012	1.02
[P ₆₆₆₁₄] ₂ [CoCl ₄]		1112.0	0.965	5.1 × 10 ⁻⁴

$$\ln\left(\frac{\eta}{\rho \times M}\right) = A + \frac{B}{T} \quad (4.1)$$

Eq. 4.1 can be decomposed in the two contributions of the Ionic liquids:

$$\ln\left(\frac{\eta}{\rho \times M}\right) = n \times \left(A^+ + \frac{B^+}{T}\right) + \left(A^- + \frac{B^-}{T}\right) \quad (4.2)$$

Where η is the viscosity (cP), ρ is the density (g cm⁻³), M is the molecular weight (g mol⁻¹), T is the absolute temperature (K), A and B are the Orrick-Erbar parameters, n stands for the number of cations chains, A^+ , B^+ are the parameters of cation contribution, and A^- , B^- are the parameters of anion contribution for the viscosity.

The phosphonium cation is common for all the MILs, although the number of cations chains is different, as well as the magnetic anion. Therefore, the global equation of the model can be written as follows:

$$\ln\left(\frac{\eta}{\rho \times M}\right) = n_i \times \left(A + B \times \frac{1}{T}\right) + \sum_i \left(A_i + B_i \times \frac{1}{T}\right) \quad (4.3)$$

Where n_i is the number of cations chains, A and B are the parameters of cation contribution and A_i and B_i are the parameters of anions contribution.

The dependent variable $\ln\left(\frac{\eta}{\rho \times M}\right)$ includes the density. The model of Orrick and Erbar uses only the density at 293K [92], however, other recent studies [99] using an extension of the Ye and Shreeve method [97], proposed a predictive method for ILs, using the density as a function of temperature. The experimental densities are reported in Table 4.2, and the

Table 4.2: Experimental Viscosities and densities of the MILs at different temperatures

Phosphonium-MILs	T(K)	η (cP)	ρ (g cm ⁻³)
[P ₆₆₆₁₄] ₃ [GdCl ₆]	293.15	28230	0.983
	298.15	18390	0.981
	303.15	13010	0.979
	323.15	2980	
	373.15	290	
[P ₆₆₆₁₄] ₂ [MnCl ₄]	293.15	112300	0.956
	298.15	75230	0.949
	303.15	41560	0.943
	323.15	13970	
	373.15	920	
[P ₆₆₆₁₄][FeCl ₄]	293.15	790	1.012
	298.15	650	1.008
	303.15	520	1.004
	323.15	230	
	373.15	44	
[P ₆₆₆₁₄] ₂ [CoCl ₄]	293.15	123500	0.965
	298.15	83450	0.962
	303.15	40250	0.959
	323.15	15360	
	373.15	11050	

density dependency with temperature is estimated according with the following equation [100]:

$$\rho = \frac{M}{NV(a + bT + cP_1)} \quad (4.4)$$

where, ρ is the density (g cm⁻³), M is the molecular weight (g mol⁻¹), N = Avogadro constant (mol⁻¹), V = molecular volume (Å³), T = temperature (K), P_1 = Pressure (MPa) and a , b and c are coefficients to be estimated by fitting. The behavior of the density with temperature was described by eq.4.4, following the same modeling procedure for the ILs group contribution model. This model includes the contribution of the density for the

final viscosity estimation [99, 100].

The density of MILs in this temperature range was estimated by the model following equation eq.4.4, all the experiments were performed at constant pressure (atmospheric pressure), P is constant, and eq.4.4 can be simplified to eq.4.5:

$$\rho = \frac{1}{(\alpha + \beta T)} \quad (4.5)$$

where,

$$\alpha = \frac{NV}{M}(a + cP) (\text{\AA}^3 \text{ Kg}^{-1} \text{ MPa})$$

$$\beta = \frac{NVb}{M} (\text{\AA}^3 \text{ K}^{-1} \text{ Kg}^{-1})$$

Equation eq.4.5 includes the parameters α and β as parameters and the estimation of the parameters has been carried out using *Fitteia* software. Results are shown in Table 4.3.

Table 4.3: Fitted parameters for the prediction of the density of the studied MILs

Phosphonium-MILs	$\alpha(\text{\AA}^3 \text{ Kg}^{-1} \text{ MPa})$	$\beta(\text{\AA}^3 \text{ K}^{-1} \text{ Kg}^{-1})$	MPD(%) (95%)	χ^2
[P ₆₆₆₁₄] ₃ [GdCl ₆]	9.3×10^{-4}	3.1×10^{-7}	0.25	0.02
[P ₆₆₆₁₄] ₂ [MnCl ₄]	5.8×10^{-4}	1.6×10^{-6}	0.28	1.9
[P ₆₆₆₁₄][FeCl ₄]	7.6×10^{-4}	7.7×10^{-7}	0.21	0.2
[P ₆₆₆₁₄] ₂ [CoCl ₄]	8.2×10^{-4}	7.4×10^{-7}	0.14	0.4
Global fit			0.22	

The MPD values obtained are between 0.14 - 0.28% , with 0.22% for the global fit when all MILs are included, in agreement with the 0.29% value previously obtained in a similar study for ILs from literature [100]. Normalized variables were used instead of their absolute values in order to avoid the influence of the absolute value on the parameter estimation. Dimensionless viscosity and $1/T$, Y^* and X^* , respectively, take the values between +1 and -1 as calculated by the eq.4.6 and eq.4.7:

$$Y^* = \frac{-Y + \left(\frac{Y_{MAX} + Y_{MIN}}{2}\right)}{\left(\frac{Y_{MAX} - Y_{MIN}}{2}\right)} \quad (4.6)$$

$$X^* = \frac{-X + \left(\frac{X_{MAX} + X_{MIN}}{2}\right)}{\left(\frac{X_{MAX} - X_{MIN}}{2}\right)} \quad (4.7)$$

The Y_{MAX} and X_{MAX} are the maximum values of $\ln\left(\frac{\eta}{\rho \times M}\right)$ and $1/T$. The Y_{MIN} and X_{MIN} are the minimum values. The values are showed in Table 4.4. To determine the dependence of the contribution of each group (cation and anion), it is necessary to define the descriptors for the MILs, shown in Table 4.5 and Table 4.6.

Table 4.4: Absolute and normalized variables for MILs viscosity and temperature

Phosphonium-MILs	T (K)	1/T(K ⁻¹)	ln($\eta/\rho \times M$)	Normalized 1/T	Normalized ln($\eta/\rho \times M$)
[P ₆₆₆₁₄] ₃ [GdCl ₆]	293.15	0.00341	2.76	-1.00	-0.48
	298.15	0.00335	2.33	-0.84	-0.37
	303.15	0.00330	1.99	-0.69	-0.28
	323.15	0.00309	0.52	-0.13	0.11
	373.15	0.00268	-1.79	1.00	0.72
[P ₆₆₆₁₄] ₂ [MnCl ₄]	293.15	0.00341	4.67	-1.00	-0.98
	298.15	0.00335	4.28	-0.84	-0.88
	303.15	0.00330	3.69	-0.69	-0.72
	323.15	0.00309	2.63	-0.13	-0.44
	373.15	0.00268	-0.02	1.00	0.25
[P ₆₆₆₁₄][FeCl ₄]	293.15	0.00341	-0.01	-1.00	0.25
	298.15	0.00335	-0.21	-0.84	0.30
	303.15	0.00330	-0.43	-0.69	0.36
	323.15	0.00309	-1.24	-0.13	0.57
	373.15	0.00268	-2.87	1.00	1.00
[P ₆₆₆₁₄] ₂ [CoCl ₄]	293.15	0.00341	4.75	-1.00	-1.00
	298.15	0.00335	4.36	-0.84	-0.90
	303.15	0.00330	3.63	-0.69	-0.71
	323.15	0.00309	2.68	-0.13	-0.46
	373.15	0.00268	2.39	1.00	-0.38

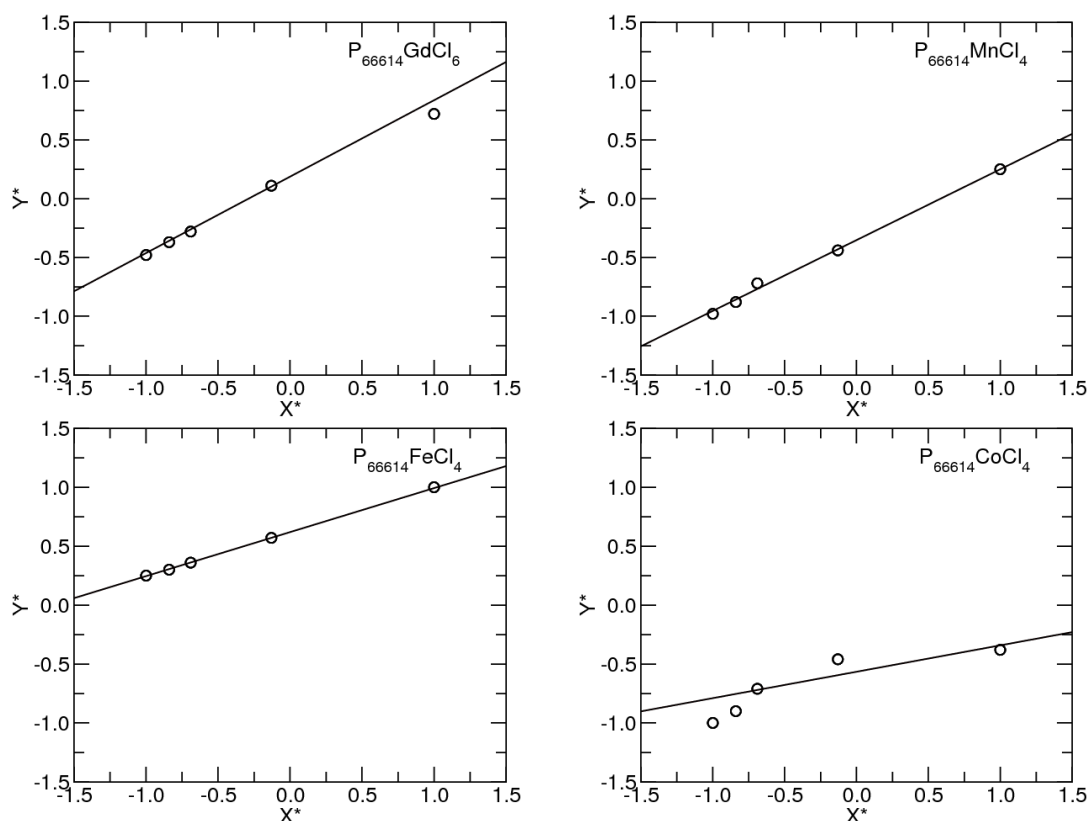
The dimensionless viscosity can be calculated by this group contribution model, following Eq.4.2, rewritten in this context:

$$Y^* = n_i \times (A^* + B^* \times X^*) + \sum_i (A_i^* + B_i^* \times X^*) \quad (4.8)$$

From the results shown in Table 4.7 and Figure 4.1, it can be observed that there is a negative anion contribution to the viscosity in the following order: [GdCl₆]³⁻ < [CoCl₄]²⁻ < [MnCl₄]²⁻ < [FeCl₄]⁻, counteracting to the positive cation effect. Considering the absolute parameters values, a higher anion contribution for the viscosity has been found when comparing with the cation.

Table 4.5: Group contribution to the dimensionless viscosity

Group	Molecular descriptor
Cation	
n	Influence of the number of cations chains (1, 2 or 3)
A* and B*	Influence of the phosphonium cation:[P ₆₆₆₁₄]. 1 if it exists and 0 if not exists.
Anion	
A ₁ * and B ₁ *	Influence of the anion: GdCl ₆ , 1 if it exists and 0 if not exists
A ₂ * and B ₂ *	Influence of the anion: MnCl ₄ , 1 if it exists and 0 if not exists
A ₃ * and B ₃ *	Influence of the anion: FeCl ₄ , 1 if it exists and 0 if not exists
A ₄ * and B ₄ *	Influence of the anion: CoCl ₄ , 1 if it exists and 0 if not exists
Number of descriptors	11


 Figure 4.1: Normalized viscosity fitted for all the MILs by Orrick-Erbar correlation using *Fitteia* software.

The temperature influence of the cation to the viscosity of MILs, is less relevant than that observed for the contribution of the anions, as is shown by the negligible B* value

Table 4.6: MILs viscosity, dimensionless viscosity Y^* and group contribution descriptors

Phosphonium-MILs	$1/T(K^{-1})$	$\ln(\eta/\rho \times M)$	Y^*	n	A^*	B^*	A_1^*	A_2^*	A_3^*	A_4^*	B_1^*	B_2^*	B_3^*	B_4^*
[P ₆₆₆₁₄] ₃ [GdCl ₆]				3	1	1	1	0	0	0	1	0	0	0
	0.00341	2.76	-0.48											
	0.00335	2.33	-0.37											
	0.00330	1.99	-0.28											
	0.00309	0.52	0.11											
	0.00268	-1.79	0.72											
[P ₆₆₆₁₄] ₂ [MnCl ₄]				2	1	1	0	1	0	0	0	1	0	0
	0.00341	4.67	-0.98											
	0.00335	4.28	-0.88											
	0.00330	3.69	-0.72											
	0.00309	2.63	-0.44											
	0.00268	-0.02	0.25											
[P ₆₆₆₁₄][FeCl ₄]				1	1	1	0	0	1	0	0	0	1	0
	0.00341	-0.01	0.25											
	0.00335	-0.21	0.30											
	0.00330	-0.43	0.36											
	0.00309	-1.24	0.57											
	0.00268	-2.87	1.00											
[P ₆₆₆₁₄] ₂ [CoCl ₄]				2	1	1	0	0	0	1	0	0	0	1
	0.00341	4.75	-1.00											
	0.00335	4.36	-0.90											
	0.00330	3.63	-0.71											
	0.00309	2.68	-0.46											
	0.00268	2.39	-0.38											

(B^* (K) = 0.07 ± 0.06).

Actually, the influence of temperature on the contribution of the anions to viscosity of MILs is considerable and increases according to the following order (as it shown in Table 4.7): $[\text{CoCl}_4]^{2-} < [\text{FeCl}_4]^- < [\text{GdCl}_6]^{3-} < [\text{MnCl}_4]^{2-}$. For the $[\text{CoCl}_4]^{2-}$ magnetic anion, the temperature has the lowest influence (B^* (K) = 0.088 ± 0.05).

The experimental and calculated viscosities are shown in Figure 4.2, which shows the parity plot.

The mean percentage deviation (MPD) obtained was 7.64% (similar to the 7.78% value obtained for a similar study of ILs from the literature [100]). Table 4.8 presents a resume of the main statistic parameters of the group contribution model of this work, with a good agreement between experimental and calculated viscosity, described with a $R^2=0.98$.

Table 4.7: Group contribution parameters fitted by Orrick-Erbar correlation eq 4.2 for the normalized viscosity and temperature of the MILs

Phosphonium-MILs	Contribution		
	A*	B* (K)	χ^2
			28.8
Cation			
[P ₆₆₆₁₄] ⁺	0.8 ± 0.03	0.07 ± 0.06	
Anion			
[GdCl ₆] ³⁻	-2.3 ± 0.09	0.45 ± 0.19	
[MnCl ₄] ²⁻	-2.0 ± 0.06	0.47 ± 0.13	
[FeCl ₄] ⁻	-0.21 ± 0.07	0.31 ± 0.07	
[CoCl ₄] ²⁻	-2.2 ± 0.06	0.088 ± 0.05	

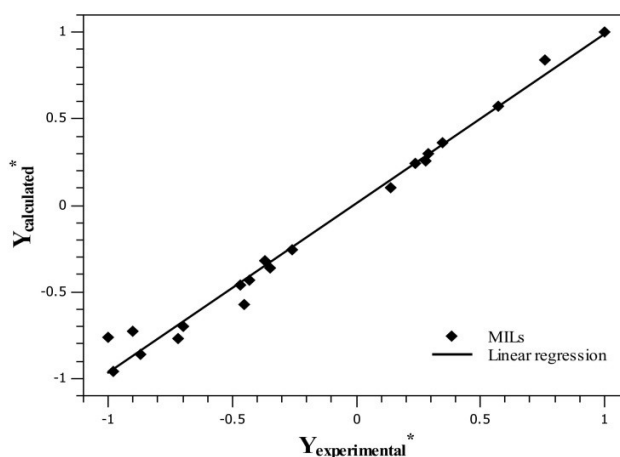


Figure 4.2: Experimental and calculated dimensionless MILs viscosity results using Orrick-Erbar correlation.

In order to compare the group contribution parameters with those described in the literature [100], the absolute values have to be fitted to obtain the absolute parameters, A and B, which are represented in Table 4.9.

Comparing the absolute values with the literature [100], there is a positive cation contribution and a negative anion contribution for the ILs and MILs viscosity. Table 4.10 shows the cation's contribution in the present work and in a previous literature study [100].

From these comparisons it can be concluded that the phosphonium cation has a lower contribution (A values) comparing with imidazolium, pyridinium and pyrrolidinium

Table 4.8: Statistic parameters of the datasheet

Data Number	20
Maximum value (Y)	4.75
Minimum value (Y)	-2.87
Average (Y)	1.71
Median	2.36
Standard deviation	2.30

Table 4.9: Absolute values of the parameters of Orrick-Erbar correlation for viscosity of the MILs

Phosphonium-MILs	Contribution		
	A	B (K)	χ^2
			18.3
Cation			
[P ₆₆₆₁₄] ⁺	1.48 ± 0.08	975 ± 2.7	
Anion			
[GdCl ₆] ³⁻	-22.9 ± 0.4	3426 ± 129.3	
[MnCl ₄] ²⁻	-19.8 ± 0.02	4333 ± 7.9	
[FeCl ₄] ⁻	-14.3 ± 0.01	2772 ± 3.2	
[CoCl ₄] ²⁻	-7.56 ± 0.95	581 ± 312.23	

cations, and the temperature (B values) has a lower influence in the viscosity for the phosphonium than the others cations. Table 4.11 shows the comparison of the anions contribution in the present work and in a previous literature study [100].

In the anions contribution of MILs, the values of parameter A for the [FeCl₄]⁻ and [CoCl₄]²⁻ have the lowest contribution, comparing to other MILs and ILs for the reduction of ILs viscosity. The temperature, parameter B, has the lowest influence in the [CoCl₄]²⁻ and [Tf₂N]⁻ anions and the larger influence in [MnCl₄]²⁻ and [Cl]⁻ anions.

Table 4.10: Comparison of the A and B parameters of Orrick-Erbar correlation for different cations of MILs and ILs

ILs and MILs cations	Contribution	
	A	B (K)
Cations		
Phosphonium ¹	1.48	975
Imidazolium ²	6.56	1757
Pyridinium ²	6.87	1704
Pyrrolidinium ²	5.43	2233

¹present work ²literature [100].

Table 4.11: Comparison of the A and B parameters of Orrick-Erbar correlation for different anions of MILs and ILs

ILs and MILs anions	Contribution	
	A	B (K)
Anions		
¹ [GdCl ₆] ³⁻	-22.9	3426
¹ [MnCl ₄] ²⁻	-19.8	4333
¹ [FeCl ₄] ⁻	-14.3	2772
¹ [CoCl ₄] ²⁻	-7.56	581
² [PF ₆] ⁻	-20.49	2099
² [BF ₄] ⁻	-18.1	1192
² [Tf ₂ N] ⁻	-17.4	510
² [Cl] ⁻	-27.6	5458
² [CH ₃ COO] ⁻	-21.3	2742
² [MeSO ₄] ⁻	-19.5	1733
² [EtSO ₄] ⁻	-19.1	1587
² [CF ₃ SO ₃] ⁻	-17.7	906

¹present work ²literature [100].

4.5 Conclusions

This work shows a group contribution method based on the Orrick-Erbar equation, for the estimation of the influence of the temperature in the viscosity for a new class of ionic liquids, the magnetic ionic liquids, based on the phosphonium cation with different number of chains and distinct magnetic anions, which are: $[P_{66614}]_3 [GdCl_6]$, $[P_{66614}]_2 [MnCl_4]$, $[P_{66614}] [FeCl_4]$ and $[P_{66614}]_2 [CoCl_4]$. The model assumes the summation of group contribution from cations and anions.

A data base with 20 points for a wide range of temperature 293.15-373.15K and viscosity 44-123500 cP was used. The results obtained are comparable with a previous study and show a 7.64% of mean percentage deviation (MPD) and $R^2 = 0.98$. This result means that the calculated viscosities based on this model are in a good agreement with the experimental values and, therefore this model is applicable for the prediction of MIL viscosities. In this work the cations with different number of chains have a positive contribution for the MILs viscosity and the anions a negative one. Further work will expand this study in order to include new magnetic ionic liquids with other cations and anions. Results agree well with previous literature data.

PERMEABILITY MODULATION OF SUPPORTED MAGNETIC IONIC LIQUID MEMBRANES (SMILMs) BY AN EXTERNAL MAGNETIC FIELD

Published as: E. Santos, J. Albo, C. I. Daniel, C.A.M. Portugal, J.G. Crespo, A. Irabien, "Permeability modulation of Supported Magnetic Ionic Liquid Membranes (SMILMs) by an external magnetic field", Journal of Membrane Science 430, (2013) 56-61.

5.1 Summary

This work is focused on the permeability modulation of Supported Magnetic Ionic Liquid Membranes (SMILMs) for CO₂ separation, when applying an external magnetic field. Four magnetic ionic liquids (MILs) have been studied ([P₆₆₆₁₄]₂ [CoCl₄], [P₆₆₆₁₄] [FeCl₄], [P₆₆₆₁₄]₂ [MnCl₄] and [P₆₆₆₁₄]₃ [GdCl₆]) in combination with a commercial hydrophobic PVDF porous support. An experimental evaluation of the membrane permeability was carried out for CO₂, N₂ and air.

The influence of the magnetic field on MILs viscosity was also studied, allowing to establish the relationship between permeability and viscosity depending on the external magnetic field. An external magnetic field between 0 and 2 Tesla increases the gas permeability for CO₂, N₂ and air without changing the permeability ratio and decreases MILs viscosity, depending on the MILs magnetic susceptibility. The MIL [P₆₆₆₁₄]₃ [GdCl₆] shows the maximum CO₂ permeability increase (21.64%) in comparison with the result when no magnetic field is applied. The permeability and viscosity product is a constant with a different value for each SMILM studied. Experimental results confirm the potential for gas permeability modulation through supported liquid membranes by tuning the external magnetic field intensity.

5.2 Introduction

The permeability of CO₂ and N₂ through Supported Ionic Liquid Membranes (SILMs) has been studied by immobilizing selected ionic liquids in polymeric porous commercial supports [101, 102, 103]. The influence of pore size, the stability evaluation regarding its hydrophobic or hydrophilic nature and the effect of water vapor in the gas stream has been reported in literature [104, 105], however, there is not yet a clear understanding of this process [106]. Although SILMs present advantages due to room temperature ionic liquids (RTILs) properties, their applications are still limited mainly associated to problems in their stability and long-term behavior [105].

Gas permeability and selectivity are the fundamental parameters characterizing membrane gas separation. There is a general trade-off between both parameters, and for polymeric materials this relationship is identified by the “upper bound” limit observed for different materials in gas separation [107, 108]. The development of new materials exceeding this trade-off line represents a main challenge in CO₂/N₂ separation.

The magnetic behavior of a new generation of RTILs containing metal ions is recently under study in the literature. The combination of general RTILs features (e.g. chemical and thermal stability, non-volatile character and non-flammability) with new properties, due to the incorporation of a metal ion, has opened a new research area which is starting to attract a wide interest. Some applications for MILs have been shown in the literature including catalysts [37, 109] or electrochromic devices [38].

The innovative character of the study comes from the unique combination of the use of membranes incorporating MILs based on different magnetic anions for selective and tunable transport of gases by applying an external magnetic field, which allows the development of a new generation of novel stimuli-responsive membrane separation processes. The possibility of permeability modulation might offer the development of new applications for MILs.

The MILs 1-butyl-3-methylimidazolium tetrachloroferrate [C₄mim][FeCl₄] and 1-butyl-3-nitrile-3-methylimidazolium tetrachloroferrate [n-bmim][FeCl₄] were the first reported MILs to respond to an external neodymium magnet of about 0.55 Tesla, possible due to changes of its organization structure [20, 110]. *Del Sesto et al.* [39] reported MILs based on different transition metal ions such as iron, cobalt, manganese or gadolinium showing a very interesting magnetic response with potential applications for magnetic and electrochromic switching. *Hamaguchi et al.* [40] demonstrated the possibility of magnetic transport of a gas in MILs, illustrated by the change in N₂ bubbles trajectory of in the presence of a magnetic field.

The application of an external magnetic field may modify the physico-chemical properties, such as solubility or surface tension, by tuning the magnetic conditions. The dependence between the magnetic field intensity and the binary MIL/water equilibrium has been also observed, showing the increase of solubility of MILs in aqueous medium [19], which could improve the process efficiency. Other recent applications, have shown

a benzene solubility increase in the paramagnetic MIL [bmim][FeCl₄] when applying a rotational magnetic field [21] or the improvement of phenolic compounds extraction in the MIL [P₆₆₆₁₄][FeCl₄] in the presence of a neodymium magnet [41].

In a previous work [36], MILs with different magnetic susceptibility based on phosphonium cation were incorporated to hydrophobic and hydrophilic PVDF porous supports obtaining stable SMILMs for CO₂ permeation. An evaluation of the membrane stability was carried out and CO₂, N₂ and air permeabilities for SMILMs, were experimentally determined. Pure gas permeation results demonstrated that these SMILMs showed much higher CO₂ permeabilities (147-259 Barrer) when comparing with N₂ (5-7 Barrer) or air (7-12 Barrer).

This work shows the influence of an external magnetic field in gas permeability (CO₂, N₂, air) of SMILMs, containing phosphonium based MILs due to the paramagnetic nature of the anion, leading to modulate the gas permeability.

5.3 Experimental

5.3.1 Materials

The gases used in the experiments were nitrogen (99.99% purity), carbon dioxide (high-purity grade (99.998%) and air (20% O₂, CO₂ ≤ 1 ppm, CO ≤ 1 ppm, H₂O ≤ 3 ppm and N₂ rest to balance (99.999% purity)) all of them obtained from Praxair (USA).

The MILs based in the phosphonium cation studied in the present work are:

- Trihexyl(tetradecyl)phosphonium hexachlorogadolinium: [P₆₆₆₁₄]₃ [GdCl₆]
- Trihexyl(tetradecyl)phosphonium tetrachloromanganate: [P₆₆₆₁₄]₂ [MnCl₄]
- Trihexyl(tetradecyl)phosphonium tetrachloroferrate: [P₆₆₆₁₄] [FeCl₄]
- Trihexyl(tetradecyl)phosphonium tetrachlorocobaltate: [P₆₆₆₁₄]₂ [CoCl₄]

All the ionic liquids used were prepared in *Faculdade de Farmácia, Universidade de Lisboa (Portugal)*, by the group of Prof. Carlos Afonso, according to published procedures [36, 39]. Their molecular weight, density, solubility and magnetic susceptibility are listed in Table 5.1. MILs density was evaluated gravimetrically with a pycnometer, CO₂ solubility was experimentally obtained by a thermogravimetric system at room temperature and atmospheric pressure while the magnetic moment measurement procedure was previously described [35, 36]. MILs water content was previously reported [36] and experiments were carried out under the same conditions (water content and humidity).

5.3.1.1 Gas Permeation experiments in Supported Magnetic Ionic Liquid Membranes (SMILMs)

The SMILMs were prepared using commercial microporous membranes from Millipore Corporation (USA). These supports are hydrophobic polyvinylidene fluoride (PVDF) membranes with a pore diameter of 0.22 μm and an average thickness of 125 μm. The immobilization procedure has been previously described [36]. To immobilize the MILs,

Table 5.1: Main properties of the Magnetic Ionic Liquids (MILs) studied.

MILs	Molecular Weight (g mol ⁻¹)	Density (g cm ⁻³)	CO ₂ solubility (% wt.)	Magnetic susceptibility (emu.K. mol ⁻¹)
[P ₆₆₆₁₄] ₂ [CoCl ₄]	1112	0.965	0.40	2.10
[P ₆₆₆₁₄][FeCl ₄]	681.51	1.012	0.50	4.29
[P ₆₆₆₁₄] ₂ [MnCl ₄]	1103	0.956	0.36	4.23
[P ₆₆₆₁₄] ₃ [GdCl ₆]	1821.54	0.982	0.25	6.51

the polymeric microporous membrane was introduced into a vacuum chamber for 1h in order to facilitate the wetting. Afterwards, drops of MILs were spread out at the membrane surface using a syringe keeping the vacuum inside the chamber and, finally, the liquid excess on the membrane surface was wiped up softly with a tissue. The increase of weight and thickness was measured before and after the immobilization procedure.

The experimental setup used for the gas permeation measurements has been previously described elsewhere [36]. Basically, it is composed by a polyvinylidene fluoride (PVDF) cell supplied by Micrux Technologies (Spain) divided by a membrane with an effective area of about 12.6 cm² into two compartments. A driving force of around 0.45 bar was established between both compartments leading to a flux across the membrane. The pressure change in both compartments over time was followed using two pressure transducers (Omega, UK). The temperature was controlled at 293.15K during the experiments using a water electromagnet chiller.

The influence of the application of an external magnetic field in the separation performance was evaluated using a GMW Dipole Electromagnet (Model 3473-70, USA) which provides magnetic fields up to 2.5 Tesla accepting pole gaps ranging from 0 to 100 mm. Permeation experiments were carried out in a vertical cell disposition with membrane pores perpendicularly positioned towards the electromagnet poles. A uniform magnetic field was applied along the membrane surface as shown in Figure 5.1.

The gas permeation through SILMs follows three different steps: (i) the solute molecule sorption into the feed/membrane interface, (ii) gas diffusion across the membrane, and (iii) desorption at the opposite side of the membrane. The sorption/desorption equilibrium depends on the solubility while the CO₂ permeability is also connected with the gas diffusion through the membrane. In general, gas permeability (P) is related to gas partition coefficient (H) and diffusivity (D) following the solution-diffusion mechanism [111]:

$$P = H.D \quad (5.1)$$

Gas permeability, P (Barrer), was calculated under room temperature and atmospheric

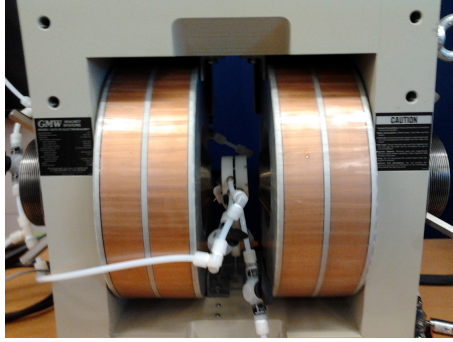


Figure 5.1: Experimental setup for CO₂ separation in the presence of an external magnetic field.

pressure from the feed and permeate compartments pressure data as previously described [36] according to eq.5.2:

$$\ln \left(\frac{[p_{feed} - p_{perm}]_0}{[p_{feed} - p_{perm}]} \right) = \ln \left(\frac{\Delta p_0}{\Delta p} \right) = \left(\frac{D.H.\beta_1}{\delta_1} \right).t \quad (5.2)$$

where p_{feed} and p_{perm} are the pressure in the feed and permeate compartments respectively (Pa), D diffusivity ($m^2 s^{-1}$), H partition coefficient (-), β_1 geometric factor (m^{-1}), t time (s) and δ_1 membrane thickness (m). Permeability, $P(Barrer)$, is obtained from the product of diffusivity and partition coefficient [111] while ideal selectivity can be calculated by the ratio between the permeabilities of two pure different gases.

5.3.1.2 Experimental viscosity determination

The influence of the application of an external magnetic field in the MILs viscosity is measured using Cannon-Ubbelohde glass capillary viscometers size 5 (9721-R95), 3C (9721-R80) and 4C (9721-R89) depending on each MIL viscosity. These capillaries were manufactured and calibrated by Cannon Instrument Company (USA) having deviations from the mean smaller than $\pm 0.2\%$. Sets of six measurements were performed. The influence of the application of an external magnetic field in MILs viscosity was also evaluated using the GMW Dipole Electromagnet applying magnetic field intensities from 0 to 2 Tesla.

5.4 Results and Discussion

5.4.0.1 Permeability-viscosity data in the absence of a magnetic field

Gas permeability through SMILMs and MILs viscosity has been measured in the absence of a magnetic field [36]. CO₂ permeability was measured using hydrophobic PVDF membranes as supporting material obtaining permeabilities between 117-198 Barrer. MILs based on the phosphonium cation studied in the current work present viscosity values

ranging from 749-110060 cP which are, except the iron based MIL, higher than the phosphonium based RTILs reported in the literature [112].

Figure 5.2 shows CO₂ permeability versus RTILs viscosity in a log-log plot assuming a constant partition coefficient (H). The Wilke-Chang equation [33] considers a strong diffusivity dependence on viscosity of dilute solutions ($P.H \propto D \propto \eta^{-1}$). Additionally, Scovazzo [107] proposed a model where the relationship between CO₂ permeability and ionic liquid viscosity in a log-log plot is a line with slope equal to -0.388, showing lower viscosity dominance in determining CO₂ permeability in SILMs for viscosity values in the range of 25-3000 cP. Present work extends this correlation by including MILs with higher viscosity obtaining a slope of -0.278 including the literature data reported in Table 5.2 [107, 112].

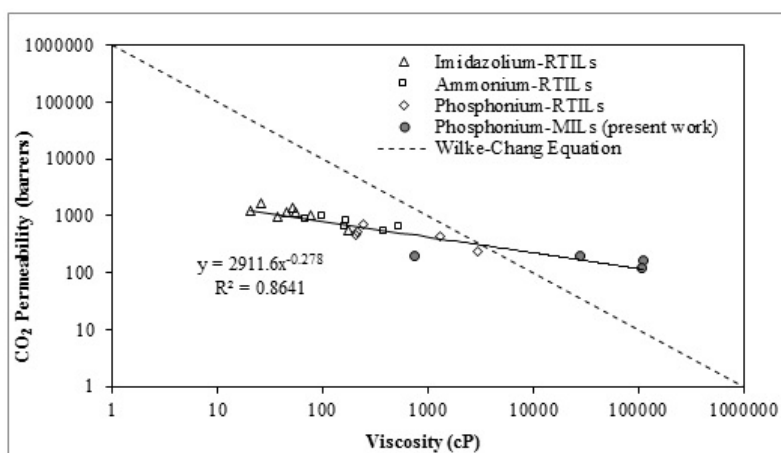


Figure 5.2: Correlation for CO₂ permeability versus viscosity.

5.4.0.2 Separation performance of SMILMs in the presence of an external magnetic field

The influence of the external magnetic field on membrane permeability was studied for CO₂, N₂ and air. Permeability was calculated as the linear relationship between the driving force versus time according to eq. 5.2 at different magnetic field intensities ranging from 0 to 1.5 Tesla at 298.15K.

Table 5.3 shows the CO₂, N₂ and air permeability, the maximum gas permeability increase (ΔP) at 1.5 Tesla magnetic field intensity, and the gas permeability ratio. The permeation ratio shows that SMILMs are highly selective for CO₂ when comparing with N₂ and air. The magnetic field leads to slight increase of the gas permeability but it does not show any influence on CO₂/N₂ and CO₂/air permeability ratio.

An increase in gas permeability will decrease the effective membrane area required to perform the gas separation performance while the constant permeability ratio hinders the achievement of the target purity. It is important to note that the presence of an

Table 5.2: Literature data used for the permeability-viscosity correlation shown in Figure 5.2

Abbreviation	Ionic Liquid	PCO ₂ (Barrer)	Viscosity (cP)
Imidazolium-RTILs			
[emim][Bf ₄]	1-Ethyl-3-methylimidazolium tetrafluoroborate	968.5	37.7
[emim][Tf ₂ N]	1-Ethyl-3-methylimidazolium bis(trifluoromethanesulfonyl)imide	1702.4	26
[emim][Pf ₆]	1-Ethyl-3-methylimidazolium hexafluorophosphate	544.3	176
[emim][dca]	1-Ethyl-3-methylimidazolium dicyanamide	1237.3	21
[bmim][Tf ₂ N]	1-Butyl-3-methylimidazolium bis(trifluoromethanesulfonyl)imide	1344.3	52
[emim][TfO]	1-Ethyl-3-methylimidazolium trifluoromethanesulfone	1171.4	45
[C ₆ mim][Tf ₂ N]	1-Hexyl-3-methylimidazolium bis(trifluoromethanesulfonyl)imide	1135.8	55
[bmim][BETI]	1-Butyl-3-methylimidazolium bis(perfluoroethylesulfonyl)imide	991.4	77
Ammonium-RTILs			
[N ₁₄₄₄][Tf ₂ N]	Trimethyl(butyl)ammonium bis((trifluoromethyl)sulfonyl)imide	523.9	386
[N ₄₁₁₁][Tf ₂ N]	Tributyl(methyl)ammonium bis((trifluoromethyl)sulfonyl)imide	830.5	71
[N ₆₁₁₁][Tf ₂ N]	Trimethyl(hexyl)ammonium bis((trifluoromethyl)sulfonyl)imide	943.2	100
[N ₁₀₁₁₁][Tf ₂ N]	Trimethyl(decyl)ammonium bis((trifluoromethyl)sulfonyl)imide	800.4	173
[N ₁₈₈₈][Tf ₂ N]	Triooctyl(methyl)ammonium bis((trifluoromethyl)sulfonyl)imide	619.4	532
[N ₆₂₂₂][Tf ₂ N]	Triethyl(hexyl)ammonium bis((trifluoromethyl)sulfonyl)imide	630.3	167
Phosphonium-RTILs			
[P ₆₆₆₁₄][Cl]	Trihexyl(tetradecyl)phosphonium chloride	426.6	1316
[P ₄₄₄₁₄][DBS]	Tributyl(tetradecyl)phosphonium dodecylbenzenesulfonate	231.7	3011
[P ₆₆₆₁₄][Tf ₂ N]	Trihexyl(tetradecyl)phosphonium bis((trifluoromethyl)sulfonyl)imide	689.1	243
[P ₆₆₆₁₄][dca]	Trihexyl(tetradecyl)phosphonium dicyanamide	513.7	213
[P ₄₄₄₁₄][DEP]	Tributyl(ethyl)phosphonium diethylphosphate	453.4	207
² Phosphonium-MILs			
¹ [P ₆₆₆₁₄] ₃ [GdCl ₆]	Trihexyl(tetradecyl)phosphonium hexachlorogadolinium	198.8	27650
¹ [P ₆₆₆₁₄] ₂ [MnCl ₄]	Trihexyl(tetradecyl)phosphonium tetrachloromanganese	161.3	110060
¹ [P ₆₆₆₁₄][FeCl ₄]	Trihexyl(tetradecyl)phosphonium tetrachloroferrate	198.4	749
¹ [P ₆₆₆₁₄] ₂ [CoCl ₄]	Trihexyl(tetradecyl)phosphonium tetrachlorocobalt	117.9	107700

Data for 30 °C otherwise noted. ¹Data at 20 °C. ²Present work.

external magnetic field increases the individual gas permeability without changing their permeability ratio.

The Robeson upper bound correlation for CO₂ permeability versus ideal CO₂/N₂ selectivity [108] was used in order to evaluate the CO₂/N₂ separation performance of these systems. Experimental results obtained on this work are below this limit, although the separation performance is enhanced since gas permeability increases in the presence of an external magnetic field.

This behavior may be related to physical properties or molecular structure changes of the ionic liquid immobilized inside the membrane pores in the presence of a magnetic field. Figure 5.3 presents CO₂/N₂ and CO₂/air separation performance enhancement for all the researched systems when a 1.5 Tesla magnetic field is applied.

Table 5.3: Gas permeability (P) increase at 1.5 Tesla intensity magnetic field and gas permeability ratio.

SMILMs	Gas	P (Barrer)		ΔP (%)	P_{CO_2}/P_{N_2}		P_{CO_2}/P_{air}	
		0 Tesla	1.5 Tesla		0 Tesla	1.5 Tesla	0 Tesla	1.5 Tesla
[P ₆₆₆₁₄] ₂ [CoCl ₄]	CO ₂	117.9 ± 4.2	124.1 ± 5.1	5.2				
	N ₂	4.9 ± 0.2	5.3 ± 0.2	5.6	23.7	23.6	14.1	14.2
	air	8.4 ± 0.3	8.7 ± 0.4	4.1				
[P ₆₆₆₁₄] ₂ [MnCl ₄]	CO ₂	161.3 ± 4.1	177.8 ± 4.3	10.2				
	N ₂	4.1 ± 0.1	4.7 ± 0.2	13.6	39.2	38.1	26.5	26.4
	air	6.1 ± 0.3	6.7 ± 0.3	10.7				
[P ₆₆₆₁₄][FeCl ₄]	CO ₂	198.4 ± 3.9	232.2 ± 3.6	17.0				
	N ₂	8.0 ± 0.2	9.3 ± 0.2	15.9	24.8	25.0	20.2	19.9
	air	9.8 ± 0.4	11.6 ± 0.3	18.8				
[P ₆₆₆₁₄] ₃ [GdCl ₆]	CO ₂	198.8 ± 3.5	241.8 ± 3.2	21.6				
	N ₂	5.7 ± 0.2	6.9 ± 0.2	21.2	34.6	34.7	19.1	19.3
	air	10.4 ± 0.3	12.5 ± 0.4	20.5				

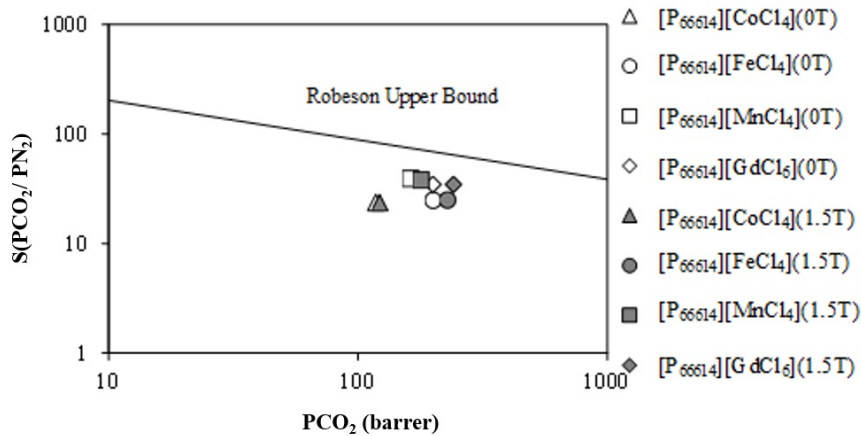


Figure 5.3: Upper bound correlation for CO₂/N₂ separation (1 Barrer = 10⁻¹⁰ cm³ (STP)cm cm⁻² s⁻¹ cmHg⁻¹)

5.4.0.3 Permeability dependence on magnetic susceptibility

Gas permeability increases as a function of the applied magnetic field depending on the MILs magnetic susceptibility, χ_{mT} , ranging from 2.10 to 6.51(emu.K. mol⁻¹). Figure 5.4

shows the influence of the permeability increase at 1.5 Tesla for different MILs, depending on their magnetic susceptibility. An increase of 3.27% in permeability can be expected per unit of magnetic susceptibility under 1.5 Tesla of magnetic field applied.

Therefore, the dependence of gas permeability with MILs magnetic behavior when applying an external magnetic field, confirms the potential to modify gas transport of different species through SMILMs allowing the permeability modulation by tuning the magnetic field.

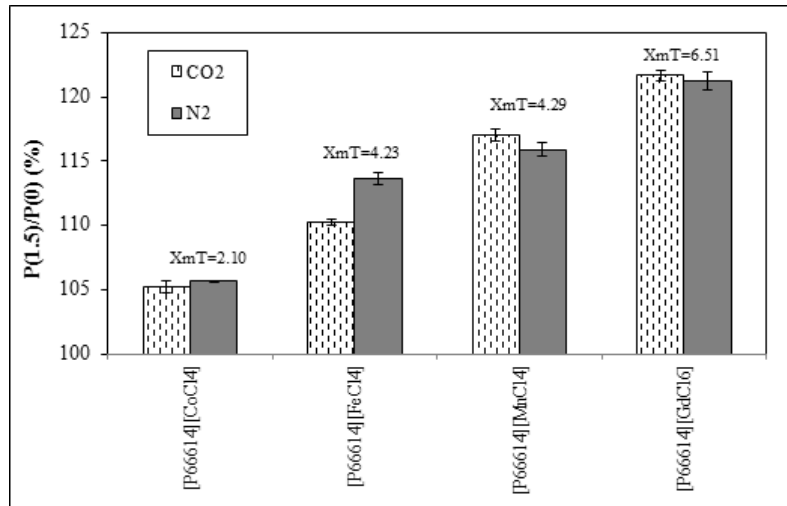


Figure 5.4: Gas permeability behavior depending on MILs magnetic susceptibility.

5.4.0.4 Influence of the magnetic field on MILs viscosity and CO₂ permeability of SMILMs

Figure 5.5 shows the behavior of CO₂ permeability ratio, $P_{(B)}/P_{(0)}$, with different magnetic field intensities ranging from 0 to 1.5 Tesla. Again, a magnetic field intensity increase reveals an increase in the gas permeability depending on the MIL magnetic susceptibility. The comparative analysis between all the studied MILs shows a higher effect of the application of an external magnetic field in CO₂ permeability for MILs with higher magnetic susceptibility values.

Table 5.4 presents MILs viscosity in the presence of a magnetic field intensity ranging from 0 to 2 Tesla. Note that viscosity values are two orders of magnitude higher for [P₆₆₆₁₄]₃[GdCl₆] and three for [P₆₆₆₁₄]₂[CoCl₄] and [P₆₆₆₁₄]₂[MnCl₄] when comparing with [P₆₆₆₁₄][FeCl₄].

5.4.0.5 Permeability-viscosity correlation in the presence of a magnetic field

Figure 5.6 shows the relationship between the permeability and viscosity under the magnetic field intensities tested in a dimensionless form referred to the result in absence of magnetic field. The fitting for all data shows a value close to unity from the slope and

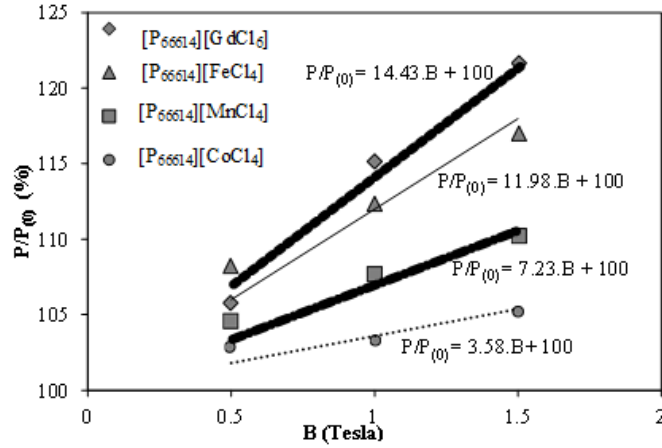

 Figure 5.5: CO₂ permeability ratio ($P_{(B)}/P_{(0)}$) at different magnetic field intensities.

Table 5.4: MILs viscosity at different magnetic field intensities from 0 to 2 Tesla.

MILs	η (cP)				
	0 Tesla	0.5 Tesla	1.0 Tesla	1.5 Tesla	2 Tesla
[P ₆₆₆₁₄] ₂ [CoCl ₄]	107700	95230	94170	93510	88950
[P ₆₆₆₁₄] ₂ [MnCl ₄]	110060	108360	107360	105730	100190
[P ₆₆₆₁₄][FeCl ₄]	749	719	702	693	672
[P ₆₆₆₁₄] ₃ [GdCl ₆]	27650	27530	25600	24290	23550

therefore, an inverse dependence for all the studied MILs is found, following the Wilke-Chang model $D \propto \eta^{-1}$. This result suggests that the product of permeability and viscosity is a specific constant (C) for each SMILM tested and independent of the applied magnetic field according to eq. 5.3:

$$P_B \cdot \eta_B = P_0 \cdot \eta_0 = C(\text{SMILMs}) \quad (5.3)$$

The constants (C) obtained from eq. 5.3 are reported in Table 5.5. These numbers describe the constant behavior of the product permeability - viscosity at different magnetic fields or without magnetic field for each SMILM.

This work has shown the permeability modulation in membranes including MILs in their porous structure. The external magnetic field produces a viscosity variation leading to tunable gas permeability. These innovative results open up the possibility for new developments based on the external magnetic field and permeability modulation in

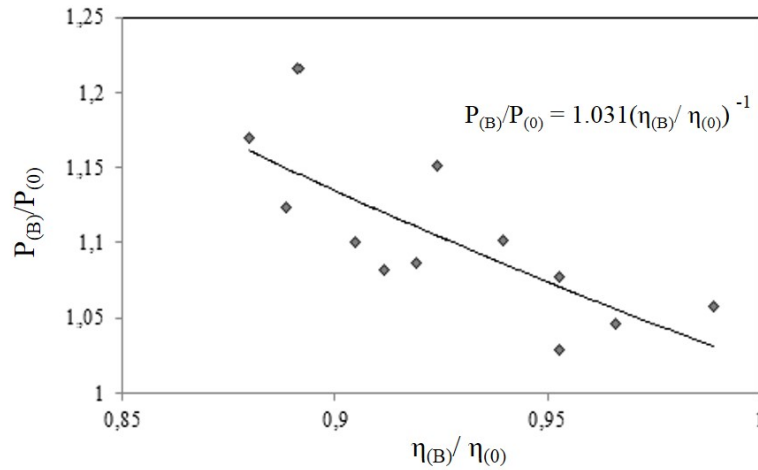
Figure 5.6: CO₂ permeability vs.MILs viscosity ratio

Table 5.5: Gas permeability - viscosity product for the different SMILMs studied.

MILs	$C \cdot 10^{10} \text{ (Kg.m.s}^{-2}\text{)} = P_0 \cdot \eta_0$
$[P_{66614}]_2[CoCl_4]$	105
$[P_{66614}]_2[MnCl_4]$	147
$[P_{66614}][FeCl_4]$	1.23
$[P_{66614}]_3[GdCl_6]$	45.6

SMILMs. In the present study, the permeability modulation by an external magnetic field has been experimentally shown in the CO₂, N₂ and air permeation through SMILMs.

5.5 Conclusions

This work has been able to show the influence of the external magnetic field application on gas permeability (CO₂, N₂ and air) through SMILMs in the range of 0-1.5 Tesla. The gas permeability variation is related to the MILs viscosity change. Experimental results show that gas permeability increases as a function of the applied magnetic field depending on the magnetic ionic liquid, while the permeability ratio (P_{CO_2}/P_{N_2}) remains constant.

An influence of the magnetic field in MILs viscosity, decreasing as a function of the magnetic field intensity, has been shown. The permeability and viscosity product is a specific constant for each SMILM and independent of the applied magnetic field. The change on gas permeability and MILs viscosity when applying an external magnetic field describes the modulation effect of permeability by tuning the magnetic field intensity.

MAGNETIC MODULATION OF THE TRANSPORT OF ORGANOPHILIC SOLUTES THROUGH SUPPORTED MAGNETIC IONIC LIQUID MEMBRANES

Accepted as: Carla I. Daniel, Aurora M. Rubio, Pedro J. Sebastião, Carlos A.M. Afonso, Jan Storch, Pavel Izák, Carla A.M. Portugal, João G. Crespo, "Magnetic modulation of the transport of organophilic solutes through Supported Magnetic Ionic Liquid Membranes", *Journal of Membrane Science*, (2015).

6.1 Summary

The present work evaluates the influence of magnetic field on the transport of two model organic compounds, ibuprofen and α - pinene, through supported magnetic ionic liquids membranes (SMILMs). The membranes studied were prepared by incorporation of magnetic ionic liquids (MILs), $[\text{C}_{11}\text{H}_{21}\text{N}_2\text{O}]_3[\text{GdCl}_3\text{Br}_3]$, $[\text{C}_4\text{mim}][\text{FeCl}_4]$ and $[\text{C}_8\text{mim}][\text{FeCl}_4]$, which act as liquid carriers. Transport studies were conducted in the absence and presence of a magnetic field with an intensity of 1.2 T.

The results obtained show that the magnetic field increases the diffusion coefficient of ibuprofen and α - pinene, improving their transport through the SMILM. The two transport studies performed, α - pinene in dodecane through a SMILM with $[\text{C}_4\text{mim}][\text{FeCl}_4]$, and α - pinene in hexane through a SMILM with $[\text{C}_8\text{mim}][\text{FeCl}_4]$, revealed a permeability increase of 51% and 29% respectively when exposed to the magnetic field, whereas transport studies of ibuprofen in dodecane through $[\text{C}_{11}\text{H}_{21}\text{N}_2\text{O}]_3[\text{GdCl}_3\text{Br}_3]$ MIL showed a permeability increase of 59% under the same magnetic field conditions.

The analysis of the magnetic field influence on solute permeation revealed that the permeability increase observed cannot be solely interpreted due to a decrease of MILs viscosity induced by the magnetic field. The magnetic dependence of solutes solubility

in the MILs should also be considered.

6.2 Introduction

Supported liquid membranes (SLMs) have been recognized as a sustainable alternative to improve the performance (permeability and selectivity) of the several separation processes [23, 113, 114, 115]. The use of SLMs finds particular interest for the removal of specific contaminants from effluents, recovery of metal ions from aqueous solutions, CO₂ capture and solute separation from gas mixtures [3, 4, 5]. However, the application of these membrane processes has been limited due to their instability and short term-performance which lead to reduced membrane fluxes and selectivities.

Different strategies, such as the adequate design of the SLM and the contacting phases, moderate operating conditions or protection of the supported membrane with a gel layer [116, 117] have been followed aiming to minimize the stability problems. SLMs generally allow for high selective separations, ruled by the chemical affinity and the diffusion of a specific solute towards to the liquid phase immobilized within the membrane porous support.

Some of the most interesting carriers in SLM systems are Ionic Liquids (ILs) which, due to their unique physicochemical properties, present some advantages over other alternatives. ILs are comprised entirely by ions and are liquid salts over a wide range of temperatures (including room temperature), presenting extremely low volatility, high thermal stability and thermal capacity, are non-flammable and reusable. Moreover, it is possible to adjust their physicochemical properties for their use in specific tasks, through suitable molecular designing attained by the selection of specific cations and anions [24].

A new class of ILs, the magnetic ionic liquids (MILs), has been recently obtained by substitution of the anion for other containing a paramagnetic metal complex. Responsive materials have been recently explored to use in membrane separation in different applications [118, 119]. MILs are included in these responsive type of liquids which are capable of changing their physicochemical properties when exposed to an external magnetic field [19, 20, 34, 35].

The possibility to module MILs properties based on their magnetic susceptibility was initially unveiled by the work performed by *S. Lee et al* [19] where the influence of the magnetic field strength on the solubility of MILs in water was evidenced by the differences in the MILs concentrations in water mixtures. Later, in a work from *Y. Jiang et al* [21] was observed that solubility of benzene in the paramagnetic MIL [bmim][FeCl₄] increased when a rotational magnetic field was applied. It was found that MILs exhibit magnetic dependent viscosity.

The viscosity of MILs containing different paramagnetic anions, [P₆₆₆₁₄]₃ [GdCl₆], [P₆₆₆₁₄]₂ [MnCl₄], [P₆₆₆₁₄] [FeCl₄] and [P₆₆₆₁₄]₂ [CoCl₄], decreases in the presence of a magnetic field with intensities up to 2 Tesla [75] as showed in the Chapter 5. Furthermore, as described in the Chapter 2 a recent comparative ¹H-NMR study of the molecular

dynamics of two ionic liquids, a non-magnetic and a magnetic ionic liquid, showed the relation between viscosity and the self-diffusion of the pure ionic liquids in the presence of a strong magnetic field. This study showed that the self-diffusion coefficient increases when the magnetic field is applied, in agreement with the decrease of the MILs viscosity [74]. Since the macroscopic properties of MILs are related with their molecular structure, it is expected that the local magnetic structures play a key role in the MILs response to an external magnetic field [20]. The influence of the magnetic field on the physicochemical properties of MILs might be explained by the dependence of the structural arrangement and molecular orientation of the ionic paramagnetic network components. Such dependence suggests that the magnetic field can control the charge density, solubility or the capacity to solvate different chemical compounds in the MILs, causing a significant impact on solute transport through the MIL's medium.

Recently, some potential applications of MILs in the development of magnetic fluids based on nanoparticles, in catalysis, extraction processes and in electrochromic devices, have been demonstrated. [37, 38, 109]. The potential impact of MILs on solute transport was evidenced by the work of *Hamaguchi et al.* [40] that showed the deviation of the ascending trajectory of N₂ bubbles through MILs bulk solution in the presence of a magnetic field. The improvement of phenolic compounds extraction with the [P₆₆₆₁₄][FeCl₄] MIL in the presence of a neodymium magnet was recently demonstrated [41]. A previous study focused on CO₂ permeation through different SMILMs – Supported Magnetic Ionic Liquid Membranes [75] described in Chapter 5 showed a successful magnetic modulation of CO₂ and N₂ transport through these membranes. That study shows that the CO₂ and N₂ permeability increases in the presence of magnetic fields up to 1.5 Tesla. In addition, the increase of the gas permeability was found to be proportional to the MILs magnetic susceptibility. A maximum increase of CO₂ permeability of 21.6% was obtained for CO₂ transport through SMILMs incorporating [P₆₆₆₁₄]₃[GdCl₆] MIL, performed in the presence of a magnetic field of 1.5T [75].

This work aims at studying the potential impact of the magnetic field on the transport of two model organic species, ibuprofen and α - pinene, in organic media, through supported magnetic ionic liquid membranes (SMILMs). Ultimately, it is our goal to infer about the possibility of modulating, non-invasively, the transport of solutes in SMILMs, envisaging the design of SMILMs for small scale purification processes, where the selective recovery of added-value organic species is a priority issue.

6.3 Experimental

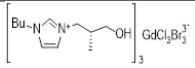
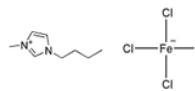
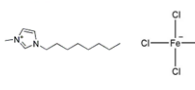
6.3.1 Materials and Methods

6.3.1.1 Magnetic Ionic Liquids (MILs)

Three distinct MILs, [C₁₁H₂₁N₂O]₃[GdCl₃Br₃], [C₄mim][FeCl₄] and [C₈mim][FeCl₄] presented in Table 6.1, were selected for the transport studies based on their polarity and

their low solubility in two different organic solvents, dodecane and hexane, used in feed and stripping phases, in order to avoid their displacement from the membrane porous support, assuring the structural and chemical stability of SMILMs along the transport process.

Table 6.1: MILs properties

MILs	Structure	Molecular Weight (g mol^{-1})	Density (g cm^{-3})	Fe^{3+} or Gd (%)
$[\text{C}_{11}\text{H}_{21}\text{N}_2\text{O}]_3[\text{GdCl}_3\text{Br}_3]$		538.91	1.465	Gd^{3+} (12.83)
$[\text{C}_4\text{mim}][\text{FeCl}_4]$		336.88	1.365	Fe^{3+} (16.39)
$[\text{C}_8\text{mim}][\text{FeCl}_4]$		392.98	1.189	Fe^{3+} (9.97)

$[\text{C}_4\text{mim}][\text{FeCl}_4]$ - 1-butyl-3-methylimidazolium tetrachloroferrate and $[\text{C}_8\text{mim}][\text{FeCl}_4]$ - 1-octyl-3-methylimidazolium tetrachloroferrate were synthesized, according to the experimental procedure described in the literature [36, 39]. $[\text{C}_{11}\text{H}_{21}\text{N}_2\text{O}]_3[\text{GdCl}_3\text{Br}_3]$ MIL was synthesized, using the method described below.

A mixture of (R)-1-butyl-3-(3-hydroxy-2-methylpropyl)imidazolium bromide (18.0 g, 64.9 mmol, 3 eq) and gadolinium(III) chloride hexahydrate (8.05 g, 21.64 mmol, 1 eq) in methanol (100 ml) was allowed to stir overnight (15 h). The solvent was removed by rotary evaporation and then dried under high vacuum for 12 hours affording desired product in nearly quantitative yield (23 g, 97%).

All other chemicals were purchased from Aldrich, Acros solvents and inorganic chemicals were purchased from Lach-Ner company S.R.O., Czech Republic. Commercially available reagents grade materials were used as received. The density of synthesized MILs was measured gravimetrically using a pycnometer and the percentage of magnetic elements, Fe^{3+} and Gd^{3+} , in each sample was determined by ICP - Inductively coupled plasma.

6.3.1.2 Model organic Solutes

Ibuprofen ($206.27 \text{ g mol}^{-1}$, in racemic form) and α - pinene ($136.23 \text{ g mol}^{-1}$) were selected as model compounds for the diffusional transport studies. Solute selection was based on their properties and applications. Ibuprofen is an amphiphilic compound and the α - pinene is a hydrophobic molecule, being of interest in a wide range of medical, pharmaceutical and food applications.

6.3.1.3 Preparation of Supported Magnetic Ionic Liquid Membranes (SMILMs)

SMILMs were prepared by immobilization of MILs in commercial microporous polyvinylidene fluoride (PVDF) membranes from Millipore Corporation (USA), with an average pore of diameter ($0.22 \mu\text{m}$). The hydrophobic character of these PVDF membranes assures a stable immobilization of MIL within the membrane porous support structure [36].

Prior to MILs incorporation, the polymeric microporous membrane was degassed by incubation into a vacuum chamber for 3h, at $50 \text{ }^\circ\text{C}$, in order to remove the air from the pores. MILs were spread at the membrane surface using a syringe, keeping the same vacuum and heating conditions in order to reduce MILs viscosity and facilitate their penetration into the porous structure. Upon MILs immobilization, the excess of liquid on the membrane surface was cleaned with a tissue. Finally, the amount of liquid impregnated in the membrane was determined gravimetrically and the membrane thickness was measured before and after MILs incorporation using a micrometer.

6.3.1.4 Transport studies

The selection of feed and stripping phases was done based on the results of preliminary stability studies. The stability of the SMILMs was evaluated by the performance of contact tests to determine possible displacement of MILs from the porous support. In the contact experiments, two organic solvents were tested, dodecane and hexane, and three different MILs: $[\text{C}_4\text{mim}][\text{FeCl}_4]$, $[\text{C}_8\text{mim}][\text{FeCl}_4]$ and $[\text{C}_{11}\text{H}_{21}\text{N}_2\text{O}]_3[\text{GdCl}_3\text{Br}_3]$.

8 mL of different organic solvents were put in contact with SMILMs with an effective membrane area of 1.77 cm^2 . Membrane area was selected taking into account the solvent volume used, in order to mimic the solvent volume/SMILMs area in the diffusion cell. Based on these tests, α - pinene diffusion was performed through two distinct SMILMs incorporating $[\text{C}_4\text{mim}][\text{FeCl}_4]$ and $[\text{C}_8\text{mim}][\text{FeCl}_4]$, using dodecane or hexane as feed and stripping solvents. Ibuprofen transport was conducted through a SMILM with immobilized $[\text{C}_{11}\text{H}_{21}\text{N}_2\text{O}]_3[\text{GdCl}_3\text{Br}_3]$ and using dodecane as feed and stripping solvent.

The transport of ibuprofen and α - pinene was performed in a glass cell with two independent feed and receiving compartments of 40mL each, divided by the magnetic membrane with an effective area of 9.6 cm^2 . Feed and receiving phases were stirred by pump recirculation or N_2 bubbling. The experiments were performed in the absence and in the presence of an external magnetic field with an intensity of 1.2 Tesla. The magnetic field was provided by a GMW Dipole Electromagnet 3473-70 comprising two poles of 75 mm of diameter from GMW Associates, USA.

In the first set of experiments, α - pinene transport studies were performed using a solution of 0.3 M of α - pinene in hexane as feed phase and pure hexane as stripping phase. α - pinene transport was followed for 31h, at a constant temperature of $24 \text{ }^\circ\text{C} \pm 1 \text{ }^\circ\text{C}$. Feed and receiving phases were sampled ($100 \mu\text{L}$) in regular time intervals. In a second set of experiments α - pinene transport was also performed using dodecane as solvent in

the feed and stripping phases. A solution with an initial concentration of α -pinene of 0.3 M was used as feed phase. Each run was performed for 5 days at constant temperature of $26\text{ }^{\circ}\text{C}\pm 1^{\circ}\text{C}$, in the absence and presence of magnetic field with an intensity of 1.2T. The α -pinene transport to the receiving phase was followed by periodic sampling of $500\text{ }\mu\text{L}$ from each phase along time.

A second transport case study was performed using ibuprofen as model solute. 3.5×10^{-3} M of ibuprofen in dodecane was used as initial feed solution, whereas pure dodecane was used as a receiving solution. The transport of ibuprofen was performed for 5 days at constant temperature of $21\text{ }^{\circ}\text{C}\pm 1^{\circ}\text{C}$ in the absence and presence of magnetic field.

Figure 6.1 shows the experimental set-up used in all transport experiments, consisting on a diffusion cell installed within the electromagnet poles.

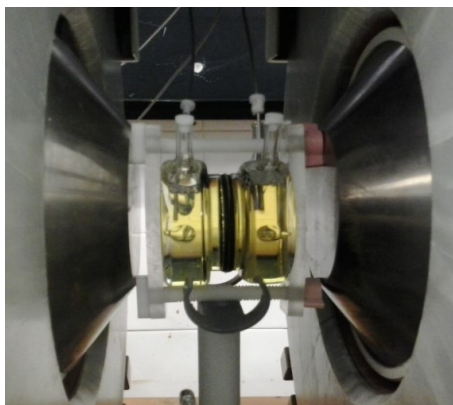


Figure 6.1: Experimental set-up showing the diffusion cell placed between the electromagnet poles during a transport study.

6.3.1.5 Analytical methods

The α -pinene concentration in both feed and stripping compartments, was analyzed over time using a gas chromatograph, GC (Varian GC) equipped with a flame ionization detector (FID). Gas Chromatography (GC) analysis were performed using a silica column, Zebron-5 (30 m length, 0.25 mm internal diameter, $0.25\text{ }\mu\text{m}$ film) coupled to a precolumn. The injector and detector temperatures were set at $280\text{ }^{\circ}\text{C}$ and the oven program temperature was varied from 50 to $300\text{ }^{\circ}\text{C}$. A split ratio of 1:50 was used and a helium flow of 1 mL min^{-1} was applied. Limonene was used as the internal standard. The chromatograms obtained were analyzed with the Varian software for determination of the chromatographic areas corresponding to the target compounds.

The transport of ibuprofen was followed by HPLC analysis of feed and receiving phase samples using a Hychrom Hypersil - 5APS column. The samples were eluted using a solution containing n-98% of hexane, 2% of isopropanol and 0.1% of trifluoroacetic acid, at a flow rate of 1 mL min^{-1} , $25\text{ }^{\circ}\text{C}$ and using a UV detector at λ of 254 nm.

6.3.1.6 Viscosity Measurements

The viscosity of the MILs, $[\text{C}_{11}\text{H}_{21}\text{N}_2\text{O}]_3[\text{GdCl}_3\text{Br}_3]$, $[\text{C}_4\text{mim}][\text{FeCl}_4]$ and $[\text{C}_8\text{mim}][\text{FeCl}_4]$ was measured using a glass capillary viscometer, Cannon 4c), Ubbelohde Viscometer – II c) and III c) respectively, in the presence and absence of a magnetic field in order to evaluate the magnetic dependence of viscosity of each MIL [74, 75]. The viscometer was mounted within the electromagnet, by centering the capillar viscometer region within the poles. The viscosity of MILs was determined at $25^\circ\text{C}\pm 1^\circ\text{C}$ and different magnetic field intensities between 0 and 2 Tesla. The viscosity values resulted from the average of three to six measurements, with deviations from the mean value smaller than $\pm 0.2\%$.

6.4 Results and Discussion

6.4.0.1 Transport results

Preliminary contact tests were performed to evaluate possible membrane instability, due to the displacement of MILs from the porous PVDF support. The displacement of MILs from PVDF supports was accessed based on the quantification of Fe and Gd (metal elements present in each MIL structure) in the contacting solvent, along time, by ICP analysis. It was noticed that for the two solvents and the three selected MILs there was no displacement of the ionic liquids from the porous supporting membranes.

Identical procedure was followed to inspect the displacement of MILs in feed and stripping phases during the transport studies. It was noticed that all feed and stripping samples were absent of iron or gadolinium at the beginning of the contact process. Only vestigial amounts (0.008%) of these elements were found in final samples evidencing that the SMILMs membranes remain stable through transport processes. In order to analyze the influence of magnetic field on the transport of solutes through SMILMs using an external magnetic field, α - pinene and ibuprofen transport studies were performed in the absence and presence of a magnetic field with an intensity of 1.2T.

The first set of experiments was performed to study the influence of magnetic field on α - pinene transport. The transport of α - pinene was studied using two different systems 1) transport of α - pinene from hexane/ α - pinene feed mixtures to pure hexane receiving phases through a SMILM with $[\text{C}_8\text{mim}][\text{FeCl}_4]$ and 2) transport of α - pinene from dodecane/ α - pinene feed mixtures to pure dodecane receiving phases, through a SMILM with $[\text{C}_4\text{mim}][\text{FeCl}_4]$. In a second experimental set it was studied the transport of ibuprofen in dodecane feed phase to dodecane receiving phase, through a SMILM with immobilized $[\text{C}_{11}\text{H}_{21}\text{N}_2\text{O}]_3[\text{GdCl}_3\text{Br}_3]$.

The solute mass transfer coefficients obtained in these experiments were determined using the diffusional model, which considers the solute concentration difference between feed and stripping compartments as the driving force for solute transport. Furthermore, it was assumed that the membrane liquid phase offers the highest resistance to solute transport, which is reasonable considering the viscosity of the liquid phases involved.

Therefore, the resistances to mass transport in the feed and stripping phases were neglected. The solute concentration profiles along time, in the feed and stripping phases, are usual described using the flux equations eq. 6.1 and 6.2. These equations relate the solute flux with the driving force evolvment along time, in both feed and stripping phases.

$$J_F = -\frac{V_F}{A_m} \frac{dC_F}{dt} = K(C_F - C_S) \quad (6.1)$$

$$J_S = \frac{V_S}{A_m} \frac{dC_S}{dt} = K(C_F - C_S) \quad (6.2)$$

where, J_F and J_S are the fluxes of the solute in the feed and stripping phases, V_F and V_S are the volumes of feed and stripping phases, A_m is the membrane area, C_F and C_S are the concentrations in the two phases and K is the overall mass transfer coefficient.

The overall mass balance of the present system was obtained by a mass balance to the solute in the feed phase, according to the equation 6.3, which includes a term that accounts for solute accumulation in the membrane $(VC)_{acc}$.

$$V_F(C_{Fi} - C_F) = (VC)_{acc} + V_S C_S \quad (6.3)$$

where V_F and V_S are the volumes of feed and stripping phases, C_F and C_S are the solute concentrations in the two phases, $(VC)_{acc}$ is the product of the volume and the concentration of the solute accumulated in the SMILM, respectively. The accumulation term was considered in the mass balance when it was found to be not negligible. Changes of the feed and stripping phase volumes were lower to 6% and, therefore, considered negligible along time.

From eq. 6.2 and 6.3, for the presented systems, the evolvment of C_F and C_S are expressed by:

$$\frac{dC_S}{dt} = \frac{KA_m}{V_S} \left(C_{Fi} - \frac{(VC)_{acc}}{V_F} - \frac{V_S}{V_F} C_S - C_S \right) \quad (6.4)$$

$$C_F = C_{Fi} - \frac{V_S}{V_F} C_S - \frac{(VC)_{acc}}{V_F} \quad (6.5)$$

Solute accumulation along time was modeled using a nonlinear regression curve-fitting model with adjustable parameters:

$$\frac{d(VC)_{acc}}{dt} = (VC)_{acc}^{eq} - \frac{(VC)_{acc}^i - (VC)_{acc}^{eq}}{(1 + (2t/\Delta t)^{d_1})^e} \quad (6.6)$$

Since the applied model is based on diffusional solute transport, permeability, $P = DS$, was calculated assuming the solubility-diffusion model, using the following expressions 6.7 and 6.9:

$$k_{imo} = \frac{D\epsilon}{\tau_m \delta_1} = \frac{D_{eff}}{\delta_1} \quad (6.7)$$

where k_{imo} represents the mass transfer coefficient through the liquid phase impregnated in support, D is the diffusion coefficient of the solute i in the impregnated liquid phase, D_{eff} is the effective diffusion coefficient, ϵ is the porosity of the membrane, τ_m is the membrane tortuosity and δ_1 the thickness of the membrane. According to the literature, the PVDF membranes used as support in this work have 70% porosity [113]. A tortuosity value of 2.4 was obtained using the following expression [113]:

$$\tau = \frac{(2 - \epsilon)^2}{\epsilon} \quad (6.8)$$

Taking into account the resistances in series theory, the higher resistance to the mass transfer is offered by the membrane liquid phase. Therefore, the overall mass transfer coefficient, K , might be calculated considering only the resistance of the membrane liquid phase to the solute transport according to the equation:

$$\frac{1}{K} \cong \frac{1}{Sk_{imo}} \Leftrightarrow K = \frac{DS\epsilon}{\tau_m\delta_1} \quad (6.9)$$

where K (cm s^{-1}) is the overall mass transfer coefficient, the product DS corresponds to the solute permeability given by the product of the diffusion coefficient, D and the solubility, S , of the solute i in the impregnated liquid phase.

From fittings to eq. 6.4, 6.5 and 6.6 the values of K were obtained for each experiment and the respective permeability $P = DS$ calculated. The three equations were fitted using a least-squares minimization routine, a 4th degree Runge-Kutta numerical solution for the differential equation and the web interface *fitteia* [56, 57].

In the case of α - pinene the data obtained for solute concentration evolvment in the feed phase is rather scattered, hampering the determination of the concentration profile in this compartment. In the case of ibuprofen, this problem was not observed and the K value was calculated using the eq. 6.4, 6.5 and 6.6. Plots of C_F and C_S , obtained for the three sets of experiment, in the function of process time are represented in Figures 6.2 and 6.3, showing the profiles of α - pinene and ibuprofen concentration along time, for the three SMIMLs in the presence and absence of an external magnetic field.

From Figures 6.2 and 6.3, it can be concluded that the transport of α - pinene and ibuprofen increases in the presence of magnetic field.

The data presented in Figures 6.2 and 6.3 were fitted with eq. 6.4 and 6.5 in order to estimate changes of the overall mass transfer coefficient, K , due to the presence of magnetic field applied. For the transport of ibuprofen, the K_{Ibu} was calculated taking into account the accumulation term of the solute in the membrane. However, since it was not possible to access changes of solute concentration in the feed phase for the α - pinene transports studies, the value of K_{Pinene} was assessed through a different strategy based on a sensitivity analysis of K with the accumulation term.

Taking into account different accumulation term, K values were estimated. Three different conditions were considered for accumulation: $C_{equilibrium} = C_i/2$, i.e. no accumulation, $C_{equilibrium} = C_i/3$ and $C_{equilibrium} = C_i/4$. The three fitted curves

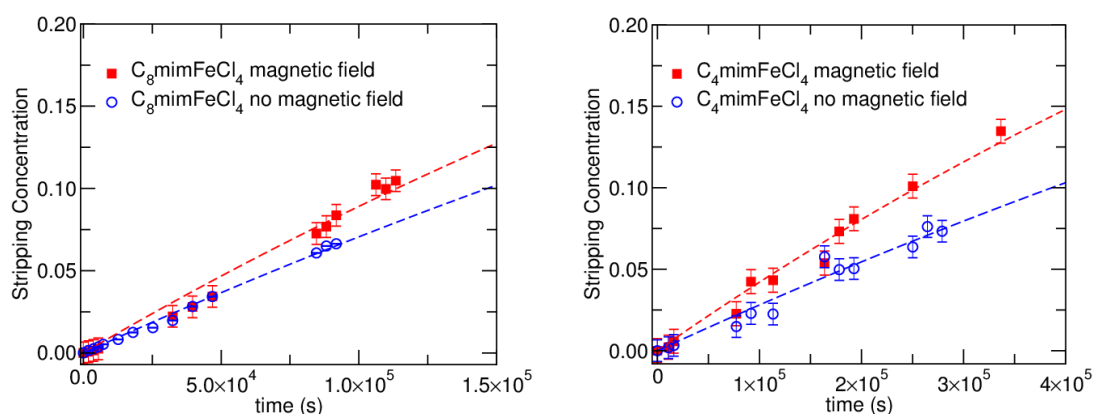


Figure 6.2: Normalized solute concentration profiles fitted along time in the stripping phase for the α - pinene transport through SMILMs with immobilized $[C_8mim][FeCl_4]$ and $[C_4mim][FeCl_4]$

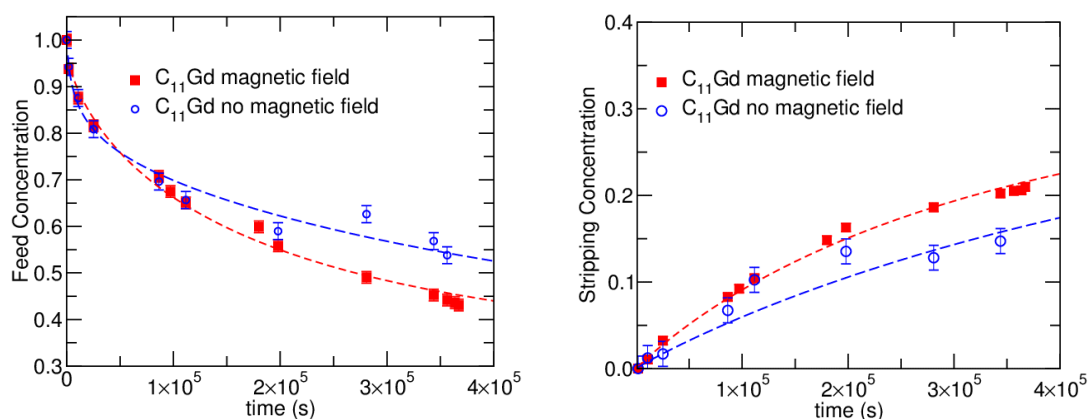


Figure 6.3: Normalized solute concentration profiles fitted along time in the feed and stripping phases for the ibuprofen transport through SMILMs with immobilized $[C_{11}H_{21}N_2O]_3[GdCl_3Br_3]$

were rather coincident with the curves shown in Figure 6.2 and was concluded that the K value does not change significantly for different accumulation terms.

The obtained values for K and for $P=DS$ for α - pinene are shown in Table 6.2.

The magnetic field led to an increase of 51% in the K and P results for the transport of α - pinene in hexane, through a SMILM containing the MIL $[C_4mim][FeCl_4]$ and an increase of 29% for the transport of α - pinene in hexane, through the SMILM with $[C_8mim][FeCl_4]$.

From Figure 6.3, it can be concluded that the magnetic field also impact positively on the transport of ibuprofen. For the calculations of ibuprofen it was considered the accumulation term. The accumulation of ibuprofen in the membrane along time is represented in Figure 6.4. Fitting curves to the concentration of ibuprofen in the membrane along time, also plotted, reveal that the accumulation factor is slightly higher in the presence of a magnetic field.

Table 6.2: K and P values resulting from the mathematical fittings for the two sets of experiments for α - pinene

SMILMs	K(10^{-6} cm s $^{-1}$)	P=DS (10^{-7} cm 2 s $^{-1}$)
[C ₄ mim][FeCl ₄] (with magnetic field)	1.49 ± 0.06	0.56 ± 0.06
[C ₄ mim][FeCl ₄] (without magnetic field)	0.987 ± 0.05	0.37 ± 0.05
[C ₈ mim][FeCl ₄] (with magnetic field)	3.35 ± 0.1	1.27 ± 0.1
[C ₈ mim][FeCl ₄] (without magnetic field)	2.6 ± 0.003	0.98 ± 0.003

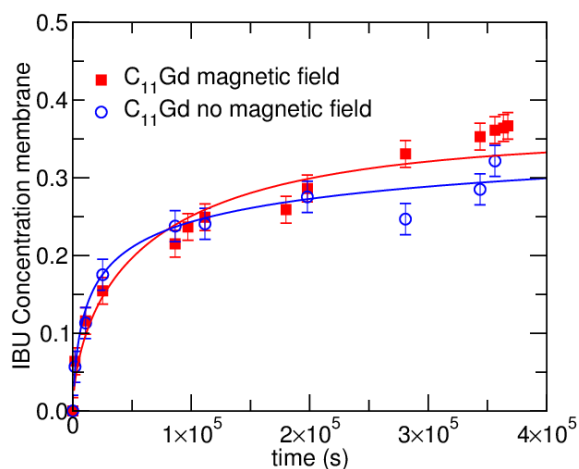


Figure 6.4: Ibuprofen normalized accumulation fittings curves along the time for the MIL

The results of K and P, considering the accumulation term are shown in Table 6.3:

The comparative analysis of K_{Ibu} values obtained in presence and absence of magnetic field, shows that the magnetic field induces an increase of 59% in the coefficient for mass transport.

From all results mentioned above for the two solutes, it can be concluded that the solute diffusional transport is favored in the presence of a magnetic field. As reported in the literature [74] the self-diffusion of the MIL [Aliquat][FeCl₄] increases when it is

Table 6.3: K and P values resulting from the mathematical fittings for the ibuprofen

SMILMs	K($10^{-6} \text{ cm s}^{-1}$)	P=DS ($10^{-7} \text{ cm}^2 \text{ s}^{-1}$)
$[\text{C}_{11}\text{H}_{21}\text{N}_2\text{O}]_3[\text{GdCl}_3\text{Br}_3]$ (with magnetic field)	4.3 ± 0.04	1.62 ± 0.04
$[\text{C}_{11}\text{H}_{21}\text{N}_2\text{O}]_3[\text{GdCl}_3\text{Br}_3]$ (without magnetic field)	2.7 ± 0.2	1.02 ± 0.2

exposed to a magnetic field. This self-diffusion increase was correlated with the magnetic field dependence of MILs viscosity. In fact, it was also described that the MILs viscosity decreases in the presence of magnetic field. Therefore, it may be rationalized that the increase of solute permeability through SMILMs is also associated with the decrease of the MIL's viscosity in the presence of a magnetic field.

6.4.0.2 Viscosity results

In order to clarify about the contribution of the magnetic dependence of MILs viscosity to the solute transport, the viscosity of the used MILs was measured under different magnetic fields. The magnetic dependence of the MILs viscosity is shown in Figure 6.5 and Table 6.4:

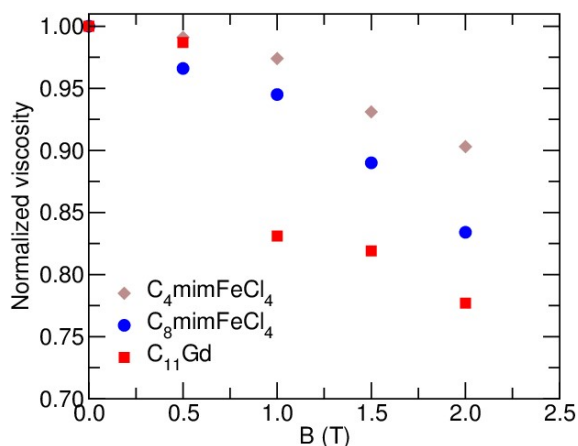


Figure 6.5: Normalized viscosity of pure MILs in the presence and absence of a magnetic field with intensities up to 2.0 Tesla

Figure 6.5 shows the normalized viscosity profiles of MILs with different magnetic field intensities. In analogy to that observed in previous studies for different MILs [74, 75], the viscosity of $[\text{C}_{11}\text{H}_{21}\text{N}_2\text{O}]_3[\text{GdCl}_3\text{Br}_3]$, $[\text{C}_4\text{mim}][\text{FeCl}_4]$ and $[\text{C}_8\text{mim}][\text{FeCl}_4]$ also

Table 6.4: Absolute viscosity results and percentage of reduction under a magnetic field.

MILs	η			% viscosity reduction (1.2Tesla)	% viscosity reduction (2.0Tesla)
	(0Tesla) (Pa.s)	(1.2Tesla) (Pa.s)	(2.0Tesla) (Pa.s)		
$[\text{C}_{11}\text{H}_{21}\text{N}_2\text{O}]_3[\text{GdCl}_3\text{Br}_3]$	49.12	40.82	38.15	17	22
$[\text{C}_4\text{mim}][\text{FeCl}_4]$	0.0317	0.0304	0.0286	4.1	10
$[\text{C}_8\text{mim}][\text{FeCl}_4]$	0.2931	0.2711	0.2444	8.1	17

decrease at increasing magnetic field intensities.

Table 6.4 presents the absolute values of viscosity for 0, 1.2 (intensity applied in the transport experiments) and 2.0 Tesla (maximum intensity allowed by the equipment) and the percentage of reduction at these two intensities. The $[\text{C}_{11}\text{H}_{21}\text{N}_2\text{O}]_3[\text{GdCl}_3\text{Br}_3]$ shows a larger percentage reduction in viscosity at both intensities, comparatively to the other two MILs, which can be due to the higher magnetic susceptibility of Gd.

Viscosity and diffusion are commonly related by the Stokes-Einstein equation. In the case of ionic liquids, the Wilke-Chang correlation [74] can be applied, showing an inverse correlation between D and η :

$$D = C \frac{T(\alpha_1^{0.5})}{\eta} \quad (6.10)$$

being D the diffusion coefficient ($\text{m}^2 \text{s}^{-1}$), C a constant defined by $C = 7.48 \times 10^{-8} M_w^{1/2} / V^{0.6}$ depending on the MIL molar mass M_w and the molar volume V , T is the temperature (K), α_1 is the association degree and η is the viscosity (Pa.s).

This inverse correlation is according with the experimental results shown above, leading us to conclude that the magnetically induced reduction of MILs viscosity contributes to the increase of solute diffusion in the presence of the magnetic field. However, when comparing the percentages of reduction of the MILs viscosity under magnetic field at 1.2Tesla: $[\text{C}_{11}\text{H}_{21}\text{N}_2\text{O}]_3[\text{GdCl}_3\text{Br}_3] = 17\%$, $[\text{C}_4\text{mim}][\text{FeCl}_4] = 4.1\%$ and $[\text{C}_8\text{mim}][\text{FeCl}_4] = 8.1\%$ with the increases observed in the respective mass transfer coefficients:

$[\text{C}_{11}\text{H}_{21}\text{N}_2\text{O}]_3[\text{GdCl}_3\text{Br}_3] = 59\%$, $[\text{C}_4\text{mim}][\text{FeCl}_4] = 51\%$ and $[\text{C}_8\text{mim}][\text{FeCl}_4] = 29\%$ it is possible to observe that solutes transport seems to be not only regulated by changes in viscosity.

Therefore, the increase of solute transport in the presence of a magnetic field may result from a combined influence of decreasing of MIL's viscosity and increasing solute solubility, S , in the MILs under magnetic field. This effect may possibly be related to the

magnetically induced structural rearrangement of the ionic network which favors solute transport and solute partition/affinity to the MILs.

To conclude about the solubility contribution, the diffusion coefficient, D , could be estimated by the Wilke-Chang and Scheibel correlations, which are commonly used to estimate the viscosity of ILs [32]. The results for the calculated D and S in the presence and absence of magnetic field are present in Table 6.5.

Table 6.5: Estimation of the D values using the Wilke Chang and Scheibel correlations and solubility values calculated for each MIL and system

SMILMs	$D_{\text{estimated(Wilke-Chang)}}$ ($10^{-6}\text{cm}^2\text{s}^{-1}$)	$D_{\text{estimated(Scheibel)}}$ ($10^{-6}\text{cm}^2\text{s}^{-1}$)	* $S_{\text{estimated1}}$	** $S_{\text{estimated2}}$
[C ₄ mim][FeCl ₄] (with magnetic field)	2.46	1.83	0.022	0.031
[C ₄ mim][FeCl ₄] (without magnetic field)	2.39	1.78	0.016	0.021
[C ₈ mim][FeCl ₄] (with magnetic field)	0.29	0.23	0.43	0.54
[C ₈ mim][FeCl ₄] (without magnetic field)	0.28	0.22	0.35	0.44
[C ₁₁ H ₂₁ N ₂ O] ₃ [GdCl ₃ Br ₃] (with magnetic field)	0.0022	0.0016	74.7	102.9
[C ₁₁ H ₂₁ N ₂ O] ₃ [GdCl ₃ Br ₃] (without magnetic field)	0.0018	0.0013	56.1	77.8

* $S_{\text{estimated1}}$ calculated by the solution-diffusion model $P=DS$ with D estimated by Wilke-Chang correlation

** $S_{\text{estimated2}}$ calculated by the solution-diffusion model $P=DS$ with D estimated by Scheibel correlation

D values were estimated by two different correlations in order to compare and validate the results. As explained before, the differences observed in the D values with and without magnetic field were attributed to the magnetic induced changes of the MILs viscosity.

α - pinene and ibuprofen solubility was determined according to the solution-diffusion model $P=DS$, in order to estimate the contribution of this parameter to the transport of these solutes. As shown in Table 6.5, the solubility of the two solutes in the three different MILs increased in the presence of the magnetic field, suggesting that the global increase of α - pinene and ibuprofen transport under magnetic field is due to both, viscosity and solubility effects.

6.5 Conclusions

This work shows that the magnetic field increases the permeability of ibuprofen and α - pinene through supported magnetic ionic liquid membranes, SMILMs. The increase of permeability was related to the magnetic susceptibility of the paramagnetic elements of MILs, $[\text{C}_{11}\text{H}_{21}\text{N}_2\text{O}]_3[\text{GdCl}_3\text{Br}_3]$, $[\text{C}_4\text{mim}][\text{FeCl}_4]$ and $[\text{C}_8\text{mim}][\text{FeCl}_4]$, and due to the MILs ability to respond to the magnetic field with changes of their physicochemical properties. A previous study [74, 75] has revealed that the MILs viscosity decreases in the presence of magnetic field. This effect was ascribed to magnetic induced structural reorganization of the MILs ionic network and associated with the increase of the MILs self-diffusion.

An identical behavior was found for the MILs used in the present work by analysis of magnetic dependence of their viscosity, as the viscosity of $[\text{C}_{11}\text{H}_{21}\text{N}_2\text{O}]_3[\text{GdCl}_3\text{Br}_3]$, $[\text{C}_4\text{mim}][\text{FeCl}_4]$ and $[\text{C}_8\text{mim}][\text{FeCl}_4]$ decreased 17%, 8.1% and 4.1%, when exposed to a magnetic field intensity of 1.2 T. However, the transport studies developed in this work show that the increase of the solute permeability through these SMILMs was not solely explained by the increase of solute diffusion coefficient in MILs, but that it might also account for the increase of the solubility of ibuprofen and α - pinene, in MILs.

Supported liquid membranes offer high selective solute transport, which makes them particularly suitable for the recovery of minority added value solutes from complex mixtures, enantiomeric resolution and for the removal of specific contaminants from liquid or gas streams. Here we show that these processes may be favored by the use SMILM systems, since they allow better control of solute permeability by non-invasively modulation of MILS viscosity and solubility by an external magnetic field. This aspect represents an important advantage for the optimization of small scale processes commonly used in pharmaceutical industry.

GENERAL CONCLUSIONS

This PhD thesis presents the development of supported magnetic ionic liquid membranes (SMILMs) prepared using a new class of ionic liquids – magnetic ionic liquids (MILs). Due to the ability of MILs to switch their physicochemical properties, such as viscosity and self-diffusion, in the presence of an external magnetic field, they are regarded as promising liquid carriers with tunable transport characteristics. In this work, the magnetic susceptibility of MILs was studied and explored towards the design of magnetic responsive membranes, aiming to improve their separation efficiency.

The impact of the magnetic behavior of MILs in the performance of SMILMs under magnetic field was evaluated. Firstly, it was studied the influence of the magnetic field on the physicochemical properties of the MILs. The studies were conducted to obtain information about the magnetic behavior and the ability of MILs to switch their physicochemical characteristics when exposed to variable magnetic field conditions. The influence of the magnetic field on the MILs' molecular dynamics and viscosity were inspected by $^1\text{H-NMR}$ relaxometry and capillary viscometry, respectively. When using the $^1\text{H-NMR}$ technique, two different systems composed by the MIL and its non-magnetic analogue, IL, $[\text{Aliquat}][\text{FeCl}_4] / [\text{AliquatCl}]$ and $[\text{P}_{66614}][\text{FeCl}_4] / [\text{P}_{66614}\text{Cl}]$ were analyzed, in order to obtain information about the diffusion mechanisms in the distinct MILs.

The spin-relaxation times of pure ILs and MIL/IL mixtures with 1% (v/v) of MIL were measured in a broad range of frequencies from 10kHz to 300MHz, for comparative purposes. An increase of the relaxation rate, R , was observed only for MIL mixtures in a range of frequencies between 10MHz-300MHz. The differences of the ILs and MILs relaxation profiles were interpreted based on a relaxation model, that took into account distinct contributions of translational and rotational motions, chain dynamics, self-diffusion, paramagnetic and cross relaxation. This analysis allowed for the estimation of self-diffusion

coefficients of the different ILs/MILs systems at low magnetic fields. By direct measurement of the MILs and ILs diffusion at high magnetic field intensities of 7 and 14T using a PFG NMR equipment, it was concluded the magnetic diffusion dependence of the MILs, not observed in the ILs systems.

Based on this analysis, it was concluded that the presence of the paramagnetic ions, increases the complexity of the system. The additional response observed for MILs at 10 MHz-300MHz was possibly attributed to the coupling of the magnetic moment of the paramagnetic ions with proton's magnetic moments, leading MILs to acquire a specific molecular mobility and dynamics, under magnetic field. Both IL/MIL systems, [AliquatCl]/[Aliquat][FeCl₄] and [P₆₆₆₁₄][FeCl₄]/[P₆₆₆₁₄Cl], depicted identical behavior. However, [P₆₆₆₁₄][FeCl₄]/[P₆₆₆₁₄Cl] system exhibited some differences, mainly relating the parameters describing the slower rotations and those associated with the *R* results in the range of frequencies below to 1 MHz.

In contrast to Aliquat, it was observed that the relaxation of the magnetic system [P₆₆₆₁₄][FeCl₄]/[P₆₆₆₁₄Cl] is smaller than the non-magnetic [P₆₆₆₁₄Cl] at low frequencies. These results lead us to conclude that in the case of phosphonium, the presence of the iron ions does not only affect the spin-lattice relaxation, but additionally, it seems to have higher influence in the molecular dynamics/motions of the cations, probably due to a higher molecular chains packing, comparatively with that observed for the Aliquat system.

Changes of MILs self-diffusion were associated to changes of MILs viscosity induced by the magnetic field. In fact, capillary viscometry measurements performed at different magnetic field conditions showed that the MILs viscosity decreases with the increase of the magnetic field intensity, corroborating the inverse correlation between viscosity and diffusion as expressed by the modified Stokes-Einstein equation. Together, resonance relaxometry and viscometry analysis, allowed for determination of the evolution of MILs self-diffusion coefficients with the magnetic field as well as the establishment of a comprehensive correlation with the magnetic induced on MILs viscosity.

The magnetic dependence of MILs viscosity and the relevance of this property in the design of new MILs, led to the development of studies aiming at estimating the contribution of cation and anion ILs/MILs counterparts to its viscosity at different temperatures. These studies were performed for four different MILs based on the phosphonium cation: [P₆₆₆₁₄][FeCl₄], [P₆₆₆₁₄][CoCl₄], [P₆₆₆₁₄][MnCl₄] and [P₆₆₆₁₄][GdCl₆] at distinct temperatures. A group contribution model was applied to predict the contribution of the phosphonium cation and the different magnetic anions. It was found that the phosphonium cation has a positive influence on the MIL's viscosity and the magnetic anions a negative impact. However, the phosphonium cation presents a lower contribution to MILs viscosity in comparison with the other cations described in further literature. Also, it was observed that the MILs viscosity is less affected by temperature when they integrate phosphonium cations.

These results are in accordance with those described in the literature for non-magnetic

ILs, being the group contribution model useful to predict other physico chemical properties of MILs. It was also concluded that, in the design of new MILs, the contribution of the cation to the MILs viscosity is more relevant than that of the anion counter-part.

To evaluate the impact of magnetic behavior of MILs on membrane separation processes, mass transport studies through supported liquid membranes containing MILs as carriers, were performed in gas and liquid phases. Gas transport studies were carried out using pure CO₂ and N₂ streams and air, through distinct SMILMs with immobilized [P₆₆₆₁₄][FeCl₄], [P₆₆₆₁₄][CoCl₄], [P₆₆₆₁₄][MnCl₄] and [P₆₆₆₁₄][GdCl₆] MILs.

These studies were conducted in the absence and presence of magnetic field intensities up to 1.5 T, in order to evaluate the impact of magnetic sensitivity of MILs on membrane permeability and selectivity. The results obtained show that the membrane permeability increased with the increase of the magnetic field intensity for the different gases (CO₂, N₂ and air) tested. This improvement was related to the decrease of the MILs viscosity, which consequently led to the increase of gas diffusion through the SMILMs. It was also observed that the increase of permeability was identical for all gases tested and thus it was concluded that the membrane selectivity was not affected by the magnetic field.

The transport of solutes in organic liquid media through SMILMs was also tested at 0T and 1.2 T. Two different model case studies were performed: 1) transport of α -pinene through SMILMs with immobilized [C₄mim][FeCl₄] and [C₈mim][FeCl₄] MILs and 2) transport of ibuprofen through SMILMs incorporating [C₁₁H₂₁N₂O]₃[GdCl₃Br₃].

Identical to that observed in gas transport studies, the magnetic field also produced an increase of the α -pinene and ibuprofen permeability coefficients. In this case, the increase of the solute permeability was not only due to the increase of solute diffusion in consequence of the magnetically induced decrease of MILs viscosity, but also it was ascribed to the increase of solute solubility in the MILs in the presence of the magnetic field. Therefore, it was possible to conclude that the magnetically responsive supported liquid membranes designed in this work, allow for non-invasive modulation of gas and liquid permeability by adjustment of the external magnetic field intensity.

FUTURE WORK

Regarding the results obtained in this thesis some suggestions for future work can be proposed.

Taking into account the characterization of the physicochemical and structural properties of the MILs, further studies based on the $^1\text{H-NMR}$ technique can be performed: 1) studies about the influence of the chain length of the MILs' cation in their molecular self-diffusion. Since the cation of the MILs act as a solvent in the magnetic ionic liquid system, it would be interesting to select cations with shorter chain lengths, in order to compare the molecular dynamics, with the two MILs already studied, [Aliquat][FeCl_4] and [P_{66614}][FeCl_4] with long alkyl chains, by the measurements of their relaxation times, T_1 , 2) The exploration of the relaxation diffusion mechanisms of MILs with different anions, having distinct magnetic susceptibilities, may be relevant, comparing their distinct nature, 3) Following the relaxation study of the MILs to be used as potential contrast agents, a $^1\text{H-NMR}$ analysis could be carried out, using new biocompatible MILs, with reduced toxicity (e.g. MILs based on choline cation with [FeCl_4] $^-$ anion), for biological tests, comparing the relaxivities with those of commercial contrast complex agents, 4) Molecular dynamics simulation is an additional tool that may be explored, in order to predict the packing of the molecular magnetic ionic liquids, estimating the distribution, orientation and motions of the molecules, e.g. MILs anions and cations, under a magnetic field. This study could lead us to a comprehensive understanding of the molecular superparamagnetic behavior of these liquids, as described in the $^1\text{H-NMR}$ work.

Additionally to the viscosity characterization of the MILs, solubility studies should be performed in the presence and absence of a magnetic field. Solubility testes of different solutes in MILs should be conducted in order to confirm the prediction that the solubility of solutes in MILs increases in the presence of a magnetic field. Concerning the impact of the magnetic field on the transport of solutes through SMILMs, it would be interesting to

perform gas permeation studies using a SMILMs integrating a task specific MIL, presenting a cation with high solubility for CO₂, in order to analyze the effect of the magnetic field on CO₂ permeability and selectivity.

A challenging task will be also to extend the use of SMILMs for the selective isolation of enantiomers, envisaging the development of separation systems able to overcome the limitations faced by alternative processes (e.g. chromatography, extraction, classical resolution) to resolve racemic mixtures. Preliminary studies of enantiomeric separation of ibuprofen were performed using SMILMs in the present work, evidenced that in the presence of a magnetic field, the enantiomeric selectivity was slightly higher. The magnetic separation of enantiomeric compounds using chiral MILs through SLMs could constitute an interesting study taking into account the knowledge already achieved in this work.

The magnetic behavior exhibited by the studied MILs and their versatility to distinct applications, mainly in separation processes, led us to develop additional studies aiming to evaluate the MILs capacity to form magnetic responsive surfactants/micelles and their potential use for magnetic selective separation of target solutes.

The potential use of MILs as magnetic responsive surfactants has been described in recent publications [120, 121]. Some studies have been focused on the capacity to control the properties of magnetic-responsive surfactant systems, mainly the surface tension, using the magnetic field. These works show promising results regarding the response of the magnetic surfactants, however, magnetic reverse micelles systems were not developed and tested for selective separation under a magnetic field so far.

Our preliminary studies (not included in this thesis) were focused on the development and characterization of reverse micelles using MILs. These studies were performed using [Aliquat][FeCl₄] as a model MIL in organic medium composed by isooctane (70%) and butanol (30%) (100mM above the CMC=50mM, W_s=9). The micellar concentration used was above the CMC (critical micellar concentration) = 50mM, to guarantee the presence of a high number of micelles formed. The organic solvent tested was the isooctane, one of the most solvent used with surfactants systems, being the butanol the co-surfactant used in order to facilitate the dissolution of the surfactant in the organic medium. In this particular case, it was necessary the addition of a small amount of the analogue IL to the organic solution of the MIL, for the stability of the system. The IL amount was defined by the ratio $W_s = [\text{Ionic Liquid}]/[\text{Surfactant}]$, where the [IL] is a small value face to the [surfactant] used [122]. The surfactant solution obtained was optically transparent and stable.

DLS – *Dynamic Light Scattering* and TEM – *Transmission Electron Microscopy* analysis were performed aiming to confirm the formation of [Aliquat][FeCl₄] reverse micelles and to determine their structure and sizes. The results from these two techniques, show the presence of particles with sizes from 5-7 nm, in solutions with MILs concentration above the CMC, closed to that commonly exhibited by a reverse cationic micellar system. However, the high light polydispersion generated by the samples, possibly attributable to sample intense color and turbidity, disturbed the quality of the analysis, disallowing

us from considering these results conclusive. Other techniques, such as X-ray or SANS (Small-angle neutron scattering), should be used in the future to confirm the DLS results, i.e. the presence of reverse micelles and their sizes. Considering the formation of reverse cationic micelles with 5-7 nm, further studies were performed to evaluate the capacity of these micelles to respond to an externally applied magnetic field.

In this case, magnetic field could then facilitate the separation of micelles from organic media. In these tests, deuterated water, D_2O , was transported to the organic phase within the hydrophilic core of the reverse micelle and used as a tracer to probe its mobility, induced by the external magnetic field.

Equilibrium tests were performed in 24h, by mixing 8 mL of organic phase (0.8M) with 8 mL of aqueous phase (D_2O – deuterated water) in a contacting cell shown in Figure 8.1. The contacting cell was placed within an electromagnet and exposed to a non-uniform magnetic field with an intensity ranging from 0.66T (higher distance from the pole) and 1.2 T (closer to the pole).

The Figure 8.1 shows the contacting cell containing the micellar system placed in the electromagnet in the absence of magnetic field (Figure 8.1a)) and in the presence of a magnetic field gradient (Figure 8.1 b)). In the presence of a magnetic field, Figure 8.1 b) it was observed the attraction of the [Aliquat][$FeCl_4$] bulk solution as a whole, not observed when the magnetic field was turned off.

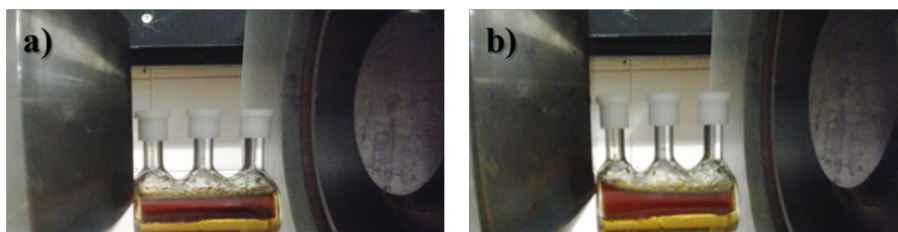


Figure 8.1: [Aliquat][$FeCl_4$] micelles solution (dark region) in equilibrium with D_2O (clear region): a) with magnetic field OFF and b) with magnetic field ON.

The solution of the magnetic micelles in equilibrium with D_2O was sampled along time at the extremes of the contacting cell, i.e. at the sampling point closer to the magnet pole and in the opposite side, in the presence and absence of the magnetic field, in order to identify a potential transport of D_2O through the contacting cell caused by the displacement of micelles towards the magnetic pole. Each sample was analyzed using 1H -NMR technique at $10.35MHz \approx 0.2T$, based on the measurement of the relaxation times of the deuterium by the identification of its specific peak. However, the deuterium peaks in 1H -NMR, obtained for the samples collected at the two extremes of the cell were similar and therefore the selective capture of the micelles by the magnetic field was not demonstrated.

As observed in Figure 8.1 b), the [Aliquat][$FeCl_4$] micelles were not exclusively attracted to the magnetic field when it was switched on. Instead, the organic solution

containing the [Aliquat][FeCl₄] micelles (upper phase) was attracted as a whole to the magnetic pole. Further studies are required to understand the behavior of such magnetic micellar system, i.e. to explain the reasons behind the inability to specifically move micelles.

Possible reasons can be related with the nature of the magnetic micelles, type of the selected MIL and polarity of the solvent. These studies are essential for the selection of conditions that may lead to micelles with improved magnetic responsive ability and thus they should anticipate the design of micelle separation systems allowing for a selective transport of target compounds.

BIBLIOGRAPHY

- [1] W. W. Ho and K. K. Sirkar. "Membrane Handbook". In: *Van Nostrand Reinhold, USA* (1992).
- [2] R. W. Baker. "Membrane Technology And Applications". In: *John Wiley & Sons Ltd* (2004).
- [3] R. M. O. Loiacano E. Drioli. "Metal-ion Separation and Concentration With Supported Liquid Membranes". In: *Journal of Membrane Science* 28 (1986), pp. 123–138.
- [4] R. Chiarizia, E. P. Horwitz, P. G. Rickert, and K. M. Hodgson. "Application of Supported Liquid Membranes For Removal of Uranium From Groundwater". In: *Separation Science and Technology* 25 (1990), pp. 1571–1586.
- [5] J. Pellegrino and R. Noble. "Enhanced transport and liquid membranes in bioseparation". In: *Trends Biotechnol* 8 (1990). Ed. by T. Biotechnol, p. 216.
- [6] A. Poliwoda, N. Llczuk, and P. P. Wieezorek. "Transport mechanism of peptides through supported liquid membranes". In: *Separation and Purification Technology* 57 (2007), pp. 444–449.
- [7] N. M. Kocherginsky, Q. Yang, and L. Seelam. "Recent advances in supported liquid membrane technology". In: *Separation and Purification Technology* 53 (2007), pp. 171–177.
- [8] B. Wang, J. Lin, F. Wu, and Y. Peng. "Stability and Selectivity of Supported Liquid Membranes with Ionic Liquids for the Separation of Organic Liquids by Vapor Permeation". In: *Industrial & Engineering Chemistry Research* 47 (2008), pp. 8355–8360.
- [9] R. Fortunato, C. A. M. Afonso, J. Benavente, E. Rodriguez-Castellon, and J. G. Crespo. "Stability of supported ionic liquid membranes as studied by X-ray photoelectron spectroscopy". In: *Journal of Membrane Science* 256 (2005), pp. 216–223.
- [10] H. Susanto, M. Balakrishnan, and M. Ulbricht. "Via surface functionalization by photograft copolymerization to low-fouling polyethersulfone-based ultrafiltration membranes". In: *Journal of Membrane Science* 288 (2007), pp. 157–167.

- [11] P. Izak, M. H. Godinho, P. Brogueira, J. Figueirinhas, and J. G. Crespo. "3D topography design of membranes for enhanced mass transport". In: *Journal of Membrane Science* 321 (2008), pp. 337–343.
- [12] T. Peng and Y. L. Cheng. "PNIPAAm and PMAA co-grafted porous PE membranes: Living radical co-grafting mechanism and multi-stimuli responsive permeability". In: *Polymer* 42 (2001), pp. 2091–2100.
- [13] L. Liang, M. K. Shi, V. V. Viswanathan, L. M. Peurrung, and J. S. Young. "Temperature-sensitive polypropylene membranes prepared by plasma polymerization". In: *Journal of Membrane Science* 177 (2000), pp. 97–108.
- [14] D. Wandera, S.R.Wickramasinghe, and S. M. Husson. "Stimuli-Responsive membranes: a review". In: *J. Membr.Sci* 357 (2010), pp. 6–35.
- [15] S. F. Medeiros, A. M. Santos, H. Fessi, and A. Elaissari. "Stimuli-responsive magnetic particles for biomedical applications". In: *International Journal of Pharmaceutics* 403 (2011), pp. 139–161.
- [16] D. Szabo, G. Szeghy, and M. Zrinyi. "Shape transition of magnetic field sensitive polymer gels". In: *Macromolecules* 31 (1998), pp. 6541–6548.
- [17] P. M. Xulu, G. Filipcsei, and M. Zrinyi. "Preparation and responsive properties of magnetically soft poly(N-isopropylacrylamide) gels". In: *Macromolecules* 33 (2000), pp. 1716–1719.
- [18] M. Zrinyi. "Intelligent polymer gels controlled by magnetic fields". In: *Colloid and Polymer Science* 278 (2000).
- [19] S. H. Lee, S. H. Ha, S.-S. Ha, H.-B. Jin, C.-Y. You, and Y.-M. Koo. "Magnetic Behavior of Mixture of Magnetic Ionic Liquid [Bmim]FeCl₄ and Water". In: *J. Appl. Phys.* 101 (2007), 09J102.
- [20] S. Hayashi, S. Saha, and H. O. Hamaguchi. "A New Class of Magnetic Fluids: bmim[FeCl₄] and nbmim[FeCl₄] Ionic Liquids". In: *IEEE Trans. Magnet.* 42 (2006).
- [21] Y. Jiang, C. Guo, and H. Liu. "Magnetically Rotational Reactor For Absorbing Benzene Emissions by Ionic Liquids". In: *China Particuology* 5 (2007), pp. 130–133.
- [22] D.Han and K.H.Row. "Recent Applications of Ionic Liquids in Separation Technology: a review". In: *Molecules* 15 (2010), pp. 2405–2426.
- [23] F. J. Hernandez-Fernandez, A. P. de los Rios, F. Tomas-Alonso, J. M. Palacios, and G. Villora. "Preparation of supported ionic liquid membranes: Influence of the ionic liquid immobilization method on their operational stability". In: *Journal of Membrane Science* 341 (2009), pp. 172–177.

- [24] Y. Hu and C. Xu. "Effect of the structures of ionic liquids on their physical-chemical properties and the phase behaviour of the mixtures involving ionic liquids". In: *Chemical Reviews* (2006).
- [25] E. Santos, J. Albo, and A. Irabien. "Magnetic Ionic Liquids - Synthesis, Properties and Applications". In: *Rsc Advances* 4 (2014), pp. 40008–40018.
- [26] P. Bernardo, E. Drioli, and G. Golemme. "Membrane Gas Separation: A Review/State of the Art". In: *Industrial & Engineering Chemistry Research* 48 (2009), pp. 4638–4663.
- [27] A. Brunetti, F. Scura, G. Barbieri, and E. Drioli. "Membrane technologies for CO₂ separation". In: *Journal of Membrane Science* 359 (2010), pp. 115–125.
- [28] D. Aaron and C. Tsouris. "Separation of CO₂ from flue gas: A review". In: *Separation Science and Technology* 40 (2005).
- [29] H. Yang, Z. Xu, M. Fan, R. Gupta, R. B. Slimane, A. E. Bland, and I. Wright. "Progress in carbon dioxide separation and capture: A review". In: *Journal of Environmental Sciences-china* 20 (2008), pp. 14–27.
- [30] A. D. Ebner and J. A. Ritter. "State-of-the-art Adsorption and Membrane Separation Processes for Carbon Dioxide Production from Carbon Dioxide Emitting Industries". In: *Separation Science and Technology* 44 (2009), pp. 1273–1421.
- [31] P. Callaghan. "Principles of Nuclear Magnetic Resonance Microscopy". In: *Oxford University Press: New York* (2003).
- [32] D. Morgan, L. Ferguson, and P. Scovazzo. "Diffusivities of Gases in Room-temperature Ionic Liquids: Data and Correlations Obtained Using a Lag-time Technique". In: *Ind. Eng. Chem. Res.* 44 (2005), pp. 4815–4823.
- [33] C. R. Wilke J. S. and P. Chang. "Correlation of Diffusion Coefficients in Dilute Solutions". In: *AIChE J.* 1 (1955), pp. 264–270.
- [34] I. de Pedro, D. P. Rojas, J. A. Blanco, and J. Rodriguez Fernandez. "Antiferromagnetic Ordering in Magnetic Ionic Liquid Emim[FeCl₄"]". In: *J. Magn. Magn. Mater.* 323 (2011), Magnetic Fluid Assoc.
- [35] I. de Pedro, D. P. Rojas, J. Albo, P. Luis, A. Irabien, J. A. Blanco, and J. Rodriguez Fernandez. "Long-range Magnetic Ordering in Magnetic Ionic Liquid: Emim[FeCl₄"]". In: *J. Phys.: Condens. Matter* 22 (2010), p. 296006.
- [36] J. Albo, E. Santos, L. A. Neves, S. P. Simeonov, C. A. M. Afonso, J. G. Crespo, and A. Irabien. "Separation Performance of CO₂ Through Supported Magnetic Ionic Liquid Membranes (SMILMs)". In: *Sep. Purif. Technol.* 97 (2012), p. 26.
- [37] H. Wang, R. Yan, Z. Li, X. Zhang, and S. Zhang. "Fe-containing magnetic ionic liquid as an effective catalyst for the glycolysis of poly(ethylene terephthalate)". In: *Catalysis Communications* 11 (2010), pp. 763–767.

- [38] A. Branco, L. C. Branco, and F. Pina. "Electrochromic and magnetic ionic liquids". In: *Chemical Communications* 47 (2011), pp. 2300–2302.
- [39] R. E. Del Sesto, T. M. McCleskey, A. K. Burrell, G. A. Baker, J. D. Thompson, B. L. Scott, J. S. Wilkes, and P. Williams. "Structure and Magnetic Behavior of Transition Metal Based Ionic Liquids". In: *Chem. Comm.* (2008), pp. 447–449.
- [40] M. Okuno, H.-o. Hamaguchi, and S. Hayashi. "Magnetic manipulation of materials in a magnetic ionic liquid". In: *Applied Physics Letters* 89 (2006), p. 132506.
- [41] N. Deng, M. Li, L. Zhao, C. Lu, S. L. de Rooy, and I. M. Warner. "Highly efficient extraction of phenolic compounds by use of magnetic room temperature ionic liquids for environmental remediation". In: *Journal of Hazardous Materials* 192 (2011), pp. 1350–1357.
- [42] R. Tao and X. Xu. "Reducing the Viscosity of Crude Oil by Pulsed Electric or Magnetic Field". In: *Energy Fuels* 20 (2006), pp. 2046–2051.
- [43] D. Sousa, G. Domingos Marques, J. M. Cascais, and P. J. Sebastião. "Desktop Fast-field Cycling Nuclear Magnetic Resonance Relaxometer". In: *Solid State Nucl. Magn. Reson.* 38 (2010), pp. 36–43.
- [44] W. S. Price. "Pulsed-field Gradient Nuclear Magnetic Resonance as a Tool For Studying Translational Diffusion .1. Basic Theory". In: *Concepts Magn. Reson.* 9 (1997), pp. 299–336.
- [45] E. Anoardo, D. J. Pusiol D. J., and C. Aguilera. "Nmr-study of the T(1) Relaxation Dispersion In the Smectic Mesophase of 4-chlorophenyl 4-undecyloxybenzoate". In: *Phys. Rev. B: Condens. Matter* 49 (1994), pp. 8600–8607.
- [46] M. Gueron. "Nuclear-relaxation in Macromolecules by Paramagnetic-ions - Novel Mechanism". In: *J. Magn. Reson.* 19 (1975), pp. 58–66.
- [47] A. Roch, R. N. Muller, and P. Gillis. "Theory of Proton Relaxation Induced by Superparamagnetic Particles". In: *Journal of Chemical Physics* 110 (1999), pp. 5403–5411.
- [48] R. Dong. "Nuclear Magnetic Resonance of Liquid Crystals". In: *Springer- New York* (1997).
- [49] P. J. Sebastião, C. Cruz, and A. C. Ribeiro. "Advances in Proton NMR Relaxometry in Thermotropic Liquid Crystals". In: *Nuclear Magnetic Resonance Spectroscopy of Liquid Crystals* (2009), pp. 129–167.
- [50] L. A. Neves, P. J. Sebastião, I. M. Coelho, and J. G. Crespo. "Proton NMR Relaxometry Study of Nafion Membranes Modified With Ionic Liquid Cations". In: *J. Phys. Chem. B* 115 (2011), pp. 8713–8723.
- [51] H. C. Torrey. "Nuclear Spin Relaxation by Translational Diffusion". In: *Phys. Rev.* 92 (1953), pp. 962–969.

- [52] N. Bloembergen, E. M. Purcell, and R. V. Pound. "Relaxation Effects in Nuclear Magnetic Resonance Absorption". In: *Phys. Rev.* 73.7 (1948), pp. 679–712. DOI: 10.1103/PhysRev.73.679.
- [53] R. Kimmich, F. Winter, W. Nusser, and K. H. Spohn. "Interactions and Fluctuations Deduced From Proton Field-cycling Relaxation Spectroscopy of Polypeptides, Dna, Muscles, and Algae". In: *J. Magn. Reson.* 68 (1986), pp. 263–282.
- [54] D. J. Pusiol, R. Humpfer, and F. Noack. "Nitrogen Nuclear-quadrupole Resonance Dips in The Proton Spin Relaxation Dispersion of Nematic and Smectic Thermotropic Liquid-crystals". In: *Z. Naturforsch., A: Phys. Sci.* 47 (1992), pp. 1105–1114.
- [55] P. Gillis, A. Roch, and R. A. Brooks. "Corrected Equations for Susceptibility-Induced T2-Shortening". In: *J. Magn. Reson.* 137 (1999), pp. 402–407.
- [56] P. J. Sebastião. "The Art of Model Fitting to Experimental Results". In: *European Journal of Physics* 35 (2014), UNSP 015017.
- [57] P. J. Sebastião. 2009. URL: <http://fittedia.org>.
- [58] C. M. Roland. "Characteristic Relaxation Times and their Invariance to Thermodynamic Conditions". In: *Soft Matter* 4 (2008), pp. 2316–2322.
- [59] S. J. Dorazio and J. R. Morrow. "The Development of Iron(II) Complexes as ParaCEST MRI Contrast Agents". In: *European Journal of Inorganic Chemistry* (2012), pp. 2006–2014.
- [60] X. L. Zhao, H. L. Zhao, Z. Y. Chen, and M. B. Lan. "Ultrasmall Superparamagnetic Iron Oxide Nanoparticles for Magnetic Resonance Imaging Contrast Agent". In: *Journal of Nanoscience and Nanotechnology* 14 (2014), pp. 210–220.
- [61] S. Kenouche, J. Larionova, N. Bezzi, Y. Guari, N. Bertin, M. Zanca, L. Lartigue, M. Cieslak, C. Godin, and G. e. a. Morrot. "NMR Investigation of Functionalized Magnetic Nanoparticles Fe₃O₄ as T-1-T-2 Contrast Agents". In: *Powder Technology* 255 (2014), pp. 60–65.
- [62] V. M. Runge, J. A. Clanton, C. M. Lukehart, C. L. Partain, and A. E. James. "Paramagnetic Agents For Contrast-enhanced Nmr Imaging - A Review". In: *American Journal of Roentgenology* 141 (1983), pp. 1209–1215.
- [63] A. Merbach, L. Helm, and E. Toth. "The Chemistry of Contrast Agents in Medical Magnetic Resonance Imaging". In: *Wiley* (2013).
- [64] M. M. Britton. "Magnetic Resonance Imaging of Chemistry". In: *Chem. Soc. Rev* 39 (2010), pp. 4036–4043.
- [65] V. C. Pierre, M. Botta, S. Aime, and K. N. Raymond. "Fe(III)-Templatedempleted Gd(III) Self-Assemblies - A New Route Toward Macromolecular MRI Contrast Agents". In: *Journal of the American Chemical Society* 128 (2006), pp. 9272–9273.

- [66] P. B. Tsitovich, P. J. Burns, A. M. McKay, and J. R. Morrow. "Redox-Activated MRI Contrast Agents Based on Lanthanide and Transition Metal Ions". In: *Journal of Inorganic Biochemistry* 133 (2014), pp. 143–154.
- [67] E. J. Werner, A. Datta, C. J. Jocher, and K. N. Raymond. "High-Relaxivity MRI Contrast Agents: Where Coordination Chemistry Meets Medical Imaging". In: *Angewandte Chemie-international Edition* 47 (2008), pp. 8568–8580.
- [68] D. L. White. "Paramagnetic Iron (iii) Mri Contrast Agents". In: *Magnetic Resonance In Medicine* 22 (1991).
- [69] P. Caravan. "Strategies for Increasing the Sensitivity of Gadolinium based MRI Contrast Agents". In: *Chemical Society Reviews* 35 (2006), pp. 512–523.
- [70] P. Caravan. "Protein-Targeted Gadolinium-Based Magnetic Resonance Imaging (MRI) Contrast Agents: Design and Mechanism of Action". In: *Accounts of Chemical Research* 42 (2009), pp. 851–862.
- [71] Z. X. Zhou and Z. R. Lu. "Gadolinium-Based Contrast Agents for Magnetic Resonance Cancer Imaging (vol 5, pg 1, 2013)". In: *Wiley Interdisciplinary Reviews-nanomedicine and Nanobiotechnology* 5 (2013), pp. 190–190.
- [72] S.-P. Lin and J. J. Brown. "MR Contrast Agents: Physical and Pharmacologic Basics". In: *Journal of Magnetic Resonance Imaging* 25 (2007), pp. 884–899.
- [73] X. Y. Liang and P. J. Sadler. "Cyclam Complexes and their Applications in Medicine". In: *Chemical Society Reviews* 33 (2004), pp. 246–266.
- [74] C. I. Daniel, F. Vaca Chavez, G. Feio, C. A. M. Portugal, J. G. Crespo, and P. J. Sebastiao P. J. "H NMR Relaxometry, Viscometry, and PFG NMR Studies of Magnetic and Nonmagnetic Ionic Liquids". In: *Journal of Physical Chemistry B* 117 (2013), pp. 11877–11884.
- [75] E. Santos, J. Albo, C. Daniel, C. Portugal, J. Crespo, and A. Irabien. "Permeability modulation of Supported Magnetic Ionic Liquid Membranes (SMILMs) by an external magnetic field". In: *Journal of Membrane Science* 430 (2013), pp. 56–61.
- [76] R. F. M. Frade, S. Simeonov, A. A. Rosatella, F. Siopa, and C. A. M. Afonso. "Toxicological Evaluation of Magnetic Ionic Liquids in Human Cell Lines". In: *Chemosphere* 92 (2013), pp. 100–105.
- [77] S. P. M. Ventura, C. S. Marques, A. A. Rosatella, C. A. M. Afonso, F. Goncalves, and J. A. P. Coutinho. "Toxicity Assessment of Various Ionic Liquid Families Towards *Vibrio fischeri* Marine Bacteria". In: *Ecotoxicology and Environmental Safety* 76 (2012), pp. 162–168.
- [78] D. M. Sousa, G. D. Marques, J. M. Cascais, and P. J. Sebastião. "Desktop Fast-Field Cycling Nuclear Magnetic Resonance Relaxometer". In: *Solid State Nuclear Magnetic Resonance* 38 (2010), pp. 36–43.

- [79] A. Aluculesei, F. Vaca Chavez, C. Cruz, P. J. Sebastiao, N. G. Nagaveni, V. Prasad, and R. Y. Dong. "Proton NMR Relaxation Study on the Nematic-nematic Phase Transition in a 131 Liquid Crystal." In: *The journal of physical chemistry. B* 116 (2012), pp. 9556–63.
- [80] A. Gradišek, T. Apih, V. Domenici, V. Novotna, and P. J. Sebastião. "Molecular Dynamics in a Blue Phase Liquid Crystal: a H-1 Fast Field-Cycling NMR Relaxometry Study". In: *Soft Matter* 9 (2013), pp. 10746–10753.
- [81] C. F. Martins, L. Neves, I. M. Coelho, F. Vaca Chávez, J. G. Crespo, and P. J. Sebastião. "Temperature Effects on the Molecular Dynamics of Modified Nafion (R) Membranes Incorporating Ionic Liquids' Cations: A H-1 NMRD Study". In: *Fuel Cells* 13 (2013), pp. 1166–1176.
- [82] H. W. Spiess, D. Schweitzer, and U. Haebleren. "Molecular Motion in Liquid Toluene from a Study of ^{13}C and ^2D Relaxation Times". In: *J. Magn. Reson.* 9 (1973), pp. 444–460.
- [83] B. d. P. Cardoso, A. Vicente, J. B. Ward, P. J. Sebastião, F. Vaca Chávez, S. Barroso, A. Carvalho, S. J. Keely, P. N. Martinho, and M. J. Calhorda. "Fe(III) SalEen Derived Schiff Base Complexes as Potential Contrast Agents". In: *Inorg. Chim. Acta* 432 (2015), pp. 258–266.
- [84] R. G. Seoane, S. Corderi, E. Gomez, N. Calvar, E. J. Gonzalez, E. A. Macedo, and A. Dominguez. "Temperature Dependence and Structural Influence on the Thermophysical Properties of Eleven Commercial Ionic Liquids". In: *Industrial & Engineering Chemistry Research* 51 (2012), pp. 2492–2504.
- [85] S. Aparicio, M. Atilhan, and F. Karadas. "Thermophysical Properties of Pure Ionic Liquids: Review of Present Situation". In: *Industrial & Engineering Chemistry Research* 49 (2010), pp. 9580–9595.
- [86] E. N. D. Andrade. "A theory of the viscosity of liquids Part II". In: *Philosophical Magazine* 17 (1934), pp. 698–732.
- [87] H. Vogel. "The Law of the Relation Between the Viscosity of Liquids and the Temperature". In: *Phys. Z.* 22 (1921), pp. 645–646.
- [88] G. S. Fulcher. "Analysis of recent measurements of the viscosity of glasses". In: *Journal of the American Ceramic Society* 8 (1925), pp. 339–355.
- [89] G. Tammann and Z. Hesse. "The Dependence of Viscosity upon the Temperature of Supercooled Liquids". In: *Anorg. Allg. Chem* 156 (1926), pp. 245–257.
- [90] T. A. Litovitz. "Temperature Dependence of the Viscosity of Associated Liquids". In: *Journal of Chemical Physics* 20 (1952), pp. 1088–1089.

- [91] M. H. Ghatee, M. Zare, F. Moosavi, and A. R. Zolghadr. "Temperature-Dependent Density and Viscosity of the Ionic Liquids 1-Alkyl-3-methylimidazolium Iodides: Experiment and Molecular Dynamics Simulation". In: *Journal of Chemical and Engineering Data* 55 (2010), pp. 3084–3088.
- [92] R. Reid, J. Prausnitz, and T. Sherwood. "The Properties of Gases and Liquids". In: (1987). Ed. by M.-H. N. York.
- [93] S. R. S. Sastri and K. K. Rao. "A new method for predicting saturated liquid viscosity at temperatures above the normal boiling point". In: *Fluid Phase Equilibria* 175 (2000), pp. 311–323.
- [94] Y. Gastonbonhomme, P. Petrino, and J. Chevalier. "Unifac Visco Group contribution Method For Predicting Kinematic Viscosity Extension and Temperature-dependence". In: *Chemical Engineering Science* 49 (1994), pp. 1799–1806.
- [95] P. Luis, I. Ortiz, R. Aldaco, and A. Irabien. "A novel group contribution method in the development of a QSAR for predicting the toxicity (*Vibrio fischeri* EC50) of ionic liquids". In: *Ecotoxicology and Environmental Safety* 67 (2007), pp. 423–429.
- [96] R. L. Gardas and J. A. P. Coutinho. "Group Contribution Methods for the Prediction of Thermophysical and Transport Properties of Ionic Liquids". In: *Aiche Journal* 55 (2009), pp. 1274–1290.
- [97] C. Ye and J. M. Shreeve. "Rapid and accurate estimation of densities of room-temperature ionic liquids and salts". In: *Journal of Physical Chemistry A* 111 (2007), pp. 1456–1461.
- [98] H. D. B. Jenkins, H. K. Roobottom, J. Passmore, and L. Glasser. "Relationships among ionic lattice energies, molecular (formula unit) volumes, and thermochemical radii". In: *Inorganic Chemistry* 38 (1999), pp. 3609–3620.
- [99] R. L. Gardas and J. A. P. Coutinho. "Extension of the Ye and Shreeve group contribution method for density estimation of ionic liquids in a wide range of temperatures and pressures". In: *Fluid Phase Equilibria* 263 (2008), pp. 26–32.
- [100] R. L. Gardas and J. A. P. Coutinho. "A group contribution method for viscosity estimation of ionic liquids". In: *Fluid Phase Equilibria* 266 (2008), pp. 195–201.
- [101] J. E. Bara, C. J. Gabriel, T. K. Carlisle, D. E. Camper, A. Finotello, D. L. Gin, and R. D. Noble. "Gas separations in fluoroalkyl-functionalized room-temperature ionic liquids using supported liquid membranes". In: *Chemical Engineering Journal* 147 (2009), pp. 43–50.
- [102] P. Luis, L. A. Neves, C. A. M. Afonso, I. M. Coelho, J. G. Crespo, A. Garea, and A. Irabien. "Facilitated transport of CO₂ and SO₂ through Supported Ionic Liquid Membranes (SILMs)". In: *Desalination* 245 (2009), pp. 485–493.

- [103] P. Scovazzo, D. Havard, M. McShea, S. Mixon, and D. Morgan. "Long-term, continuous mixed-gas dry fed CO₂/CH₄ and CO₂/N₂ separation performance and selectivities for room temperature ionic liquid membranes". In: *Journal of Membrane Science* 327 (2009), pp. 41–48.
- [104] P. Cserjesi, N. Nemestothy, and K. Belafi-Bako. "Gas separation properties of supported liquid membranes prepared with unconventional ionic liquids". In: *Journal of Membrane Science* 349 (2010), pp. 6–11.
- [105] L. A. Neves, J. G. Crespo, and I. M. Coelho. "Gas permeation studies in supported ionic liquid membranes". In: *Journal of Membrane Science* 357 (2010), pp. 160–170.
- [106] A. Criscuoli, E. Drioli, A.K.Pabby, S.S.H.Rizvi, and A. (Eds.) "Membrane contactors for gaseous streams treatments in: Handbook of Membrane Separations: Chemical, Pharmaceutical, Food, and Biotechnological Applications". In: *CRC Press, Taylor & Francis Group Boca Raton* 1041–1055 (2008).
- [107] P. Scovazzo. "Determination of the upper limits, benchmarks, and critical properties for gas separations using stabilized room temperature ionic liquid membranes (SILMs) for the purpose of guiding future research". In: *Journal of Membrane Science* 343 (2009), pp. 199–211.
- [108] L. M. Robeson. "The upper bound revisited". In: *Journal of Membrane Science* 320 (2008), pp. 390–400.
- [109] M. D. Nguyen, L. V. Nguyen, E. H. Jeon, J. H. Kim, M. Cheong, H. S. Kim, and J. S. Lee. "Fe-containing ionic liquids as catalysts for the dimerization of bicyclo[2.2.1]hepta-2,5-diene". In: *Journal of Catalysis* 258 (2008), pp. 5–13.
- [110] S. Hayashi and H. O. Hamaguchi. "Discovery of a magnetic ionic liquid [bmim]FeCl₄". In: *Chemistry Letters* 33 (2004), pp. 1590–1591.
- [111] E. Cussler. "Diffusion. Mass Transfer in Fluid Systems". In: *Cambridge University Press, USA* 21–23, 434–435, 438–439 (1997).
- [112] L. Ferguson and P. Scovazzo. "Solubility, diffusivity, and permeability of gases in phosphonium-based room temperature ionic liquids: Data and correlations". In: *Industrial & Engineering Chemistry Research* 46.4 (Feb. 2007), pp. 1369–1374.
- [113] R. Fortunato, C. A. M. Afonso, M. A. M. Reis, and J. G. Crespo. "Supported liquid membranes using ionic liquids: study of stability and transport mechanisms". In: *Journal of Membrane Science* 242 (2004), pp. 197–209.
- [114] S. Schlosser, E. Sabolova, R. Kertesz, and L. Kubisova. "Factors influencing transport through liquid membranes and membrane based solvent extraction". In: *Journal of Separation Science* 24 (2001), pp. 509–518.

- [115] J. D. Clark, B. B. Han, A. S. Bhowan, and S. R. Wickramasinghe. "Amino acid resolution using supported liquid membranes". In: *Separation and Purification Technology* 42 (2005), pp. 201–211.
- [116] A. J. B. Kemperman, H. H. M. Rolevink, D. Bargeman, T. van den Boomgaard, and H. Strathmann. "Stabilization of supported liquid membranes by interfacial polymerization top layers". In: *Journal of Membrane Science* 138 (1998), pp. 43–55.
- [117] P. R. Danesi, L. Reichleyyinger, and P. G. Rickert. "Lifetime of Supported Liquid Membranes - the Influence of Interfacial Properties, Chemical-composition and Water Transport On the Long-term Stability of the Membranes". In: *Journal of Membrane Science* 31 (1987), pp. 117–145.
- [118] H. H. Himstedt, X. Qian, J. R. Weaver, and S. R. Wickramasinghe. "Responsive membranes for hydrophobic interaction chromatography". In: *Journal of Membrane Science* 447 (2013), pp. 335–344.
- [119] A. Y. Gebreyohannes, M. R. Bilad, T. Verbiest, C. M. Courtin, E. Dornez, L. Giorno, E. Curcio, and I. F. J. Vankelecom. "Nanoscale tuning of enzyme localization for enhanced reactor performance in a novel magnetic-responsive biocatalytic membrane reactor". In: *Journal of Membrane Science* 487 (2015), pp. 209–220.
- [120] P. Brown, C. P. Butts, J. Cheng, J. Eastoe, C. A. Russell, and G. N. Smith. "Magnetic emulsions with responsive surfactants". In: *Soft Matter* 8 (2012), pp. 7545–7546.
- [121] P. Brown, A. Bushmelev, C. P. Butts, J. Cheng, J. Eastoe, I. Grillo, R. K. Heenan, and A. M. Schmidt. "Magnetic Control over Liquid Surface Properties with Responsive Surfactants". In: *Angewandte Chemie-international Edition* 51 (2012), pp. 2414–2416.
- [122] D. Blach, M. Pessego, J. J. Silber, N. Mariano Correa, L. Garcia-Rio, and R. Dario Falcone. "Ionic Liquids Entrapped in Reverse Micelles as Nanoreactors for Bimolecular Nucleophilic Substitution Reaction. Effect of the Confinement on the Chloride Ion Availability". In: *Langmuir* 30 (2014), pp. 12130–12137.

APPENDIX - SUPPORTING INFORMATION

A.0.1 Theoretical models

A.0.1.1 Translational self-diffusion

In the case of isotropic liquids or isotropic phases of liquid crystal compounds the contribution of translational self-diffusion (SD) to the relaxation can be expressed by the Torrey's model [51] with a

$$\left(\frac{1}{T_1}\right)_{\text{SD}} = C_d \frac{n\tau_D}{d^3} [\mathcal{T}(\omega\tau_D) + 4\mathcal{T}(2\omega\tau_D)], \quad (\text{A.1})$$

where $\omega = 2\pi\nu_L$, $C_d = (1/2)(3\mu_0\gamma^2\hbar/(8\pi))^2$ is the strength of the dipolar interaction and $\mathcal{T}(\omega\tau_D)$ is a dimensionless analytical function that depends on the average time between diffusion jumps τ_D , the mean-square jump distance $\langle r^2 \rangle$, and the molecular width d . τ_D is related with the self-diffusion constant D by the relation $\langle r^2 \rangle = 6\tau_D D$. n is the density of ^1H spins.

A.0.1.2 Rotations/reorientations

Molecular rotations/reorientations (Rot) may be characterized by one or more correlation times according to the number of independent rotational axis considered to describe this motion. Usually, rotations along the molecular long axis and rotations/reorientations along a molecular transverse axis have different correlations times and the most simple model used to describe this relaxation process is given a $\text{Rot}_1 + \text{Rot}_2$ where Rot_i is given by the Bloemberger, Purcel and Pound (BPP) model:

$$\left(\frac{1}{T_1}\right)_{\text{Rot}_i} = A_{\text{Rot}_i} \left[\frac{\tau_{\text{Rot}_i}}{1 + \omega^2\tau_{\text{Rot}_i}^2} + \frac{4\tau_{\text{Rot}_i}}{1 + 4\omega^2\tau_{\text{Rot}_i}^2} \right] \quad (\text{A.2})$$

with $A_{\text{Rot}_i} = 9\mu_0^2\gamma^4\hbar^2/(128\pi^2r_{i_{\text{eff}}}^6)$ where $r_{i_{\text{eff}}}$ is an effective inter-spin distance [52].

A.0.1.3 Cross-relaxation

^{35}Cl has nuclear spin $3/2$ and cross-relaxation (CR) between the proton spins and ^{35}Cl nuclear spins can occur. Cross-relaxation has indeed been observed between proton spins and nitrogen and also between proton spins and ^{35}Cl spins [45, 53, 54]. Cross-relaxation may become significant when the proton's Larmor frequency is close to each one of the quadrupole frequencies of the other nucleus. The relaxation rate can be expressed by [53]

$$\left(\frac{1}{T_1}\right)_{\text{CR}i} = A_{\text{CR}i} \frac{\tau_{\text{CR}i}}{1 + (\omega - \omega_i)^2 \tau_{\text{CR}i}^2} \quad (\text{A.3})$$

where ω_i , with $i = 1, 2, \dots$, are the frequencies that correspond to the ^{35}Cl spin energy levels and $A_{\text{CR}i}$ are parameters related with the strength of the interaction.

A.0.1.4 Paramagnetic relaxation induced by superparamagnetic particles

Proton spin-lattice relaxation can be affected by the presence of magnetic ions in two ways: i) the so-called *inner-sphere* relaxation, which occurs when relaxing protons bind temporarily to ions or ion complexes, and the ii) *outer-sphere* applies to protons that do not bind but move or diffuse close to magnetic ions or particles [55]. In a recent study of molecular dynamics in magnetic ionic liquid systems by proton spin-lattice relaxometry, [74] it was shown that the paramagnetic relaxation observed was better described considering an effective superparamagnetic outer-sphere contribution given by equation:

$$\left(\frac{1}{T_1}\right)_{\text{PM}} = 6\tau_d c \left\{ S_c^2 j_1(\omega, \tau_d, \tau_s \rightarrow \infty) + \left[S(S+1) - S_c \cotg \frac{x}{2S} - S_c^2 \right] j_1(\omega, \tau_d, \tau_s) \right\} \quad (\text{A.4})$$

where S is the electronic spin along the applied magnetic field, c is a quantity proportional to the molar concentration of magnetized particles, $[M]$. r is the distance of closest approach between the anion and the protonated cation, $\tau_d = \langle r^2 \rangle / D$, D is the diffusion time constant, τ_s is the longitudinal electronic relaxation time and ω is the proton Larmor frequency. S_c is given by

$$S_c = \frac{2S+1}{2} \tanh^{-1} \left((2S+1) \frac{\omega}{\omega_r} \right) - \frac{1}{2} \tanh^{-1} \left(\frac{\omega}{\omega_r} \right) \quad (\text{A.5})$$

where $\omega_r = 2\gamma kT / (\hbar\gamma_S)$ and γ_S is the electron's gyromagnetic ratio. The corresponding spectral density for outer-sphere relaxation is [55]

$$j_1(\omega, \tau_d, \tau_s) = \text{Re} \left\{ \frac{1 + \Omega^{1/2}/4}{1 + \Omega^{1/2} + 4\Omega/9 + \Omega^{3/2}/9} \right\} \quad (\text{A.6})$$

where $\Omega = (i\omega + 1/\tau_s)\tau_d$.

A.0.1.5 Relaxivity Dispersion

In the case of the magnetic ionic liquid/DMSO solutions presented in this work we considered the inner-sphere relaxivity contribution expressed by [63]:

$$r_1^{is} \approx \frac{1}{1000} \frac{q^{st}}{14.04} \frac{1}{T_{1m}^H} \quad (\text{A.7})$$

being q^{st} the number of DMSO molecules temporarily bind to the iron particles and $T_{1m}^H \gg \tau_m$ where τ_m is the DMSO residence binding time to the FeCl_4^- (or FeCl_3).

$$\frac{1}{T_{1m}^H} = \frac{2}{15} \left(\frac{\mu}{4\pi} \right)^2 \frac{\hbar^2 \gamma_I^2 \gamma_S^2}{r_{Fe}^6} S_p (S_p + 1) [3J(\omega_I, \tau_{d1}) + 7J(\omega_S, \tau_{d2})] \quad (\text{A.8})$$

$$J(\omega, \tau_{di}) = \frac{S^2 \tau_{dig}}{1 + \omega^2 \tau_{dig}^2} + \frac{(1 - S^2) \tau_{di}}{1 + \omega^2 \tau_{di}^2} \quad (\text{A.9})$$

$$\tau_{di} = \frac{1}{\tau_{mH}} + \frac{1}{T_{iS}} \quad (\text{A.10})$$

$$\tau_{dig} = \frac{1}{\tau_{mg}} + \frac{1}{T_{iS}} \quad (\text{A.11})$$

$$\frac{1}{T_{1s}} = 2C \left[\frac{1}{1 + \omega_s^2 \tau_v^2} + \frac{4}{1 + 4\omega_s^2 \tau_v^2} \right] \quad (\text{A.12})$$

$$\frac{1}{T_{2s}} = C \left[\frac{5}{1 + \omega_s^2 \tau_v^2} + \frac{2}{1 + 4\omega_s^2 \tau_v^2} + 3 \right] \quad (\text{A.13})$$

with

$$C = \frac{1}{50} \Delta^2 \tau_v [4S_p(S_p + 1) - 3] \quad (\text{A.14})$$

The outer-sphere relaxivity contribution is given by:

$$r_1^{os} = \frac{32N_A \pi}{405} \left(\frac{\mu}{4\pi} \right)^2 \frac{\hbar^2 \gamma_I^2 \gamma_S^2}{RD} S_p (S_p + 1) [3J^{os}(\omega_I, \tau_d), T_{1s} + 7J^{os}(\omega_S, \tau_d), T_{2s}] \quad (\text{A.15})$$

with $\tau_d = R^2/D$

$$J^{os} = \text{Re} \left\{ \frac{1 + \frac{z}{4}}{1 + z + \frac{4}{9}z^2 + \frac{1}{9}z^3} \right\} \quad (\text{A.16})$$

being, $z = i\omega\tau_d + \frac{\tau_d}{T_{iS}}$ is a complex and $j = 1, 2$

A.0.1.6 DMSO/ FeCl_3 and DMSO/[P_{66614}][FeCl_4]

It is presented the relaxivity results and fitting curves obtained for DMSO/hexahydrated FeCl_3 for comparison with the DMSO/[P_{66614}][FeCl_4] solution.

fitteia Report

(internet based fitter service)

*The Art of Model Fitting to Experimental Results*¹

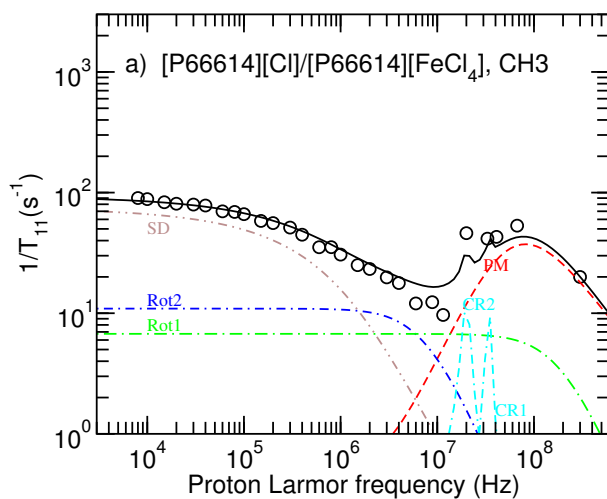
Subject	Plots-Paper-P66614, CH3_final
Date	Wednesday 5 th November, 2014, 18:11
Affiliation	carla.daniel@dq.fct.unl.pt 194.210.232.202
Abstract	Fit report produced with the fit results of function: $y = ((T < 2) ? iT1ISpara(f, 300.0, \tau_{d1}/(1 + \text{pow}(2*\pi*f*\tau_{d1}, p)), \tau_{d1}, M, r, S) : 1e-9) +$ $BPP(f, Arot, \tau) + BPP(f, Arot1, \tau1) + (T < 2) ? CROSSRELAX(f, adip, tdip, fdip)$ $: 1e-10 + (T < 2) ? CROSSRELAX(f, adip1, tdip1, fdip1) : 1e-10 + (T < 2) ? Torrey1(f,$ $d, r*1e10, n, \tau_{d1}/(6.0*(1 + \text{pow}(2*\pi*f*\tau_{d1}, p)))) : Torrey1(f, d, r*1e10, n, \tau_{d1})$ to the 55 experimental points, considering 10 free parameters.

$$\begin{aligned} \tau_{d1} &= 6.3465 \times 10^{-09} \pm 5.9527 \times 10^{-10} \\ \tau_{d1} &= 1 \times 10^{-11} \pm 6.431 \times 10^{-13} \\ \tau_{d1} &= 7.3387 \times 10^{-08} \pm 3.4833 \times 10^{-09} \\ Arot &= 1.85 \times 10^{+08} \text{ (fixed)} \\ \tau &= 1.18 \times 10^{-08} \text{ (fixed)} \\ Arot1 &= 2.81 \times 10^{+09} \text{ (fixed)} \\ \tau1 &= 4.8 \times 10^{-10} \text{ (fixed)} \\ M &= 0.014 \text{ (fixed)} \\ r &= 2.5314 \times 10^{-10} \pm 1.3679 \times 10^{-12} \\ S &= 400 \text{ (fixed)} \\ d &= 8 \pm 0.017602 \end{aligned}$$

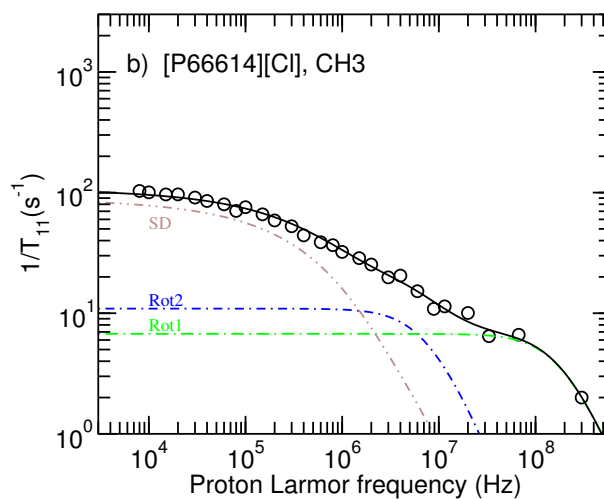
$$\begin{aligned} n &= 7 \times 10^{+22} \text{ (fixed)} \\ \tau_{d1} &= 1.4574 \times 10^{-08} \pm 6.9147 \times 10^{-10} \\ adip &= 2.5352 \times 10^{+07} \pm 1.108 \times 10^{+07} \\ tdip &= 5 \times 10^{-07} \pm 3.2912 \times 10^{-07} \\ fdip &= 3.4 \times 10^{+07} \text{ (fixed)} \\ \tau_{d1} &= 3.85 \times 10^{-10} \text{ (fixed)} \\ p &= 1.1303 \text{ (fixed)} \\ adip1 &= 2.518 \times 10^{+07} \pm 9.2404 \times 10^{+06} \\ tdip1 &= 5 \times 10^{-07} \text{ (fixed)} \\ fdip1 &= 2 \times 10^{+07} \pm 3.1437 \times 10^{+05} \end{aligned}$$

$$\begin{aligned} \chi^2[2] &= 13.727 \\ \chi_t^2 &= 146.008 \end{aligned}$$

$$\chi^2[1] = 132.281$$



recta-1.pdf



recta-2.pdf

¹"The Art of Model Fitting to Experimental Results", P.J. Sebastião, *Eur. J. Phys.* **35** (2014) 015017

fitteia Report

(internet based fitter service)

*The Art of Model Fitting to Experimental Results*¹

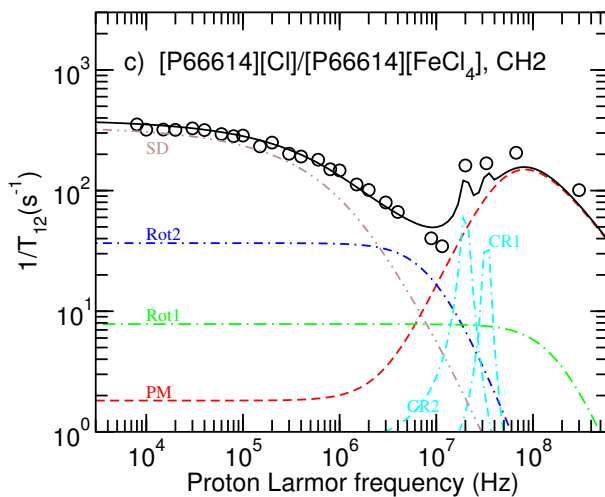
Subject	Plots-Paper-P66614, CH2_final
Date	Wednesday 5 th November, 2014, 18:12
Affiliation	carla.daniel@dq.fct.unl.pt 194.210.232.202
Abstract	Fit report produced with the fit results of function: $y = ((T < 2) ? iT1ISpara(f, 300.0, \tau_{aud1}/(1 + \text{pow}(2*\pi*f*\tau_{aud}, p)), \tau_{aus}, M, r, S) : 1e-9) +$ $BPP(f, Arot, \tau) + BPP(f, Arot1, \tau_{au1}) + (T < 2) ? CROSSRELAX(f, adip, tdip, fdip)$ $: 1e-10 + (T < 2) ? CROSSRELAX(f, adip1, tdip1, fdip1) : 1e-10 + (T < 2) ? Torrey1(f,$ $d, r*1e10, n, \tau_{aud}/(6.0*(1 + \text{pow}(2*\pi*f*\tau_{aud}, p)))) : Torrey1(f, d, r*1e10, n, \tau_{aud})$ to the 53 experimental points, considering 10 free parameters.

$$\begin{aligned} \tau_{aud1} &= 6.0183 \times 10^{-09} \pm 7.3524 \times 10^{-10} \\ \tau_{aus} &= 1 \times 10^{-11} \pm 1.7137 \times 10^{-12} \\ \tau_{aud} &= 7.34 \times 10^{-08} \text{ (fixed)} \\ Arot &= 7.33 \times 10^{+08} \text{ (fixed)} \\ \tau_{au} &= 1.0009 \times 10^{-08} \text{ (fixed)} \\ Arot1 &= 3.03 \times 10^{+09} \text{ (fixed)} \\ \tau_{au1} &= 5.16 \times 10^{-10} \text{ (fixed)} \\ M &= 0.014 \text{ (fixed)} \\ r &= 1.5859 \times 10^{-10} \pm 2.6898 \times 10^{-12} \\ S &= 400 \text{ (fixed)} \\ d &= 4.5148 \pm 0.068607 \end{aligned}$$

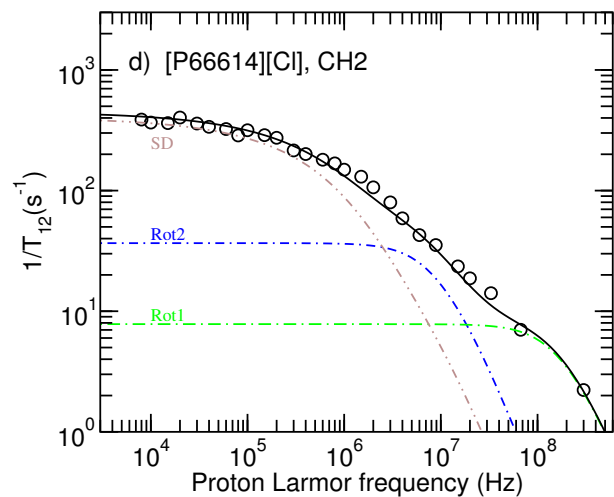
$$\begin{aligned} n &= 7 \times 10^{+22} \text{ (fixed)} \\ \tau_{auD} &= 1.46 \times 10^{-08} \text{ (fixed)} \\ adip &= 1.2856 \times 10^{+08} \pm 4.3852 \times 10^{+07} \\ tdip &= 5 \times 10^{-07} \pm 3.2303 \times 10^{-07} \\ fdip &= 3.3206 \times 10^{+07} \pm 1.6025 \times 10^{+06} \\ \tau_{auv} &= 3.85 \times 10^{-10} \text{ (fixed)} \\ p &= 1.1303 \text{ (fixed)} \\ adip1 &= 1.479 \times 10^{+08} \pm 3.2848 \times 10^{+07} \\ tdip1 &= 5 \times 10^{-07} \pm 1.9932 \times 10^{-08} \\ fdip1 &= 2 \times 10^{+07} \pm 3.356 \times 10^{+05} \end{aligned}$$

$$\begin{aligned} \chi^2[2] &= 28.6349 \\ \chi_t^2 &= 98.3727 \end{aligned}$$

$$\chi^2[1] = 69.7377$$



recta-1.pdf



recta-2.pdf

¹"The Art of Model Fitting to Experimental Results", P.J. Sebastião, *Eur. J. Phys.* **35** (2014) 015017

fitteia Report

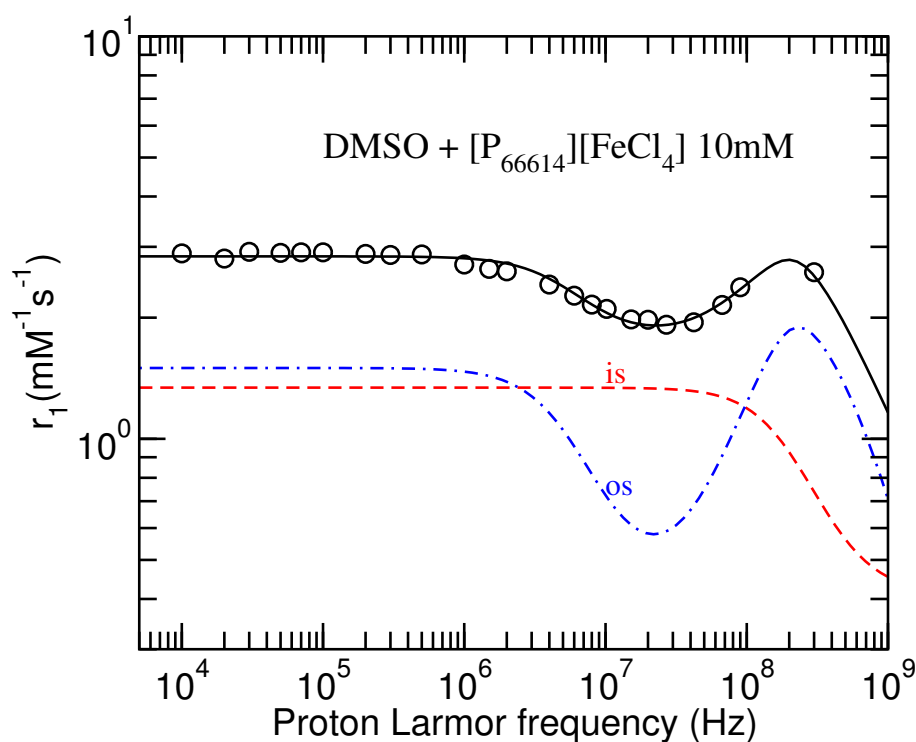
(internet based fitter service)

*The Art of Model Fitting to Experimental Results*¹

Subject	P66614-FeCl4-DMSO, Fit-10mM-r1-final
Date	Friday 24 th July, 2015, 15:02
Affiliation	carla.daniel@dq.fct.unl.pt 84.90.100.162
Abstract	Fit report produced with the fit results of function: $y=x/14040*iT1innerSmallS(f, 295.0, tmg, tmH, tv, ZFS, r, S0*n, S) + iT1outerSmallS(f, 295.0, D, tv, ZFS, R, S0*n)$ to the 23 experimental points, considering 5 free parameters.

$tmg = 1$ (fixed)	$D = 7 \times 10^{-10}$ (fixed)
$tmH = 1.1197 \times 10^{-12} \pm 6.5915 \times 10^{-14}$	$tv = 2.5882 \times 10^{-12} \pm 2.5312 \times 10^{-13}$
$r = 3.5 \times 10^{-10} \pm 2.2172 \times 10^{-11}$	$ZFS = 2.8787 \times 10^{+10} \pm 2.1614 \times 10^{+09}$
$S0 = 3$ (fixed)	$R = 7.9588 \times 10^{-10} \pm 2.9725 \times 10^{-11}$
$n = 1.0001$ (fixed)	$x = 8$ (fixed)
$S = 0$ (fixed)	

$$\chi^2[1] = 5.28254 \quad \chi_t^2 = 5.28254$$



recta-1.pdf

¹"The Art of Model Fitting to Experimental Results", P.J. Sebastião, *Eur. J. Phys.* **35** (2014) 015017

fitteia Report

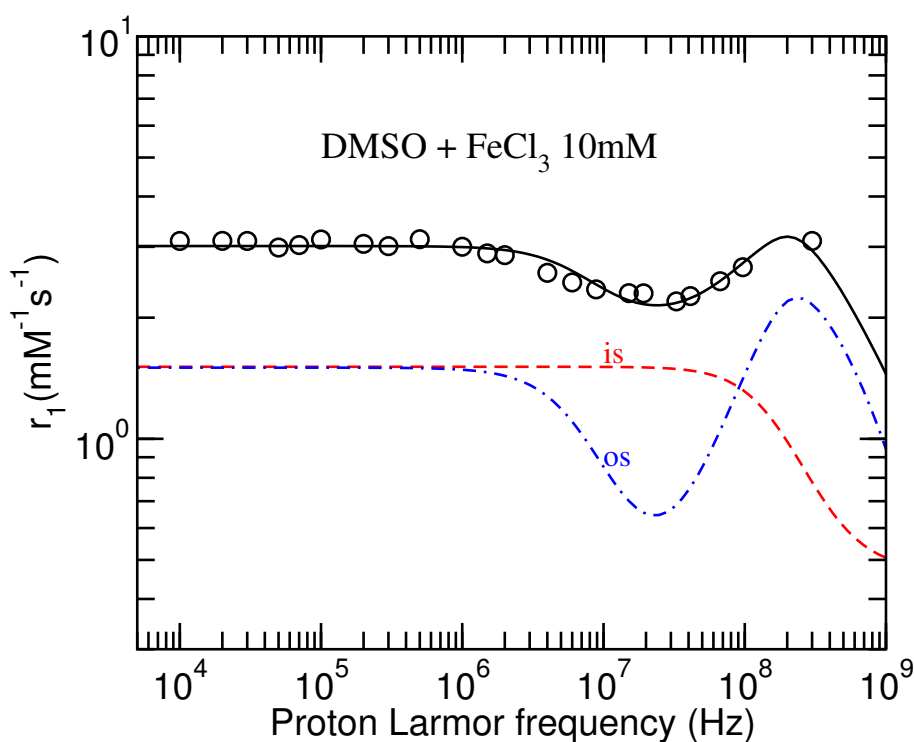
(internet based fitter service)

*The Art of Model Fitting to Experimental Results*¹

Subject	FeCl3-DMSO, Fit-10mM-r1-final
Date	Friday 24 th July, 2015, 15:03
Affiliation	carla.daniel@dq.fct.unl.pt 84.90.100.162
Abstract	Fit report produced with the fit results of function: $y=x/14040*iT1innerSmallS(f, 295.0, tmg, tmH, tv, ZFS, r, S0*n, S) + iT1outerSmallS(f, 295.0, D, tv, ZFS, R, S0*n)$ to the 23 experimental points, considering 6 free parameters.

$tmg = 1$ (fixed)	$D = 7 \times 10^{-10}$ (fixed)
$tmH = 1.2759 \times 10^{-12} \pm 8.5858 \times 10^{-14}$	$tv = 3.0213 \times 10^{-12} \pm 2.6997 \times 10^{-13}$
$r = 3.5 \times 10^{-10} \pm 1.3408 \times 10^{-11}$	$ZFS = 3.0863 \times 10^{+10} \pm 2.5376 \times 10^{+09}$
$S0 = 3$ (fixed)	$R = 7.2522 \times 10^{-10} \pm 3.0103 \times 10^{-11}$
$n = 1.0001$ (fixed)	$x = 8 \pm 4.347$
$S = 0$ (fixed)	

$$\chi^2[1] = 11.9318 \quad \chi_t^2 = 11.9318$$



recta-1.pdf

¹"The Art of Model Fitting to Experimental Results", P.J. Sebastião, *Eur. J. Phys.* **35** (2014) 015017